M 2015

U.PORTO
FEUP FACULDADE DE ENGENHARIA
UNIVERSIDADE DO PORTO

ASSESSMENT OF ANTICANCER DRUGS' EFFECTS ON MEMBRANE BIOPHYSICAL PROPERTIES USING MODEL MEMBRANES

DANIELA FILIPA PINTO RIBEIRO

MASTERS DISSERTATION PRESENTED
TO FACULDADE DE ENGENHARIA DA UNIVERSIDADE DO PORTO IN
BIOENGINEERING – MOLECULAR BIOTECHNOLOGY

This page was intentionally left blank.

Faculdade de Engenharia da Universidade do Porto
Instituto de Ciências Biomédicas Abel Salazar

Assessment of Anticancer Drugs' Effects on Membrane Biophysical Properties using Model Membranes

Daniela Filipa Pinto Ribeiro

Thesis Dissertation for the degree of Master of Science in Bioengineering
-Specialization in Molecular Biotechnology

Supervisor: Prof. Dr. Salette Reis
Co-supervisors: Dr. Cláudia Nunes and MSc Ana Catarina Alves

March 31st, 2015

Abstract

Cancer is a pathology that affects a large portion of the world's population [1]. It is an assembly of diseases with various symptoms that significantly decreases the patient's life quality and has a high rate of mortality [2]. One of the most commonly used treatments for this pathology is chemotherapy, involving the use of combinations of drugs to kill cancer cells. Since these drugs either act directly on the membrane or have to cross it to reach their targets, the interactions between anticancer drugs and biological membranes are of high importance.

The structure of biological membranes consists of a phospholipid bilayer. In healthy cells, phosphatidylcholine (PC) and phosphatidylserine (PS) are some of the most common lipids, the PS being found on the inner leaflet, but cancer cells' membranes usually present higher heterogeneity in constitution, higher fluidity and the PS exposed to the extracellular media [3]. The complexity of the membrane and all the variables associated with the cells' functions makes it a very difficult model to study. As such, artificial model membranes like liposomes might present a viable alternative, being a simpler and easier to manipulate model that accurately simulates the cell membrane's constitution and behaviour.

That being said, the aim of our study was to assess the effects of two anthracyclines used in chemotherapy, daunorubicin and doxorubicin, on the lipid membranes of four LUV formulation models, two of them constituted by dimyristoyl-phosphatidylcholine (DMPC) with and without cholesterol, mimicking the normal cell membrane, and the other two simulating the tumoral cell membrane, constituted of a mixture of dimyristoyl-phosphatidylcholine (DMPC), dioloyl-phosphatidylcholine (DOPC) and dipalmitoyl-phosphatidylserine (DPPS) at the proportions 3:1:1, respectively, also with and without cholesterol. Hepes buffer at pH 7.4 and Tris buffer at pH 6.3 were used to mimic the normal and tumoral tissue's pH, respectively.

Dynamic Light Scattering (DLS) was used to determine liposome size and Electrophoretic Light Scattering (ELS) liposome zeta potential. The partition coefficient (K_p) of the drugs was determined through derivative spectroscopy using liposome/water sytems. Membrane location of daunorubicin involved spectrophotometry, spectrofluorimetry and lifetime fluorimetry measurements. Membrane fluidity and the effect of the two drugs on it were assessed through fluorescence anisotropy.

These techniques were employed on the four formulations of liposomes mentioned before. Membrane location and anisotropy techniques were also performed on tumoral cells, the cell line MDA-MB-231, to assess the ability of the designed models of mimicking the actual biomembranes.

Size measurements confirmed that the models were prepared as intended, with liposome sizes being close to 100 nm. Neither drug seemed to affect liposome size. Zeta potential confirmed that normal model membranes had a surface charge close to neutral and tumoral model membranes were slightly negatively charged, which is consistent with what happens naturally. Increase in drug concentration made the zeta potential in tumoral models less negative, meaning that the drug, positively charged, was interacting with the surface of these membrane models.

K_p determination showed that the two drugs, although very similar, partition very differently. The highest K_p is found for the normal model. Partition for the two drugs decreases with the presence of cholesterol in the membrane for normal models, but the opposite occurs for the tumoral models. Doxorubicin partitions more than daunorubicin for all models except the tumoral with cholesterol model.

Daunorubicin appears to localize between the acyl chains of phospholipids in the membrane but still interacting through electrostatic interactions with the polar heads, so it appears to locate at an intermediate region.

In terms of fluidity, the normal model with cholesterol appears to be the most rigid of all and remains unchanged by the addition of the drugs tested, while the normal model is highly fluid. Contrarily to what was expected, the tumoral model with cholesterol becomes less fluid with the presence of drug, which does not happen in the tumoral model without cholesterol.

Summarily, K_p values prove that there is interaction between both drugs and the four models studied. Both drugs partition significantly less into the normal model with cholesterol than the normal model without it. The opposite occurs in the tumoral models, where cholesterol seems to be causing some adjuvant effect on the partition of the drugs. Evidence suggests that the drug daunorubicin located at a more interfacial region, probably the cooperative zone. The tumoral model with cholesterol also seems to become more fluid at the physiological temperature for both drugs at the cooperative zone. Similar results were found for tumoral cells. From all the gathered information it can be hypothesized that cholesterol might be forming microdomains with some of the lipids of the tumoral model, increasing the rigidity of the membrane in certain areas but leaving the remaining areas permeable to the drug, hence the higher K_p values and higher overall fluidity. It could also be observed that the designed model membranes, although simple, replicated biomembranes quite well. This study and follow-up work can be a big step towards the validation of liposomes as models for cell membranes, and in the future allow the facilitation of drug-membrane interaction studies. Possible future applications would involve not only the use in research but the introduction of the models at an industrial level for an easier, less expensive and quicker development of new drugs or delivery systems for the treatment of several diseases that are more efficient and possess fewer side effects.

Acknowledgements

I would first like to acknowledge the "Trinity" that made this work possible:

To Professor Salette Reis I would like to thank immensely for allowing me to work in her research group, but much more than that I would like to thank Professor Salette for all the support, guidance and counseling. Thank you for being a guiding star in this work and an example of what I one day can only dream of being like, so thank you for the pleasure of working under your supervision.

To Doctor Claudia Nunes, for all the help, and guidance as well, for sharing your immense knowledge with me and at the same time bringing a smile (or laughter) to both of our faces. Thank you for the "coolness" and all the high fives that always calmed me down, and in general, thanks for always lending a helping hand even if you didn't have to.

To Master Catarina Alves, for everything and a little more. Thank you for the guidance and support but also for all the care and inspiration. You are a remarkable researcher and were a great supervisor. Thank you for keeping me focused and grounded as well. I just hope I was up to the expectation.

These three people were able to, in only about 6 months, completely change my life. They shaped the researcher I am now and the one I want to be in the future, inspiring me to better myself personally and professionally every day. For that you have my deepest gratitude.

I'd like to acknowledge all of my labmates a send a huge "thank you" their way! You made it all so much easier and more pleasant just by being incredible people and creating the most uplifting work environment I could hope for. A special thanks to Mara and José for being there when times got hard, and to Joaninha for always helping whenever needed.

To my "Tecos", a big hug and a "cheers!", for dealing with me even though you didn't need to, for the conversations and support. You truly are a second family, you've been there for me not only these past few months but for the last 3 years, and I am here for you as well.

To my friends from back home, even though you don't have a clue of what this was I was working with, you did your best to understand and support me through it and cheer me up without the need for me to even say a word. Thank you for being there for me, always.

To Francisco I would like to thank for all the love and patience, for often being a safe haven, and for so much more that I know I don't need to say.

And lastly and most of all, I would like to thank my family, my parents, sister and grandma, who made all of this possible. Obrigada aos meus pais, irmã e avó, que fizeram com

que tudo isto fosse possível. Obrigada por todo o esforço e dedicação para me proporcionarem tudo o que tive, especialmente os últimos 5, quase 6 anos que sei que foram difíceis para vocês também. Obrigada por me acompanharem nesta jornada que já vai longa mas ainda está a começar.

After all, this is just the beginning.

Index

Figure List

Table List

Abreviations and Symbols

2-OHOA	2-Hydroxyoleic Acid
ALP	Alkyl Lysophospholipids
BRCA1	Breast Cancer Tumor Suppressant Gene 1
BRCA2	Breast Cancer Tumor Suppressant Gene 2
CD	Circular Dichroidism
CEU	1-Aryl-3-(2-Chloroethyl) Urea
CLL	Chronic Lymphatic Leukemia
Dan	Daunorubicin
DLS	Dynamic Light Scattering
DMPC	Dimyristoyl Phosphatidylcholine
DMPG	Dimyristoyl Phosphatidylglycerol
DMSO	Dimetyl Sulfoxide
DNA	Desoxyribonucleic Acid
DOPC	Dioleoyl Phosphocholine
DOTAP	1,2-Dioleoyl-3-(Trimethylammonium) Propane
Dox	Doxorubicin
DPH	1,6-Diphenyl-Hexatriene
DPPC	Dipalmitoyl Phosphatidylcholine
DPPG	Dipalmitoyl Phosphatidylglycerol
DSC	Differential Scanning Calorimetry
ELS	Electrophoretic Light Scattering
EPC	Egg Phosphatidylcholine
EPR	Electron Spin Resonance
FBS	Fetal Bovine Serum
FT-IR	Fourier Transform Infrared Spectroscopy
GUV	Giant Unilamellar Vesicle
HCL	Hairy Cell Leukemia
K_D	Dynamic Constant
Kp	Partition Coefficient
Ks	Static Constant
Ksv	Stern-Volmer Constant
Kq	Bimolecular Constant
LB	Langmuir-Blodgett
LUV	Large Unilamellar Vesicle
MLV	Multilamellar Vesicle
NaCl	Sodium Chloride
NMR	Nuclear Magnetic Resonance
PA	Phosphatidic Acid

PC	Phosphatidylcholine
PE	Phosphatidylethanolamine
PEG	Polyethileneglycol
PG	Phosphatidylglycerol
pHe	Extracellular pH
PI	Phosphatidylinositol
PIP	Phosphatidylinositol Phosphate
PIP2	Phosphatidylinositol Biphosphate
pKa	Acid Dissociation Constant
POPC	Palmitoyl Phosphatidylcholine
PS	Phosphatidylserine
RPMI	Roswell Park Memorial Institute
SAXS	Small Angle X-Ray Scattering
SM	Sphingomyelin
SUV	Small Unilamellar Vesicle
Tm	Phase Transition Temperature
TMA-DPH	1-(4-Trimethylammoniumphenyl)-6-Phenyl-1,3,5-Hexatriene
TME	Tumor Microenvironment
UV-Vis	Ultraviolet and Visible
VEGF-A	Vascular Endothelial Growth Factor A
WAXS	Wide Angle X-Ray Scattering

Chapter 1

Introduction

Cancer is a pathology that affects a large portion of the world's population. It affects people from any region regardless of culture or wealth and is one of the biggest causes of death. Over the last 35 years, the global burden of cancer has more than doubled, with 12.4 million new cases diagnosed and 7.6 million cancer-related deaths just in 2008. With the continuous growth and aging of the world, predictions point towards about 27 million new cancer cases diagnosed and approximately 17 million deaths as a result of cancer in the year 2030 [1].

In the past, many of the greatest scientific and medical accomplishments were achieved in developed countries, resulting in higher exposure of the people to different kinds of radiation, radioactivity (from nuclear accidents, nuclear weapons…) and chemical carcinogens. Such events could explain why cancer was, in the past, a developed country disease [3-5]. However, in the current years, the trend was balanced out if not overturned, with at least half of the global cancer cases being found in low or medium resource countries. In fact, in 2008 five out of every ten diagnosed cancer cases occurred in these regions [6]. These countries are clearly more affected as the increase in cancer cases presents a far more complicated issue due to the lack of proper sanitary and health care conditions. In low to medium resource countries cancer treatment facilities and life-extending treatments are often unavailable for economic reasons [3].

According to the American Cancer Society, cancer is not a disease but encompasses a group of diseases that have in common the uncontrolled growth and spread of abnormal cells. It can cause virtually any sign or symptom depending on the tumor's characteristics. The abnormal cells compete with the healthy cells for oxygen and nutrients, eventually leading to the death of healthy cells. If the spread of abnormal cells is not controlled, it can result in death [7-9].

There is still no definitive and 100% effective cure for cancer. There are, however, treatments with a high rate of success that can eradicate the disease from an individual [7]. One of these treatments, chemotherapy, involves the use of drugs to eliminate cancer cells through a variety of mechanisms. However, they act on all cells undergoing cellular division, so rapidly growing tissues like skin, liver or the intestinal tract, are also under the attack of these drugs, which leads to a number of undesirable and severe side effects that reduce the patients' life quality throughout the treatment sometimes to a state of disability and can also interfere with the success of the treatment [5, 10]

The main targets of chemotherapeutic drugs are intracellular and therefore the drugs must be able to surpass the plasma and possibly the nuclear and organelle membranes. Therefore, the study of anticancer drug-membrane interactions is an important field of research since it provides understanding on the drugs' pharmacology and pharmacokinetics [3]. The basic structure of all cell membranes is a curved lipid bilayer composed of various lipids which serves as a permeability barrier to the hydrophilic molecules on either side of it and host many peripheral and transmembrane proteins. As such, the biophysical properties of the lipids that compose the bilayer may modulate its behaviour in contact with drugs as well as the behaviour of associated proteins and other molecules. Therefore, it is important to study the effect of anticancer drugs on the membranes to evaluate their efficacy, but this may be complicated due to the high complexity of cells. Artificial lipid model membranes appear as a novel way to study drug-membrane interactions since they can be made of cell membrane components or derivatives and mimic its behaviour while the conditions involved are much easier to control [11].

1.1 - Cancer Ethiology and Pathophysiology

1.1.1. Cancer Ethiology

Cancer is a pathology that is characterized by the abnormal growth and development of cells that acquired new characteristics through genetic mutations that provide them with specific capabilities, such as the ability to proliferate independently of the mechanisms that regulate cellular growth [12, 13]. An agglomerate of abnormal cells is called a tumor or neoplasia and it is not necessarily malignant. A tumor becomes a cancer when its cells gain the ability to migrate through different tissues and therefore invade other regions of the organism [11, 14].

When in a tissue, the tumor cells compete with the normal cells for energy and nutrients. Since neoplastic cells have a higher growth ability, they have an advantage, and therefore inhibit the normal proliferation of healthy cells leading to the deterioration of the tissue and failure of its functions [15].

Tumors constitute complex tissues that include various different cell types which establish a number of heterotypic interactions in order to satisfy its necessities. A good example could be the process through which the tumor recruits regular cells to form tumor-associated stroma, a support structure that actively contributes to the emergence of certain decisive cancer-related capabilities [8].

When a tumor is forming, the local conditions are altered, which means that the developing tumor will be enclosed in an environment completely different from the one that is associated with normal cells. This is called the tumor microenvironment (TME) and includes surrounding non-tumor cells like endothelial cells, fibroblasts and immune cells that are embedded into the tumor tissue by extracellular matrix proteins. Soluble factors, signaling molecules and mechanical cues that promote malignant transformation and support the tumor's growth and invasion are also part of the TME [16, 17].

The microenvironment is characterized by low oxygen levels or hypoxia, low glucose concentrations and overexpression and hypersecretion of a number of hydrolytic enzymes in different stages of tumor progression that form the *liquid milieu* of the TME. A micro-acidic environment is common in most solid tumors, with an extracellular pH (pHe) ranging from 5.3

to 7.2, as a consequence of the aforementioned events. The acidity may favour the activity of proteases with a slightly acidic optimal pH such as cysteine and aspartic cathepsins, as well as the redistribution of lysosomes in the cell surface for the release on their proteases [16, 18].

The interactions between all of the TME's components are essential for the correct regulation of the self-renewal and differentiation processes fulfilled by the tumor's stem cell niche to promote the tumor cells' indefinite proliferation [17]. Elements of its microenvironment can actually be instructive to tumor cells, making them more or less tumorigenic and even maintaining or inducing a cancer stem-like state through the secretion of certain molecules (the secretion of hepatocyte growth factor by myofibroblasts in the microenvironment of colorectal cancer is an example) [17, 19]. Although its general constitution remains the same, a specific tumor developed in a certain tissue will have determined factors, signals and molecules that might not be present in another tumor type since their differences implicate other kinds of stimuli. Research on the specific microenvironments of, for instance, breast [20, 21] and lung [22] cancer, Hodgkin lymphoma [23], B-cell chronic lymphocytic leukemia [21] and neuroblastoma [24] produced results that prove as much.

The genesis and progression of cancer is a process that occurs through a sequence of steps, which is confirmed by the fact that the transformation of normal cells into malignant ones requires progressive genetic alteration [25]. Cancer genesis can be divided into three phases: initiation, promotion and progression [5]. The first step is initiation and involves a change in the normal cells' phenotype due to irreversible mutations in its DNA. These are induced by initiators, which, if not already reactive with DNA, are altered by drug-metabolizing enzymes, being then able to cause mutations in the DNA [26, 27]. Promotion is the process through which the initiated cells progress into a visible tumor [28]. This process is undoubtedly related to epigenetic factors. The promoters do not directly interact with the DNA. Instead many bind to cell membrane receptors and affect internal pathways – specific promoters. Nonspecific promoters, on the other hand, alter gene expression without the presence of a known receptor. Both of them generally further alter the cell so it proliferates and divides, which results in their ability to grow unregulated. Promoters do not act on cells that have not undergone initiation and are usually specific to a certain type of tissue [3, 29, 30]. At this point the lesion is benign. To acquire malignancy, the cells must undergo heritable mutations that greatly influence their histopathological characteristics of cellular morphology, invasiveness, growth, and differentiation. This process is called progression. The three stages are represented in figure 1.

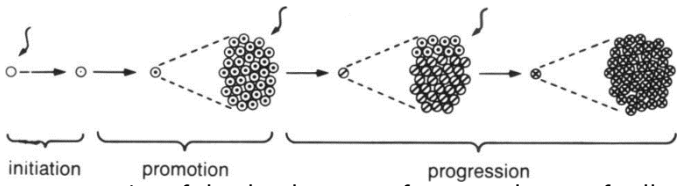

Figure 1 Schematic representation of the development of a tumoral mass of cells. Here are represented the three main steps of cancer ethiology – initiation, promotion and progression [31].

These mutations can be caused by variability inducing phenomena, namely point mutations, genetic amplification or chromosomal translocation. Usually, the occurrence of malignant phenotype in a cell requires not only one but several alterations of its genome that

are accumulated over time. The cell's DNA can suffer spontaneous mutations or they can be inherited from parents. An example for the last case is related to breast cancer – women that inherit a defective copy of the BRCA1 and BRCA2 genes are on greater danger of developing pathology [32]. Many external factors, usually combined, are also involved in the generation of cancer associated mutations. An unhealthy diet, excess body weight and little physical activity are all factors that can increase the risk of cancer. The abuse of substances such as alcohol and tobacco also increases the risk of cancer [15]. Moreover, Ultraviolet (UV) radiation, which comes from the sun and man-made sources like tanning beds, is able to affect cells of the epidermis, the most superficial layer of the skin, originating basal and squamous cell skin cancer or the less common but more serious melanoma, most frequently on more exposed areas such as the face, neck and arms [25]. Other high energy radiation types, like the X rays and gamma radiation used for medical purposes and nuclear power plants, are also associated with tumor generation, as well as some chemicals and infectious agents [3, 15, 25]. Carcinogen types are as listed below:

-Lifestyle factors (nutrition, tobacco use, physical activity, etc.);

-Naturally occurring exposures (ultraviolet light, radon gas, infectious agents, etc.);

-Medical treatments (chemotherapy, radiation, immune system-suppressing drugs, etc.);

-Workplace exposures;

-Household exposures (food irradiation, consumer products containing radiation);

-Pollution [5].

Any healthy nucleated cell possesses mechanisms to repair its DNA and maintain the stability of its genetic content. These mechanisms regulate cellular processes that increase the probability of mutations, such as DNA replication, chromosome segregation and others. When the repair mechanisms are surpassed, the DNA cannot be repaired. As a consequence, the control of the production and release of growth factors that happens regularly in healthy cells ceases to be done efficiently [33]. The subsequent mutations generate more and more variability in the genome of the daughter cells and the ones with a higher survival rate are selected leading to a higher cellular heterogeneity and finally to a state of chronical proliferation associated with tumor cells [5].

The transformation of healthy cells into cancer cells results of mutations mainly in genes of the following types:

-Proto-oncogenes: genes that usually regulate cell division, apoptosis and differentiation; through the action of carcinogens they can become oncogenes, which promote malignant alterations;

-Tumor suppressant genes: genes that suppress alterations that could lead to cancer; as a result, their inactivation is involved in carcinogenesis [27].

The tumor cells achieve immortality by controlling their own proliferative signals. This happens through a few alternative mechanisms. Cells can produce their own growth factors, to which they respond by expressing specific receptors for them – autocrine proliferative stimulation. Alternatively, they can stimulate normal cells in the supporting tumor-associated stroma to supply the cancer cells with the required growth factors [25, 33]. They can also increase the expression of surface receptors or change their conformation in order to make them hyperresponsive to growth factor ligand concentrations that would be limiting otherwise. Several studies using DNA sequencing analysis of cancer cell genomes have revealed somatic mutations that implicate the constitutive activation of signaling circuits usually triggered by activated growth factor receptors [34].

The growth of functional cancer cells also requires cellular senescence to be stopped or delayed and that the cells in the interior of the tumor mass are being supplied with nutrients. The first need is satisfied by the fact that the enzyme telomerase, almost inexistent in normal cells, is present and active in cancer cells, which supports the knowledge that, during the transformation process to malignance, the cells suffer dedifferentiation and loss of function [5, 33]. Nutrients are carried to the interior of the tumor by blood vessels formed for that exact purpose through angiogenesis motivated by the vascular endothelial growth factor A (VEGF-A), for instance, and its expression can be stimulated by oncogenes [15, 27, 35].

Another characteristic of cancer is the acquisition by the cells of the ability to invade tissues besides the one they were originally formed in. This is a process named metastization and involves the propagation of cancer cells to different tissues of the body, starting by the insertion of cancer cells in the lymphatic and blood vessels near the original tumor. These cells then circulate in these systems and end up diffusing to the parenchyma of distant tissues where they constitute cancer cell nodes (micro-metastasis) that then develop into macroscopic tumors.

It can therefore be concluded that cancer cells possess a setting of capabilities that strictly differentiate them from normal cells [8], such as:

- Enabling replicative immortality;
- Inducing angiogenesis;
- Resisting cell death;
- Sustaining proliferative signaling;
- Evading growth suppressors;
- Activating invasion and metastasis.

1.1.2. Conventional Therapies

Throughout the years the knowledge on the pathophysiology of cancer has been enlarged through constant research. The better understanding of its causes and types favored the development of therapies that succeed in the treatment or restriction of cancer. The concept of targeted therapy is still under development but there are nowadays techniques that produce good results in treating cancer. Although hyperthermia, immunotherapy and stem cell transplant are also being used, the most used and also most effective techniques until now will be described below [25, 36].

Surgery is a type of treatment that can be performed for diagnosis, to evaluate the stage of the disease and for reduction or removal of the tumor mass. Surgeries performed for diagnosis are called biopsies and involve the removal of a small portion of tissue from various regions of the affected organ to be analyzed. Surgeries that aim the treatment of the condition consist, as said, in tumor removal or are performed to mitigate the effects of the disease. Surgeries can be very invasive (open body surgery, laparoscopy) or less invasive (laser surgery, endoscopy) [25]. The choice depends on factors such as the stage of the disease, the patient's age and other health problems they might suffer from [37, 38]. If surgical remotion of the entire tumor is possible, this therapy can rapidly eliminate the pathology practically by itself. However, it poses some disadvantages since it is useless in the case of liquid or circulating tumors and very ineffective in metastized tumors, being mostly used in association with one of the next therapies. It is also an invasive procedure that makes patients vulnerable to a number of other complications such as infection [3, 39].

Radiotherapy on the other hand consists of the application of radiation, usually X or Gamma, to the treatment of cancer. Radiation damages the DNA of the dividing cancer cells, which become unviable and undergo cell death. Therefore, radiotherapy allows the reduction of tumor size by leading to the death of the cells that form it. However, this is more a contemption procedure than it is a cure, being usually utilized coupled with other treatment options, mainly chemotherapy. Another problem with this technique is that it doesn't affect only cancer cells. It acts on cells undergoing division in every tissue, damaging healthy cells as well and causing secondary effects in short (skin, intestines and other rapid-growing tissues) and long term (bone and nervous tissue). Consequently, the therapy needs to be used while assuring the balance of the organism upon the damage caused, which poses some difficulties in its use [2, 3, 40, 41].

Chemotherapy is the most used type of treatment for cancer since it seems to very effective [32]. It involves the use of natural or synthetic chemical compounds in order to destroy infecting agents or cancer cells. It can be performed on its own or coupled with one or more of the aforementioned alternative therapy methods, depending on the type and stage of the pathology [3].

Chemotherapy can be administered in different clinical settings, such as: primary induction chemotherapy, for the treatment of advanced, metastatic cancer, for which the possibility of cure is remote and the goal is to increase the survival time and the quality of the patient's life; neoadjuvant chemotherapy, used for localized tumors (anal, bladder, breast, esophageal, laryngeal and non-small cell lung cancers) for which alternative methods exist but are less efficient than desirable, leads to good results when coupled with radiotherapy; and adjuvant chemotherapy, used after another treatment option to prevent recurrence, is effective in prolonging the survival of the patients after removal or remission of the tumors [7].

The therapies that involve drugs are constantly evolving once, much like microorganisms, cancer cells have the ability to develop genetic alterations that grant them drug resistance. This was also the motive that led to the development of combined chemotherapy, which consists of the introduction of more than one type of drug in the organism, which allows the treatment of the disease on different levels and through distinct mechanisms leading to a higher efficacy and lower susceptibility to possible resistance by the cells [3, 42].

Nowadays it is known that a determined dose of drugs used in chemotherapy could be enough to eradicate a certain amount of malignant cells. Thus, correlating the dose with the size of the tumor, it would be theoretically possible to eliminate it quickly and definitively. However, the fact the cancer cells derive from cells from the same individual makes it so that they share a few characteristics with cells in various tissues of the body. Therefore, the effects of the drugs occur also in healthy cells and so a drastic session is not an option. Instead, sequential but spaced chemotherapy sessions have to be scheduled so the patient doesn't sustain lethal injuries from the treatment [3, 42].

Most currently used drugs on chemotherapy act on a particular characteristic of cancer cells – cell division. Consequently, cells in the G0 stage of the cell cycle are unaffected. On the other hand, cells in the S stage suffer damage to their DNA that leads to apoptosis. Just like radiation would, these drugs act both on malignant and rapidly growing healthy cells, causing side effects such as impaired wound healing, lower leukocyte production (compromising the immune system), hair loss, infertility and teratogenicity.

Table 1 Some of the most used chemotherapeutic agents from each type and their mechanisms of action and main side effects [7].

Type	Drug	Mechanism of Action	Side Effects
Alkylating agent	Cyclophosphamide	Alkylates the DNA at the N7 position of guanine; inhibits DNA synthesis.	Nausea, vomiting, Bone marrow suppression, leukopenia, thrombocytopenia, alopecia, hemorrhagic cystitis
	Cisplatin		Nausea, vomiting, Bone marrow suppression, renal dysfunction, acoustic nerve dysfunction.
	Procarbazine		Nausea, vomiting, myelosuppression, hemolytic anemia, pulmonary effects.
	Dacarbazine		Nausea, vomiting, myelosuppression
	Mustines	Alkylates the DNA through cross-linking.	Nausea, vomiting, myelosuppression.
Antimetabolite	Methotrexate	Binds to the catalytic side of dihydrofolate reductase, inhibiting the folic acid pathway.	Bone marrow suppression; dermatological damage and to the gastrointestinal mucosa.
	Mercaptopurine	Activation by hypoxanthine-guanine phosphoribosyl transferase (HGPRT) to form 6-thioinosinic acid which inhibits enzymes involved in purine metabolism.	Hyperuricemia, acute gout, nephrotoxicity.
	Thioguanine	Substitution of guanine bases leading to inhibition of DNA and RNA synthesis.	
	5-Fluorouracil	One derivative inhibits thymidine synthesis, the other incorporates RNA, in general, DNA and RNA synthesis is inhibited.	Myelosuppression, mucositis.
	Cytarabine	Active form competes and inhibits DNA polymerase, inhibiting DNA synthesis but not RNA.	Nausea, alopecia, stomatitis, severe myelosuppression.
	Gemcitabine	Competes with cytidine and replaces it in DNA formation, inhibiting replication.	Nausea, fever, headache, fatigue, vomiting, poor appetite, allergic reaction, difficulty sleepy, shortness of breath.
Plant Alkaloid	Vinblastine	Microtubule depolarization, which interferes with chromosome segregation causing mitotic arrest at metaphase.	Nausea, vomiting, alopecia, bone marrow suppression.
	Vincristine		Bone marrow suppression, neurotoxic reactions.
	Etoposide	Inhibits topoisomerase II, which leads to DNA damage and cell cycle arrest at late S or G2 phase.	Nausea, vomiting, alopecia, hematopoietic and lymphoid toxicity.
	Paclitaxel	Enhanced microtubule polymerization, forming bundles that lead to mitotic arrest.	Vomiting, diarrhea, alopecia, neutropenia, thrombocytopenia, peripheral neuropathy.
Antibiotics	Anthracyclines (doxorubicin and daunorubicin, epirubicin)	Intercalate the DNA and affect topoisomerase II inhibiting DNA and RNA synthesis, alter membrane fluidity and ion transport, and produce and oxygen radical species.	Permanent heart damage, nausea, vomiting, myelosupression, alopecia.
	Bleomycin	Produces single and double stranded breaks due to free radical formation, arresting the cell cyle in phase G2.	Anaphylactoid reaction, fever, anorexia, hyperkeratosis, blistering.
Hormonal Agent	Tamoxifen	Partially competes with estrogen, binding to estrogen receptors and suppresses serum levels of insulin-like growth factor-1; and up-regulates local TGF-beta production.	Hot flashes, nausea, fluid retention

Miscellaneous	Hydroxyurea	Blocks an enzyme which converts the cytosine nucleotide into the deoxy derivative and the incorporation of the thymidine nucleotide into the DNA strand, inhibiting DNA synthesis.	Drowsiness, nausea, vomiting, diarrhea, alopecia, anorexia, mucositis, stomatitis, bone marrow suppression.
	L-asparaginase	Depletes serum asparagines that the tumor cells need but cannot produce, leading to cell death.	Allergy, anaphylaxis, pancreatitis.
	Oxaliplatin	Forms both inter- and intra-strand cross links in DNA which prevent DNA replication and transcription.	Nausea, vomiting, diarrhea, neurotoxicity, neutropenia, ototoxicity.

1.1.3. Anticancer Drugs

The most used types of anticancer drugs are called cytotoxic agents and can be divided in various categories.

Alkylating agents and derivatives establish covalent bonds with the DNA and prevent its replication. Antimetabolites block or subvert metabolic mechanisms of DNA synthesis. In this category there are purine anthagonists, like mercaptopurine and gemcitabine, and pirimidine anthagonists, such as 5-fluorouracil and cytarabine, which are drugs that compete with regular bases and are added as such to forming chains or influence enzymes associated with their metabolism or synthesis. Other pathways can also be affected by this type of drug, being a good example the folate metabolism. The cells need folate naturally to perform regular and essential functions like synthesising, repairing and methylating DNA. Fast growing cells like cancer cells need an even higher amount of folate. In the case of folate anthagonists like methotrexate, the drug binds to the enzyme responsible for converting folate to its active form, inhibiting this process and therefore depriving the cell of folate. Cytotoxic antibiotics are able to interfere with several mechanisms (depending on the antibiotic) in DNA replication and protein synthesis. Plant derivatives, such as alkaloids, taxanes and campothecins, impair the correct functioning of microtubules, interrupting the mitosis. Hormones are also used, especially steroids, as well as compounds that suppress or antagonize hormone secretion. A number of compounds that include the recent tumor-related targets cannot be included in any of the previous categories [3, 43]. Table 1 shows some of the most applied chemotherapeutic drugs along with their type, mechanism of action and side effects.

Due to the development of resistance by the cancer cells to the anticancer drugs and the lack of definitive and 100% successful cure, new drugs are currently being researched for their possible advantageous effects comparing to the ones already in use. An interesting new category are the alkyl lysophospholipids, ALP. Edelfosine appears to be the most potent anticancer ALP. It is particularly interesting since, unlike most chemotherapeutic drugs, it does not attack DNA. Instead, edelfosine accumulates in the lipid rafts of the membranes of tumor cells, apparently inducing apoptosis through a redistribution of lipid raft protein composition [44, 45]. 1-aryl-3-(2-chloroethyl) ureas or CEUs also present strong anticancer effects that led their intensive use in several studies. CEUs are hybrids of two also potent anticancer agents, aromatic nitrogen mustards and aliphatic nitrosoureas. They have shown to be very cytotoxic, devoid of mutagenicity and show no signs of systemic toxicity in animal models with tumors. They are weak alkylating agents that are unable to alkylate either cellular DNA or gluthatione, so the low alkylating potency is only partially responsible

for their cytotoxicity. These are amphiphilic drugs that therefore can interact with the lipids in the membrane, so alteration of the membrane's fluidity is thought to be the major cause of cytotoxicity [46]. The general structure of CEUs can be seen in figure 2.

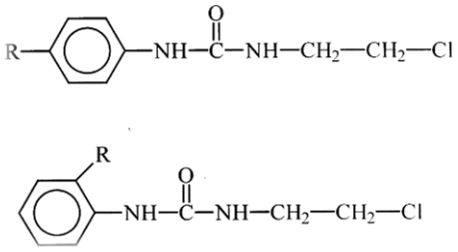

Figure 2 General structures of CEU derivatives substituted at positions four (top) and two (bottom). "R" representes the substituent groups (also called radical groups). The only difference between distinct CEUs is this R (radical) substituent [46].

Although chemotherapy can be performed using only one agent, introducing a combination of different drugs into the organism is much more common. That is because the combination of different types of drugs can target different pathways on the cells, making the therapy more efficient, and also provide a way to surpass drug resistance by cancer cells [32]. In Table 2 are shown a few common established combination regimens for 8 distinct types of cancer.

Table 2 An assortment of very common and established combination chemotherapy regimens. Adapted from Corrie et al. 2011 [47].

Cancer	***Combination of Drugs***
Breast	-Cyclophosphamide, methotrexate, 5-fluorouracil; -Doxorubicin, cyclophosphamide.
Hodgkin's Disease	-Mustine (nitrogen mustard), vincristine, procarbazine, prednisolone; -Doxorubicin, bleomycin, vinblastine, dacarbazine.
Non-Hodgkin's Lymphoma	-Cyclophosphamide, doxorubicin, vincristine, prednisolone.
Germ Cell	-Bleomycin, etoposide, cisplatin.
Stomach	-Epirubicin, cisplatin, 5-fluorouracil.
Bladder	-Methotrexate, vincristine, doxorubicin, cisplatin.
Lung	-Cyclophosphamide, doxorubicin, vincristine (etoposide).
Colorectal	-5-fluorouracil, folinic acid, oxaliplatin.

It can be gathered from Table 2 that each drug combination includes drugs with different mechanisms of action, which may be associated with the importance of eliminating as much cancer cells as possible as well as overcoming possible drug resistance as mentioned before. Also, the differences in combinations support the idea that different types of cancer involve different mechanisms and molecules [48].

Targeted cancer therapies, on the other hand, are more specific as they try to eliminate the pathology by acting on specific molecular targets associated with cancer, blocking the growth and spread of cancer cells. Through these therapies, side effects can be minimized since the specificity towards cancer-related targets decrease or halt the action of the drugs on normal cells [49]. Although targeted cancer therapies are relatively new, very subjective

and still under development, the kind of strategy they present might be key in the future of cancer treatment.

1.2 - Biological Membranes

Cellular membranes are some of the most important components of cells. Besides their essential function in the compartmentalization of the cells, whether it is separating the cell contents from the environment in the case of the plasmatic membrane or creating a boundary between the inside of the cell's organelles and its cytoplasm, biological membranes are involved in a number of other processes that are crucial for the development of cells and organisms in general [50]. These functions are mainly regulated and made possible by the very diverse constitution of the membranes.

The universal basis for cell membranes' structure has been since 1925 established to be the lipid bilayer [3]. The lipid bilayer is formed by a variety of amphiphilic molecules unevenly distributed and held together by hydrophobic interactions between their acyl chains. In 1972, Singer and Nicholson proposed that the membrane was structured as a fluid mosaic, a highly dynamic, heterogeneous and asymmetric structure composed of lipids and proteins that moved and changed conformation freely within the membrane's plane. The fluid mosaic model is still the basis of knowledge in regards to the membrane bilayer, but currently there is much more information regarding its constitution and the interaction between its constituents at a molecular level [50, 51].

Cell membranes are characterized by an asymmetric distribution of lipids along the bilayer. These lipids are mostly phosphatidylcholine (PC), phosphatidylethanolamine (PE) and phosphatidylserine (PS), as well as sphingomyelin (SM), phosphatidylinositol (PI) and cholesterol in smaller proportions, represented in figure 3 [50]. Cholesterol is a very important constituent of the membrane because it is the main molecule responsible for the maintenance of membrane's fluidity. This molecule has a hydroxyl group that interacts with the hydrophilic head groups of the other lipids in the membrane, while its bulky steroid groups interact with their hydrophobic acyl chains, as can be seen in figure 4.

These interactions modulate the packing of the lipids within the membrane, influencing its fluidity [50]. Membrane fluidity is one of the most important psychochemical characteristics of biological membranes since it affects several cell functions such as cell growth, carrier-mediated transport and enzyme and receptor-related signalling pathways like apoptosis. Proteins also integrate the membranes. Integral proteins span the entire membrane while peripheral proteins usually adhere to the surface of the membrane via protein-protein interactions. Proteins can contribute as molecule or ion transporters or anchors and are involved in a variety of biological processes [52].

This asymmetric distribution of lipids on the membrane is associated with the aforementioned lipid rafts and is maintained purposely by the cell at the expense of energy, which confirms its importance to the cell's functioning [53]. An important aspect of this asymmetry is that in normal cells anionic aminophospholipids (mainly PS) are maintained on the inner leaflet of the membrane [53-55]. This is important because PS exposure at the surface of cells has been correlated with the maintenance of the membrane structure as well as some of its functions, allowing the binding of membranes proteins, being a cofactor for protein kinase C or PKC and the Na^+/K^+ ATPase and the promotion of a blood clotting cascade, and so it is essential that, at a normal state [54, 56], PS is not exposed. Contrarily,

it has been shown that PS is exposed in high amounts on the outer leaflet of tumoral cell membranes [54], and that has actually became a major hallmark that could in the future be an excellent target for the delivery of drugs. The same seems to happen with PE, although its involvement in the membrane behaviour seems to be smaller [56].

So it is clear that the constitution and structure of the cell membrane differs greatly from normal to tumoral cells. Interestingly, slight changes can be seen even between the structure and composition of the membranes of different types of cancer cells. Studies on hepatoma cells showed that their membranes contained four times more SM than normal ones, as well as an increase in choline plasmalogen and unsaturated fatty acids, which might indicate higher membrane fluidity [57]. In human colorectal cancer cells, increased levels of all phospholipids were found, including PI, PS, PE and PC, which is associated with enhanced cell membrane synthesis [53, 58]. The membranes of lymphocites from patients with Chronic Lymphocitic Leukemia or CLL present an increase in general phospholipid concentration as well as cholesterol, SM and glucosylceramide and lactosylceramide while a decrease of the PC levels was observed when comparing the membrane fraction with the general homogenate [59]. Hairy cells from hairy cell leukemia (HCL) have membranes with higher content in cholesterol and lower fluidity than CLL lymphocites. However, the cholesterol content is similar to that found in normal monocytes [60]. It becomes therefore evident that cell type influences plasma membrane constitution, which could be a stepping stone towards developing new therapies or drug delivery systems specifically targeting certain tissues or tumoral cell types.

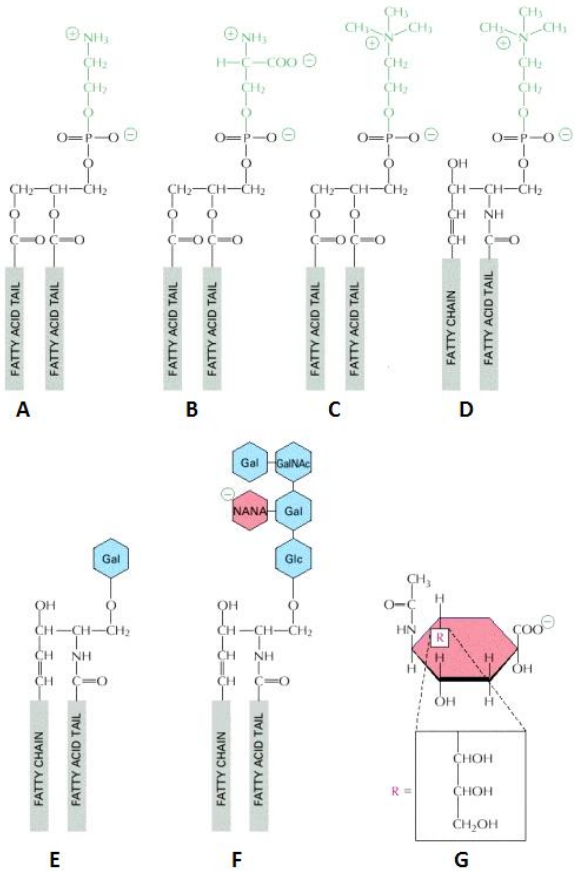

Figure 3 Representation of the structures of some of the main lipids found in animal plasma membranes: phosphatidylethanolamine (A), phosphatidylserine (B), phosphatidylcholine (C) and sphingomyelin (D), which are phospholipids. Glycolipids appear in a much smaller amount, but the most common are galactocerebroside (E), GM1 ganglioside (F) and sialic acid or NANA (G). Adapted from Alberts et al. 2002 [2].

The membrane's heterogeneity leads to the formation of microdomains in its structure [50]. Some of these microdomains are called lipid rafts and are made of cholesterol and sphingolipids [glycosphingolipids and shpingomyelin (SM)]. The lipid rafts actively participate in metabolic and signal transduction processes, and some of these processes are even involved in the promotion of cell death (like the Fas receptor death pathway)[51].

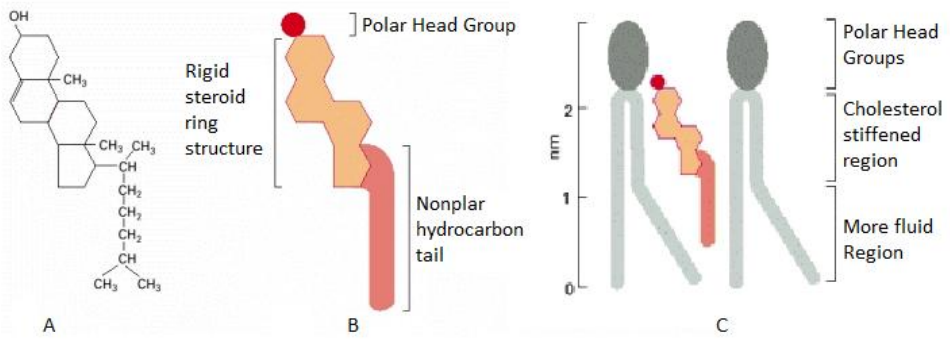

Figure 4 The structure of cholesterol is represented by formula (A) and by schematic drawing (B). (C) represents the cholesterol's interaction with lipids in the bilayer. Adapted from Alberts et al. 2002 [61].

1.2.1. Importance for drug-membrane interaction studies

Plasma membrane is a complex and intricate structure involved in a variety of life-defining events for the cell. Besides the already mentioned importance of membrane proteins, changes in lipid levels have been described in a number of pathologies, namely cardiovascular diseases and cancer [3, 62-64]. Due to the highly prolific character of cancer cells, they have constitutive activation of fatty acid biosynthesis, which has been demonstrated to lead to altered phospholipid and fatty acid profiles in breast cancer cells and surrounding tissue [65]. Gangliosides were shown to be aberrantly distributed in a number of tumors and an accumulation of esterified cholesterol was associated with cell cycle progression and tumor growth. Sphingomyelin levels were reduced in a number of cancers as well [66].

It appears that the plasma membrane is also a very important participant in chemotherapy-induced cell death since the targets for the main chemotherapeutic drugs are thought to be intracellular, as well, as in the effect of a variety of other decisive drugs (antibiotics, antifungal drugs, etc.), but very little is understood about the actual processes and the way that the membrane is involved in them [51, 65, 67]. Indeed, the ultimate effect of the drug might be a consequence of the actual interaction of the drug with the plasma membrane or be related to the interaction with an intracellular target. Certain drugs can interact with the membrane's proteins, which can act as receptors, signal transducers, transporters or enzymes. Others act on the actual lipid bilayer, altering its biophysical properties such as permeability (so the drug can enter the cell or to disrupt the membrane leading to cell death), phase behavior and conformation. Either way, an interaction with or penetration of the cell membrane is a crucial step in the drug's activity, especially in the case of anticancer drugs [65, 68]. Other membranes (such as nuclear envelope, Golgi and reticulum membranes) might also be involved in the mentioned processes. Several studies have actually proved that there is a correlation between the cytotoxicity of certain antitumor agents and, for instance, membrane fluidity, as well as other parameters [46]. Therefore, the study of the interactions between these drugs and membranes is of vital importance since it

could shed light on the drugs' activity and therefore on its pharmacology, pharmacokinetics, efficacy and toxicity [69]. Furthermore, the knowledge that can be obtained from the study of drugs-membrane interactions could allow the improvement of drugs mechanism of action and the development of new drug delivery systems [68, 70].

1.2.2. Types of Model Membranes

The complex constitution of the membrane as well as its behavior is very beneficial for the cell in a way that they modulate very important processes as previously mentioned. However, besides the difference in phospholipidic constitution and the existence of microdomains, the molecular shape (polymorphism) of lipids, the different degrees of affinity between them, the charge, the differential electrostatic interactions and other factors also affect the membranes' behavior and structure. This intricacy and complexity creates great difficulties in the study of the referred processes, and, most importantly in the case of this review, in the study of anticancer drug-membrane interactions [50, 68, 71]. The solution lies in the use of artificial model membranes. These model membranes can be manufactured with the desired constitution and maintained in controlled conditions, and can be used to mimic simple or complex cases by just varying its lipid composition. Lacking the remaining constituents of an actual cell, these models are not subjected to several factors that could arise from differences in intracellular molecules, processes or conditions, which could interfere with the results obtained.

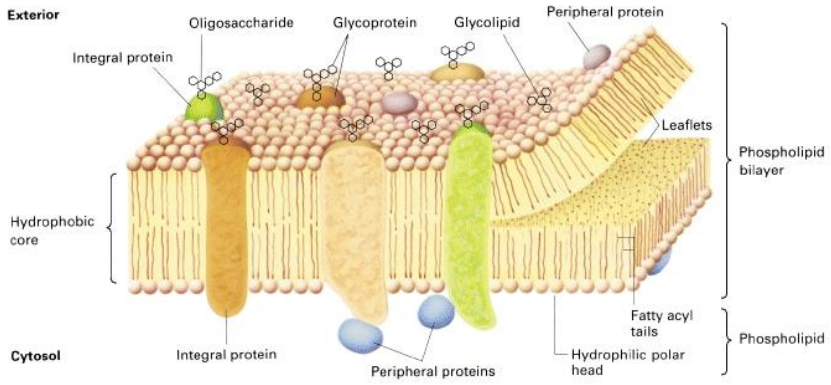

Figure 5 Schematic representation of a biological membrane and its constituents [3].

A wide variety of mimetic model systems exists and is currently used for the study of drug-membrane interactions. In this particular case, the review will center our attention on those used for studies regarding the effect of anticancer drugs on model membranes. The review of these studies, discussed in the section below, resulted in the conclusion that lipid monolayers, lipid bilayers and liposomes are the most used model membrane systems used to assess the effects of anticancer drugs, although micelles also play a smaller but important role in these.

A. Lipid Monolayers

Lipid monolayers may be the simplest form of lipid model. They can also be called Langmuir monolayers and are formed at the air-water interface in a Langmuir through by accumulation of the lipids with a cylindrical shape in the lipid solution at the surface with the

hydrophilic head in contact with the water and the hydrophobic tails turned upwards [68]. Since these type of lipids have a shape that does not allow the formation of curvature, the structure is maintained as a plane layer [66].

B. Lipid Bilayers

Lipid bilayers are basically two monolayers placed together. Their structure is generally the one that can be found in plasma membranes: a bilayer of lipids in which the polar heads are turned to the outside, where they can interact with water and aqueous solutions, and the hydrophobic lipid tails are placed on the core of the bilayer [72].

Both monolayers and bilayers can also be supported lipid monolayers or bilayers. In this case, instead of being at an air-water interface, these structures are adsorbed to a solid surface like mica or gold [73].

C. Micelles

Micelles are vesicles delimitated by a lipid monolayer of conical-shaped lipids. This shape makes the monolayer curve until a closed vesicle is formed. Depending on the shape of the lipid, the micelle can be a regular one, with the polar heads turned outwards and the hydrophobic tails turned to the inside, or an inverted micelle in which the opposite occurs [66, 69].

D. Liposomes

Liposomes are a more complex but also a much more versatile model to study drug-membrane interactions. These structures are basically vesicles with a lipid bilayer as a surrounding membrane. These vesicles can differ both in size and number of bilayers. Liposomes with multiple concentric bilayers separated by liquid are designated multilamellar lipid vesicles (MLVs); while unilamellar vesicles have only one lipid bilayer and, depending on their size, they are classified as small unilamellar vesicles (SUVs), large unilamellar vesicles (LUVs) or giant unilamellar vesicles (GUVs) [74].

1.3 - Anticancer Drug-Membrane Interaction Studies

1.3.1. Techniques applied in anticancer drug-membrane interaction studies

It has so far been described the importance of lipid model membranes in the study of drug-membrane interactions, but its importance only exists if there are techniques to study those interactions. Along with the development of novel model membranes, a wide variety of techniques have been develop to better understand these interactions and in order to assess not only the partition or location of the drug in the membrane, but also its conformation and orientation upon interaction with it, as well as the changes in lipid phase, structure, stability and even at a molecular or elementary level upon drug presence [75, 76]. Table 3 correlates the most used techniques in this field with the model membranes that are frequently used with and its respective goal.

Table 3 Experimental techniques applied to the study of anticancer drug-membrane interaction studies using different membrane mimetic models.

Technique	Type of model membrane	Biophysical parameter studied	References
DSC	MLVs	Effect of squalene-gemcitabine, tamoxifen, paclitaxel, cisplatin and methotrexate on the lipid phase transition temperatures	[77-82]
	SUVs	Effect of paclitaxel, etoposide and cytarabide on the lipid phase transition temperatures	[80, 83]
SAXS	MLVs	Effect of squalene-gemcitabine on structural parameters and phase behavior of bilayers	[77]
	Lipid Bilayers	Effect of squalene-gemcitabine on structural parameters above and below the transition	[84]
	LUVs	Effect of doxorubicin on the packing details of the membranes	[85]
WAXS	MLVs	Effect of paclitaxel on structural parameters and phase behavior of bilayers	[77]
	Lipid Bilayers	Effect of squalene-gemcitabine on structural parameters above and below the transition	[84]
Monolayer Techniques	Lipid Monolayers	Assessment of edelfosine, doxorubicin and paclitaxel's capacity of penetrating into the monolayer	[44, 45, 86-90]
Fluorescence measurements	Lipid Monolayers	Effect of edelfosine on the lipid structure; assessment of the formation of edelfosine-lipid micelles	[44]
	LUVs	Effect of doxorubicin, edelfosine and 2-hydroxyoleic acid (2 OHOA) on the membrane structure and permeability; partition of the drug	
	SUVs	Assessment of doxorubicin's capacity of penetrating into the bilayer	[87]
	Micelles	Assessment of doxorubicin's capacity of penetrating into the monolayer	[87]
Turbidity	LUVs	Assessment of bilayer solubilization as an effect of edelfosine	[44]
FT-IR	SUVs	Determination of changes in membrane structure and dynamics upon interaction with etoposide and cytarabide	[83]
	MLVs	Effects of acyl chain length on structural parameters such as lipid order and the strength of hydrogen bonding under the effect of tamoxifen	[78, 79]
	MLVs	Determination of changes in membrane structure and dynamics upon interaction with CEUs	[46, 91]
	Lipid Bilayers	Effects of CEUs on the gel-to-liquid-crystalline phase transition temperature of the acyl chains of the lipid; study of CEU incorporation into the bilayer	[46]
Phase Contrast	GUVs	Effects of ODPC on membrane structure	[92]

Microscopy			
BAM	Lipid Monolayers	Effects of edelfosine on the morphology of the monolayer	[45]
NMR	MLVs	Study of the influence of CEUs on the membrane phase behavior and conformation	[91]
	Lipid Bilayers	Study of the influence of cisplatin on the phase behavior and conformation of the bilayer	[93]
	Liposomes	Study of the influence of cisplatin on the phase behavior and conformation of the bilayer	[94]
EPR	MLVs and SUVs	Determination of changes in membrane structure and dynamics as an effect of paclitaxel presence	[80]
Circular Dichroidism	LUVs	Assessment of doxorubicin's partitioning	[85, 95]
DLS	MLVs	Determination of the effect of doxorubicin on phase transition temperature	[88]
Cyclic Voltametry	Supported Lipid Monolayers	Assessment of doxorubicin's partitioning conditions	[89]
SERRS	Supported Lipid Monolayers	Assessment of doxorubicin's interactions with the monolayer (penetration or binding)	[89]
QCM and SPR	Supported Lipid Monolayers	Quantification of the doxorubicin that is able to interact with the monolayer	[89]
2D TLC	MLVs	Study of the complexation of cisplatin with the membrane in the presence of a competitor (glutathione)	[96]

From the information presented in Table 3 it appears that the most used model membranes are lipid monolayers and bilayers (MLVs and LUVs). Lipid monolayers are the simplest model membrane, with a typically smooth structure that is easy to create and monitorize. The main conditions to have in mind, such as pH, ion content, temperature, and surface pressure are easily controlled [97]. Bilayers, although a little more complex in structure, share some of these characteristics, which also makes them a preferred model [97]. In the case of liposomes, some techniques benefit from the use of a higher amount of sample, and so MLVs are a good choice [76]. However, unilamellar vesicles also have its relevance, particularly LUVs due to the fact that their membrane curvature is similar to that of cells [75, 76].

In the case of liposomes and lipid bilayers that can be generically called models with bilayered membranes, differential scanning calorimetry (DSC) is one of the most often used techniques, along with SAXS and WAXS, NMR, FT-IR and Circular Dichroidism (CD).

The physicochemical properties of phospholipids lead them to form bilayers spontaneously, and the bilayer's physical organization highly depends on temperature, type of phospholipid and water-lipid ratio. For instance, at higher temperatures, a bilayer can be organized in the liquid crystalline phase (L_α) and as the temperature decreases it changes to the gel phase (L_β) with limited movement of the hydrocarbon chains. This is important because the lipid phase of the majority of the phospholipids in a membrane is directly related to the degree of disorder of its lipids and therefore the membrane's fluidity. This can be better understood in figure 6. DSC is a thermodynamics technique that is able to asses changes in phase transition by measuring the heat exchange associated with cooperative lipid phase transitions in model and biological membranes. One of the most important parameters to be obtained seems to be the change in the main phase transition temperature, which is the peak of the gel-to-liquid crystalline endotherm, T_m. A decrease in T_m suggests higher disorder of the hydrocarbon chains and, therefore, an increased fluidity of the membrane can be inferred [98]. Zhao et al. used DSC to determine the phase transition temperatures of MLV and SUV lipids under the influence of CEUs [80], while Speelmans and Pignatelo performed similar experiments using cisplatin[81] and methotrexate[82] respectively on MLVs.

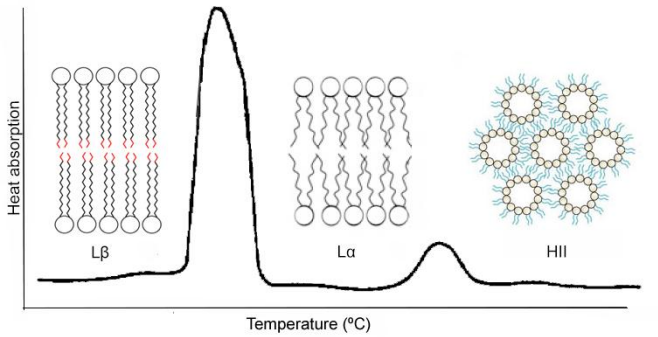

Figure 6 Structures adopted by phospholipids in aqueous media. Most phospholipids adopt only the first two phases, while some other such as DPPE form hexagonal phases. L_β and L_α (gel and liquid crystalline) states exists at low and intermediate temperatures respectively, while the inverted cylinder (hexagonal) H_{II} state is found at high temperatures. Adapted from Seydel et al. (2002) [98].

Fluorescence measurements include a variety of methods that use fluorescence to determine a number of parameters. A few of these fluorescence methods will be described where relevant along this topic.

Fluorescence measurements are actually very useful in this field and versatile, allowing the evaluation of parameters such as membrane organization, permeability and fluidity as well as drug location in model membranes. The techniques are fairly simple and involve the coupling of a fluorescent probe to the drug or the membrane lipids, depending on the goal of the study. The fluorescence can then be followed through fluorescent microscopy or spectrometry [98].

Fluorescence anisotropy can be used to determine the size and shape of molecules, interactions between molecules and rigidity of many molecular environments, having been employed in the study of membrane fluidity [99, 100]. Fluorescence anisotropy is a phenomenon through which the light emitted by a fluorophore has different intensities along different axes of polarization. In other words, this is a method based on the photoselective excitation of fluorophores by polarized light. These preferentially absorb protons whose electric vectors are aligned parallel to the transition moment of the fluorophore. As a result, upon excitation with a polarized light, one is selectively exciting the fluorophores whose absorption transition dipole is parallel to the electric vectors of the excitation [100]. Emission occurs also with a polarized light through a fixed axis. The relative angle between these two axis determines the maximum anisotropy measure [100].

In a regular experiment using this method, the fluorescence intensities with the excitation polarizer aligned vertically while the emission polarizer is aligned vertically as well (I_{vv}) and horizontally (I_{vh}) are measured. Through the following equation, the anisotropy value, A, can be obtained:

$$A = \frac{Ivv - G \times Ivh}{Ivv + 2 \times G \times Ivh}$$

Where G is the grating factor, which is a correction factor for the polarization by the interior components of the fluorometer that is determined by $\frac{Ihv}{Ihh}$. I_{hv} and I_{hh} are the measured intensities with the excitation polarizer aligned horizontally while the emission polarizer is oriented first vertically and then horizontally, respectively [99, 100].

The anisotropy, A, depends on the fraction of fluorescent solute interacting with a macromolecule, in this case, an anticancer drug molecule, and on the rigidity of the complex[99]. In the paper by Martin et al., fluorescence anisotropy showed a decrease in membrane lipids order in the presence of 2-hydroxyoleic acid (2OHOA) [101].

Certain substances have the ability to decrease the intensity of fluorescence of a fluorophore. That process is called quenching, and the causing substance or molecule is a quencher. This is a very useful in membrane-drug interaction studies. Let's suppose that the drug studied is coupled with a fluorophore that suffers quenching by a certain region of the hydrocarbon chains of the membrane's phospholipids. The membrane is put in contact with the drug, which penetrates it. The fluorescence can be measured then. Depending on the amount of quenching the fluorophore suffered, it can therefore be determined how close to the quencher region of the hydrocarbon chain the drug partitioned to [98, 102]. Also to determine partition, fluorescence microscopy can be used and the fluorophore-drug complex can be visualized in the compartment it partitioned into. The same can be performed with confocal microscopy [98].

De Wolf measured the quenching doxorubicin bring upon itself when it self-associates and through this knowledge was able to determine that doxorubicin complexes dissociated and bonded to SUVs [87]. To test the effect of edelfosine on the membrane's permeability, Busto et al. used LUVs containing a fluorescent substrate and added the drug to the medium. By

measuring the fluorescence on the outside of the vesicles it was possible to determine vesicle efflux caused by edelfosine and that the drug increased the membrane's permeability [44]. Li performed similar experiments using doxorubicin on MLVs [85].

X-ray diffraction techniques (small angle, SAXS, or wide angle x-ray scattering, WAXS) are very useful to obtain information regarding the localization of the drug on the membrane and the conformational changes of the membrane. The principle behind it consists of comparing the electron density profile of untreated lipid membranes with the profile of lipid membranes under the effect of the drug [98]. If the sample is partially hydrated, probes are used and a coherent Bragg-like scattering can be obtained with reasonable resolution. The differences observed give information on the drug location within a bilayer, as well as on the structural changes that it caused to the membrane [98]. Pili and Bildstein used the techniques SAXS and WAXS to determine the effect of a hybrid anticancer drug made of squalene and gemcitabine on structure parameters at varying temperatures and on phase transition [77, 84]. Li and colleagues analyzed the effect of doxorubicin on the packing of lipids using SAXS [85].

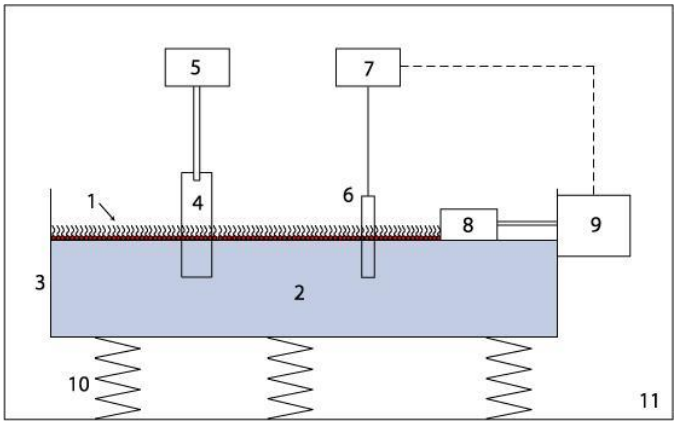

Figure 7 A schematic of a Langmuir Blodgett trough: 1. Amphiphilic monolayer 2. Liquid subphase 3. LB Trough 4. Solid substrate 5. Dipping mechanism 6. Wilhelmy Plate 7. Electrobalance 8. Barrier 9. Barrier Mechanism 10. Vibration reduction system 11. Clean room enclosure.

DSC and x-ray diffraction techniques are often coupled with nuclear magnetic resonance (NMR) spectrometry, a technique that is also able to evaluate the effect of ligands (drugs in the case) on the membrane structure as well as its motional characteristics. NMR techniques provide detailed information about molecular conformation and ordering, and relaxation time measurements probe the amplitude and time scale of motions and allow interaction phenomena to be studied. Solid-state NMR allows a more direct approach to ligand–receptor interactions, normally with enhanced sensitivity, resolution and assignments, by specifically incorporating NMR isotopes (2H, 13C, 15N, 19F). Solid-state NMR can provide information on the orientational constraints of labeled groups in ligands and peptides caused by the spectral anisotropy of certain nuclei. Magic angle spinning (MAS) solid-state NMR methods have been applied to determine spin-coupled distances through dipolar coupling determinations, to high resolution (0.3Å) and chemical shifts to define the ligand-binding environment [98]. Jensen studied the effect of cisplatin on the phase behavior and conformation of lipid bilayers [93] and liposomes [94].

Fourier transform infrared spectroscopy (FT-IR) also provides organizational information on the lipid membrane but at a molecular level. The spectra are characterized by the wavelength of the maximum of the absorption signal and the width and intensity of the signal as a function of the direction of the polarized light beam. The analysis of the signals obtained

for the hydrophobic and hydrophilic regions of the phospholipids can give insight regarding intra- and intermolecular interactions. When amphiphilic drugs are added, local phase changes can be detected if the drug has interacted with the membrane, providing information regarding the phase changes [98]. Therefore, the orientation and degree of organization of substructures within the phospholipids can be assessed through this method, as well and the possibility of drug partitioning into the bilayer [98]. Therefore, FT-IR data can complement or even substitute the information that can be obtained through NMR [98]. FT-IR has been used, for example, to determine the effect of etoposide and cytarabide on the membrane structure of SUVs [83] and to study the changes in membrane structure and phase transition temperatures as well as the drug incorporation in lipid bilayers and MLVs suing CEUs [46, 91].

Circular Dichroidism also focuses on determining drug location and conformation on the membrane [98]. Li and Gallois used this technique to assess the partitioning of doxorubicin into LUVs [85, 95].

Lipid monolayer techniques are some of the most used techniques to study the effect of anticancer drugs on lipids of the membrane. Although the monolayer structure differs from the general structure of cell membranes (bilayer), it is thought that they provide an organized interfacial structure similar to that found in cell membranes. With this model, the tendency of drugs to accumulate in the interface of the membrane can be studied as well as its behavior there. Drug-monolayer interactions can be characterized by changes in the surface pressure, surface potential or binding [98]. Langmuir monolayers, which are basically monolayers constituted of only one molecule type, are often chosen due to the simplicity of preparation and control of the conditions, with main focus on surface pressure for example. Busto and colleagues were able to study the effect of edelfosine on Langmuir monolayers, namely the drug's capacity of penetrating the monolayer [44]. There is also the Langmuir-Blodgett (LB) monolayer, and its preparation involves the transfer of a Langmuir monolayer to a solid substrate in order to make highly ordered, ultra-thin, defectless films with controllable architecture, orientation and thickness [103]. Studies of these models were used to determine the adsorption of doxorubicin to the monolayer [89]. The monolayers are usually formed and analyzed in an apparatus called Langmuir-Blodgett trough, schematized in figure 7.

Another method used to determine surface potential is electrophoretic light scattering (ELS). The principle of ELS is fairly similar to that of dynamic light scattering or DLS – a laser beam directed at a sample will produce a frequency or phase shift that depends on the dispersed particles' mobility. While, in the case of DLS, Brownian movements are responsible for particle motion, in ELS that is caused by an oscillating electric field [102]. The ELS technique is mainly useful to determine the zeta potential of a particle. The zeta potential is the potential difference between the dispersion medium and the stationary layer of fluid attached to the dispersed particle [104].

It is a good indicator of the magnitude of repulsive electrostatic interactions between particles, and as such can provide insight on molecule adhesion, flotation and, in membranes for example, rigidity [104]. Park et al. used this technique to determine particle size, polydispersity index and zeta potential of nanoparticles loaded with doxorubicin [105].

It is evident that different techniques can give different data that overlap amongst them.

Determination of drug partition was for many years performed using the octanol-water partitioning method. However, it is being put aside due to its limitations compared to

partitioning into the membranes. In fact, the octanol-water partition coefficient has been proven to not always be the most accurate. Therefore, membranes are recently being used for this purpose and have demonstrated enormous discrepancy with the older method's values. It appears that the octanol-water partition coefficient alone is unable to account for variations in biological selectivity, which might be related to, besides hydrophobicity, hydrogen-bonding substituents.

Lipid vesicles are models that can replicate cellular conditions, since they present a curvature of the membrane like what is observed in cells, besides the possibility of being produced with components very similar to those existing in biological membranes. All of these extra parameters in regards to structure and composition, these models allow the study of other interactions besides hydrophobic, such as electrostatic interactions. Using lipid vesicles, the partition can be detected by simply coupling with spectroscopy, a method described above. Alternatively, HPLC could also be used depending on the constituents of the membranes. Appropriate columns, with, for instance, irreversively bound phosphatidylcholine are currently commercially available.

Circular Dichroidism and FT-IR, as well as cyclic voltametry are other techniques are currently used for the determination of the partition of the drug. [98].

A few studies also contemplate the relative affinity of anticancer drugs to the membrane comparing with other drugs, such as neomycin. Burger and colleagues used the two-dimensional thin-layer chromatography (2D TLC) to distinguish and separate the drugs regarding their affinity [96, 98].

1.3.2. Effect of anticancer drugs on biophysical parameters of model membranes

The previous topic showed that model membranes are being considerably used in several research areas nowadays. Actually, contrary of what could be believed, using lipid membranes as models to study the behavior of cell membranes while interacting with drugs is not a new concept and has been the goal of numerous studies for more than 20 years [87, 106-108]. However, since the membrane is such a complex structure, and there are many parameters involved in the study of its interactions with drugs, more information is still to be gathered. This field continues to be of high importance in the general overview of scientific and health-related research, as the understanding of the penetration and state changes in membranes as a result of its interaction with anticancer drugs could benefit the development of new and possibly more efficient drugs as well as provide higher amounts of base knowledge that could be used in other fields as well, like in nanotechnology [97].

Table 4 presents a summary of the main effects of different anticancer drugs on various model membranes as well as the techniques used to study them.

It has been previously stated that the membrane's lipid composition determines its characteristics as well as its behavior under different conditions. Consequently, it makes sense that the lipid composition of model membranes plays a similar role. Therefore, one of the most important aspects to have in mind in drug-membrane interaction studies is the lipids that constitute the model membrane.

The most used lipids in these studies, according to table IV, seem to be derivatives of phosphatidylcholine (PC), such as dipalmitoyl phosphocholine (DPPC), dioleoyl phosphocholine (DOPC), palmitoyl oleoyl phosphocholine (POPC) and egg PC (EPC).

Phosphatidylcholine is, as previously stated, one of the major components of naturally occurring biological membranes, so the use of PC derivatives in model membranes promotes a proximity in the natural and artificial membranes' characteristics, theoretically producing a model membrane that is more similar to a biological one, not only in structure but also in curvature and behavior when interacting with external substances, in the present case, anticancer drugs [50, 61]. Dimyristoyl phosphoglycerol (DMPG) and dipalmitoyl phosphocholine (DPPG) are also amongst the most used components of model membranes for similar reasons, being derivatives of an important and very simple phospholipid found in biological membranes, phosphatidylglycerol (PG) [50].

However, biological membranes naturally contain other molecules in lesser amounts that can also modulate its behavior. Important examples are sphingomyelin (SM) and cholesterol, which appear to have some importance in regulating the membrane's stability and signal transducing properties [50, 51], and therefore are also used in drug-membrane interaction studies, whether it is in combination with each other [45] or as a part of model membranes made of a variety of lipids [46, 80, 85, 88, 90, 95, 108, 109]. Also, comparisons between single lipid models and mixtures allow the determination of the effect of specific lipids in drug-membrane interactions [97].

Other lipids that also appear in cell membranes in lower quantities, such as phosphatidic acid (PA) and phosphatidylinositol (PI) and its derivatives (phosphatidylinositol-1-phosphate, PIP, and phosphatidylinositol-2-phosphate, PIP2), are also used in some studies [87, 93, 95, 108].

Table 4 Overview of the state of the art regarding drug-membrane interaction studies – the effects of anticancer drugs on lipid model membranes.

Anticancer Drug studied	Drug Concentration	Type of Model Membrane	Composition (proportion)	Technique	pH	Drug Effects (and location) on the membrane	Refs.
Squalene+Gemcitabine	7 mM	MLVs	DPPC	SAXS; WAXS	7.4	-Penetration into the membrane.	[77]
	SqGem/DPPC ratio = 0 to 0.45	Lipid Bilayers	DPPC	SAXS; WAXS	7.4	-Formation of a bicontinuous cubic phase (between gel and fluid phases); -Drug partitions between the lipid acyl chains of the bilayer.	[84]
	SqGem/DPPC ratio = 0 to 0.45	Lipid Bilayers	DPPC	DSC	7.4	-Higher lipid disorder – more fluidity.	[84]
	1.4 mM	Lipid Monolayers	DOPC; DOPC:DSPC(1:1);DOPC:DSPC:Chol(4.5:4.25:1.25)	BAM; Langmuir balance	7.4	-The drug penetrated in all the tested monolayers - smoother and faster for pure DOPC monolayer; slow for DOPC:DSPC due to closer packing of the lipids. -Presence of cholesterol improved drug adsorption to the membrane.	[109]
Edelfosine	0–20 μM	Lipid Monolayers	POPC	Langmuir balance; Fluorescence spectrometry	7.4	-Insertion into the monolayer at surface pressure above those supported by cell membranes; - Increased permeability of the monolayer.	[44]
	Mole fraction 0; 0.025; 0.05; 0.1; 0.2; 0.3 and 0.5	Lipid Monolayers	DPPC	Langmuir isotherms	7.4	-Drug and lipid are miscible in monolayers; -Weak interactions and only at low levels of surface pressure.	[86]
	Mole fractions 0.1, 0.3, 0.5, 0.7 and 0.9	Lipid Monolayers	SM:Chol (2:1; 1:1;1:2)	Langmuir isotherms	6.5	-Disorder of the lipid chains, more pronounced at lower proportions of cholesterol; -Increased permeability of the monolayer.	[45]

	Mole fractions 0.1, 0.3, 0.5, 0.7 and 0.9	Lipid Monolayers	SM:Chol (2:1; 1:1;1:2)	BAM	6.5	-Alterations in the liquid and gaseous phases; -Alteration of the monolayer's morphology, becoming inhomogeneous.	[45]
	18 μM; 37,5 μM; 75 μM; 250 μM.	LUVs	EPC	Fluorescence spectroscopy	7.4	-Increased permeability of the membrane.	[44]
CEUs	Lipid/CEU molar ratios 0.1 and 0.25	MLVs	DMPC; DOTAP; DOTAP:DMPC (1:1)	FT-IR	7.4	-No changes in fluidity of DMPC liposomes' membranes; higher fluidity of DOTAP liposomes' membranes at low drug concentrations; -Increased fluidity and permeability in DOTAP:DMPC monolayers.	[91]
	Lipid/CEU molar ratios 5:1, 20:1 and 50:1	Lipid Bilayers	DMPC; DMPC:Chol(7:3)	FT-IR	7.5	-Smaller and/or more branched R groups, sulfur atoms attached to the aromatic ring or low concentrations cause increase in fluidity; CEUs substituted in different positions lead to differences in fluidity; -Less disorder and fluidity in cholesterol-containing membranes.	[46]
	Lipid/CEU molar ratios 5:1, 20:1 and 50:1	Lipid Bilayers	DMPG	FT-IR	7.5	-Increased fluidity, but less than for DMPC membranes.	[46]
	Lipid/CEU molar ratios 5:1, 20:1 and 50:1	Lipid Bilayers	POPC:DMPC (1:1)	FT-IR	7.0	-Increased fluidity, similarly to that noted for DMPC bilayers.	[46]
Paclitaxel	23.4, 58.6 and 117 mM	MLVs and SUVs	DPPC; DPPC:Chol (9:1)	DSC	6.5	-Higher fluidity of the membrane; detection of a maximum solubility value of the drug; -Membrane containing cholesterol is more stable; -Drug located in the outer hydrophobic cooperative zone of the bilayer, i.e., region of carbon atoms C1–C8 in the acyl chain.	[80]

23.4 and 234 mM	MLVs and SUVs	DPPC; DPPC:Chol (9:1)	EPR	6.5	-Higher fluidity and penetration of the DPPC membrane; -For the DPPC:Chol membrane, fluidity increases with temperature increase until Tm; from Tm up the opposite happens; -Drug located in the outer hydrophobic cooperative zone of the bilayer, i.e., region of carbon atoms C1–C8 in the acyl chain.	[80]
11.7, 23.4, 58.6, 117 mM	SUVs	DPPC; DEPC; DPPE; DSPC	DSC		-Little change observed for the DSC profiles of the DPPE and DSPC liposomes; noticeable change in the thermographs of DPPC and DEPC liposomes; -Paclitaxel localized in the outer hydrophobic cooperative zone of the bilayer, i.e, in the region of atoms C1-C8 of the acyl chain or binding at the polar head group of the phospholipid.	[110, 111]
23.4, 58.6 and 117 mM [110-112]; 5, 10, 300 and 600 nM [90];	Lipid Monolayers	DPPC; DEPC; DPPE; DSPC	Langmuir balance		-Drug penetration occurs rapidly until a solubilization limit. -Drug located in the outer hydrophobic cooperative zone of the bilayer, i.e., region of carbon atoms C1–C8 in the acyl chain.	[90, 110-112]
5, 10, 300 and 600 nM	Lipid Monolayers	Cancerous cervical lipid extract	Langmuir balance		-Drug penetration occurs rapidly until a solubilization limit for lower initial surface pressure values; for the higher value tested, rapid penetration of the drug is detected but after the maximum penetration desorption of the drug starts to occur gradually.	[90]
5, 10, 300 and 600 nM	Lipid Monolayers	Normal cervical tissue lipid extract	Langmuir balance		-Very different results compared to DPPC and cancerous cervical lipid monolayers; -At lower initial surface pressure values, equilibrium is achieved rapidly; at the highest initial pressure, membrane destabilization occurs.	[90]

	5, 10, 300 and 600 nM	Lipid Monolayers	DPPC:SM(8:2; 5:5; 7:3)	Langmuir balance		-Paclitaxel penetration is inversely proportional to the concentration of SM.	[90]
Doxorubicin, Pirarubicin and Daunorubicin	1 μM	LUVs	PC:PA:Chol (75:5:20, 60:20:20 and 52:3:45)	Fluorescence measurements	6	-Permeability coefficient is the highest in LUVs which contain the lowest amount of cholesterol and PA; -Pirarubicin is more rapidly encapsulated than the rest; doxorubicin is the opposite.	[108]
Doxorubicin and Daunorubicin	5 x 10^{-4} M^{-1}, 100 μM and μM	LUVs	PC:PA:Chol(95:5:0,75:5:20,55:5:40, 80:20:0,75:20:5, 70:20:10,65:20:15,60:20:20,55:20:25, 50:20:30,45:20:35, and 40:20:40)	Circular Dichroidism	7	-Doxorubicin: at low concentrations of PA, interaction is mainly through electrostatic forces; increases in PA amount lead to hydrophobic interactions predominating. -Daunorubicin: moves directly from the aqueous phase to the embedded site within the polar head region; -For both drugs, cholesterol concentration seems to produce no significant change in drug penetration.	[95]
Idarubicin and Idarubicinol	5 x 10^{-4} M^{-1}, 100 μM and μM	LUVs	PC:PA:Chol(95:5:0,75:5:20,55:5:40, 80:20:0,75:20:5, 70:20:10,65:20:15,60:20:20,55:20:25, 50:20:30,45:20:35, and 40:20:40)	Circular Dichroidism	7	-Idarubicin: no or low PA causes embedding of idarubicin into the bilayer as a monomer; high concentrations of PA induce embedding with formation of a complex of 2 or 3 molecules of the drug with molecules of PA and cholesterol; -Idarubicinol: penetrating as a monomer; -For both drugs, cholesterol is an essential factor for the penetration process.	[95]
Doxorubicin	3.4 mM and 0.34 mM	LUVs	EPC:Chol (55:45)	Confocal Microscopy	7.5	-No observable membrane invaginations.	[85]
	3.4 mM and 0.34 mM	LUVs	EPC:Chol (55:45)	Circular	4	-Interaction drug-membrane is detectable regardless of drug	[85]

			Dichroidism	and 5	concentration; -Doxorubicin's complexed form seems to be the predominant form inside the liposomes.	
10^0 to 10^3 μM	Lipid Monolayers	PIP_2	Langmuir balance	7.4	-The drug penetrates into the monolayer; -Doxorubicin has similar affinity to this monolayer as neomycin.	[87]
5, 10, 25, 50, 100 and 200 μM	Lipid Monolayer	Pure lipids: PI; PIP; PIP2; DOPA; Cardiolipin; SAPA. Mixtures: 80% of DOPC+ 20% of each of the previous	Langmuir balance	7.4	-More penetration in the PIP and PIP2 monolayers especially with DOPC (mixtures).	[87]
10 μM	SUVs and Micelles	Pure lipids: PI; PIP; PIP2; DOPA; Cardiolipin; SAPA. Mixtures: 80% of DOPC+ 20% of each of the previous	Fluorescence spectroscopy	7.4	-More penetration in PIP and PIP2 membranes, especially those containing also DOPC (similar as seen in the previous study.	[87]
20 and 40 nM	Lipid Monolayers	DPPC:Chol:PEG-PE (100:0:0; 100:20:0; 100:0:4; 100:20:4)	Langmuir balance	7.4	-In pure DPPC monolayers, doxorubicin penetrates creating a less condensed state; presence of cholesterol increased the rigidity of the membrane; -Drug localized between the DPPC acyl chains.	[88]
40 nM	MLVs	DPPC:Chol:PEG-PE (100:0:0; 100:20:0;	DLS	7.4	-Higher fluidity in all liposomes; -Presence of cholesterol reduced the aforementioned effect;	[88]

			100:0:4; 100:20:4)			-Presence of PEG-PE lowers the penetration of the drug; -Drug localized between the DPPC acyl chains.	
	1×10^{-5} M	Lipid Monolayers	Octadecanethiol:octadecylamine (C18-SH:C18NH2) and octadecanethiol:dihexadecyl phosphate (C18-SH:DHP)	Langmuir balance		-Higher penetration for C_{18}-SH:DHP than for C_{18}-SH:$C_{18}NH_2$ monolayers.	[89]
	1×10^{-5} M	Langmuir-Blodgett monolayers (on gold surface)	C_{18}-SH:$C_{18}NH_2$ and C_{18}-SH:DHP	Cyclic Voltametry		-Time of drug adsorption/partitioning on/into mixed monolayers is relatively short (~= 1 min); much faster adsorption/partitioning of doxorubicin into two-component monolayers.	[89]
	1×10^{-5} M	Langmuir-Blodgett monolayers (on gold surface)	C_{18}-SH:$C_{18}NH_2$ and C_{18}-SH:DHP	SERRS, SPR and QCM		-Doxorubicin adsorbs at the monolayer surface but does not penetrate it; -Drug located at the surface of the biomimetic film; the sugar moiety of the drug is expected to be away from the metal.	[89]
Cisplatin	1 mM and 5 mM	MLVs	DOPS:DOPC (1:1)	2D TLC		-Molar excess of glutathione prevents cisplatin-PS complexation. This also happens in cells. -Drug located in the inner leaflet of the membrane, in the polar head region.	[96]
	10 and 30 mol%	Lipid Bilayers	PE 16.7%:PS 10.6%:PC 9.6%:PA 2.8%:PI 1.6% and total pig brain	NMR	7.4	-Increase in fluidity; -Drug binds to the carboxyl groups in the polar head.	[93]

			lipid extract 58.7%				
	10 and 30 mol%	Liposomes	POPS	NMR	7.4	-Cisplatin–POPS complex formation, possibly with cisplatin binding to one of the oxygen atoms of the POPS phosphate moiety.	[94]
	25 to 250 μM	LUVs	DPPC; DPPG; DOPE:DOPC (1:1)	Binding assays	6 and 7.4	-Interaction involved negatively charged phospholipids and only in buffers with low Cl^- concentration, indicating that aquated, positively charged cisplatin is involved. -Drugs binds to the polar heads of PS and PA.	[81]
	5 mM	MLVs	DPPC; DPPG; DOPE:DOPC (1:1)	DSC		-Less fluidity but a high amount of bounds; -Drugs binds to the polar heads of PS and PA.	[81]
Methotrexate	Drug-DMPC molar ratios of 0.01 to 0.09	MLVs	DMPC	DSC	7.4	-Methotrexate conjugates increase membrane fluidity in a concentration-dependant way.	[82]
Tamoxifen	1, 6, 9 and 15 mol%	MLVs	DMPC; DPPC	DSC	7.4	-Increased membrane fluidity; -Drug locates at the polar head region.	[79]
	1, 6, 9 and 15 mol%	MLVs	DMPC; DPPC; DPPG	FT-IR	7.4	-For DPPG, higher fluidity is observed at low concentration of the drug (1 mol%); -Drug locates at the polar head region.	[79]
	1, 6, 9 and 15 mol%	MLVs	DMPC	DSC and FT-IR	7.4	-Higher membrane fluidity with increase in drug concentration; -Drug partitions to the hydrophobic core of the bilayer.	[78]
Cytarabide	5×10^{-3} M	SUVs	DPPC	DSC, NMR and FT-IR	7.4	-Penetration into the bilayer observed; interactions with the choline group of DPPC;	[83]
Etoposide	5×10^{-3} M	SUVs	DPPC	DSC, NMR and FT-IR	7.4	-Cytarabide ring and etoposide ring insert into the bilayer at the same depth and therefore can compete to penetrate it.	[83]

From Table 4 we gather that the effects of different drugs vary even when the same model membrane is used. This is expected, since an assortment of very different drugs is currently being studied, with very different structures and conformations.

This review focuses on some of the most used anticancer drugs for chemotherapy, namely doxorubicin, daunorubicin, cisplatin, paclitaxel, metothrexate and tamoxifen, and on few new drugs that seem promising and as a result have been widely studied ever since its discovery, such as ALPs, especially edelfosine, CEUs and a hybrid of gemcitabine and squalene.

Even inside the same class of drug, for example, the anthracyclines, we find differences in the effects they exert on a model membrane. Doxorubicin and daunorubicin, for example, differ in terms of lipophilicity, and so they interact differently with the same membrane. In membranes with PC, PA and cholesterol, doxorubicin binds mostly through electrostatic forces, maintaining its dihydroxyanthraquinone moiety in the aqueous phase, while the more lipophilic daunorubicin requires mostly hydrophobic bonds, and as a result it partitions into different regions and through different processes [95]. More on this subject will be explained further ahead.

Gemcitabine is a prodrug that has been studied for membrane interactions after being coupled with squalene, a natural lipid precursor of cholesterol biosynthesis. The resulting conjugate spontaneously self-assembles in water to form nanoparticles with an inverse hexagonal phase [97] and is apparently much more effective than the drug on its own [113]. The gemcitabine-squalene hybrid seems to generally increase DPPC membranes' fluidity by causing disorder of the lipid acyl chains. It is able to penetrate both single lipid monolayers and bilayers [77, 84, 109], contrarily to gemcitabine that, at neutral pH, partitions between the aqueous medium and the lipid water interface, barely interacting with DPPC. The hybrid molecules insert between the lipid acyl chains while maintaining their polar head group anchored at the aqueous interface [97]. The gemcitabine-squalene bioconjugate induces the formation of an unusual inverse bicontinuous cubic phase over time, with a lipid order between those of the gel and fluid phases of DPPC, partly reminiscent of the "liquid ordered" phase Lo formed in saturated mixtures of PC or SM with cholesterol. When the temperature increased, a reversible transition to the fluid lamellar phase was observed. This influence has been correlated with the ability to alter the spontaneous curvature of the cell membrane leaflets, so this hybrid proves to be of relevance in the present context [84]. Edelfosine has been mainly studied using Langmuir monolayer techniques. It has been found that it also penetrates the monolayers, namely constituted of POPC and DPPC [44, 86]. This anticancer drug could increase the permeability of the membrane inserting in it also in LUVs made of EPC [44]. More complex models, such as lipid bilayers with different proportions of sphingomyelin and cholesterol, have provided not only information on the action of the drug over the membrane but also regarding the effect of cholesterol in the stabilization of the membrane when in contact with the drug. In fact, edelfosine was able to insert the bilayer, but this penetration was less effective in bilayers with higher amounts of cholesterol, which leads to believe that this molecules is able to stabilize the membrane and thus impair the penetration and general effects of edelfosine [45].

CEUs are a type of novel anticancer drug that are being exhaustively studied. There are a wide variety of these compounds and the difference in their properties resides in the composition and structure of their radical (R) group. Studies showed that 4-n-butyl CEU did not interact with DMPC liposomes, but that at low concentrations it did interact with DOTAP

liposomes or liposomes constituted of equal parts of DMPC and DOTAP, leading to believe that DOTAP could promote the insertion of 4-n-butyl CEU into the membrane [91]. 4-sec-butyl CEU however acts on both DMPC and DOTAP membranes leading to acyl chain disorder, although in different (but not quite defined) ways [91]. The effect of differences in R group was tested by applying CEUs with R groups of different lengths or branching on pure DMPC lipid bilayers and studied with FT-IR. CEUs composed of R groups with higher branching led to bigger decreases in Tm, which indicates that more branched CEUs fluidize the membrane better. The effect of the length of the R group was tested in a similar fashion and proved that smaller lengths lead to bigger decreases in Tm and therefore a more fluid membrane. The same effect was observed for CEUs possessing a sulfur atom bound to the aromatic ring. The effect of the position in which the CEU is substituted was also studied, and it was observed that the CEU substituted at the position four has a much higher influence in increasing the fluidity of the membrane and inserting in it than the one substituted at the position two [91].

The effects of 4-butyl CEU and 4-sec-butyl CEU were further tested with membranes constituted of DMPC with 30% of cholesterol. The presence of cholesterol markedly decreased the cooperativity of the lipid phase transition, but the effects on the lipid hydrocarbon chains were similar to those observed for DMPC systems in the absence of cholesterol [91].

Zhao and colleagues (2007) described the interactions of paclitaxel with MLVs and SUVs of DPPC in the absence and presence of cholesterol through DSC and EPR. They observed that the membrane became more flexible as a result of interaction with paclitaxel at a concentration up to 5%, which led to believe that there was a solubility limit for this drug in these membranes [80]. This concentration of the drug corresponded to the most stable mixed monolayers obtained, as inferred from the excess free energy of mixing [112]. The same models formed by DPPC and 10% of cholesterol produced similar results regarding the lipid disorder caused by paclitaxel and its insertion, but cholesterol seemed to stabilize the final membrane by strengthening the interactions between DPPC and paclitaxel, impairing further penetration of the drug [80]. Preetha et al. (2006), on the other hand, used lipid monolayers to study the effect of paclitaxel. Simple DPPC monolayers became more fluid after interacting with the drug, allowing it to rapidly penetrate the monolayer until a solubility limit was achieved. This is congruent with the findings of Zhao et al. (2007) [80, 114]. This data was then compared with the effect of paclitaxel on monolayers made of normal cervical lipid extract and of cancerous cervical lipid extract. Three initial surface pressures were used in the study – 10, 20 and 30mN/m. For monolayers constituted of cancerous cervical lipid extract, the first (and lower) two initial pressure values produced results no different than those found for DPPC monolayers. However, at the highest initial value, 30mN/m, after a maximum of solubilization of paclitaxel into the membrane, there appears to be desorption of the drug from the monolayer. The normal cervical lipid extract monolayers presented very different kinetics of drug penetration.

In this case, at 10 and 20mN/m, very rapid drug adsorption occurs and the equilibrium is achieved much faster than in the previous monolayer types. However, at 30mN/m the opposite occurs, the equilibrium being achieved after much more time than for the other monolayers, and beyond that point a progressive decrease in surface pressure is observed down to values even below zero, indicating membrane destabilization [114]. So, higher drug penetration was observed for DPPC monolayers compared to the other two. Comparing the two lipid extract monolayers, drug penetration was higher for the one formed by normal cervical lipids. This may be due to the different composition of the two lipid extracts.

Posterior quantification of these two lipid extract monolayers showed that cholesterol was 1.5 times higher in amount in cancerous than in normal cervical tissue. Sphingomyelin (SM), phosphatidylcholine (PC), phosphatidylethanolamine (PE), phosphatidylserine (PS), phosphatidylinositol (PI) and phosphatidylglycerol (PG) were also present in higher amounts in cancerous cervical tissue [114]. Cholesterol was found to reduce drug penetration when present in DPPC membranes [115]. Preetha and colleagues proved also that sphingomyelin prevented drug penetration. Consequently, it is possible to infer that the higher amount of both lipids in the cancerous cervical tissue and in the resulting extract creates a more rigid monolayer that impairs paclitaxel penetration, which would explain these results, and this is in agreement with a previous study by the same authors that actually showed that the cancerous cervical lipid extract monolayer was more rigid than the normal cervical lipid extract one [114, 116].

Doxorubicin is perhaps the anticancer drug studied using the widest variety of model membranes, but in all studies it was shown that interaction with the membranes occurred and that doxorubicin could actually penetrate lipid membranes, even using very different lipids in each study [85, 87-89]. Interestingly, once again, membranes formed of more than one component appear to produce more relevant results. SUVs and micelles studied by De Wolf and colleagues allowed the penetration of doxorubicin in membranes of PIP and PIP2 and even more if these contained also DOPC, being the latter more physiologically relevant [87]. Similarly to what is observed for paclitaxel, the presence of cholesterol in DPPC:PEG-PE monolayers and MLVs decreases the drug penetration into the membrane; PEG-PE appears to have a similar effect, which might be related to its binding partly to the hydrophobic region and partly to the polar heads of the lipid membrane [89].

The studies by Speelmans (1994), Frézard and Gallois (1998) focused in comparing the effects of various anthracyclines derivatives on the membrane of LUVs encapsulating DNA, and therefore being one step closer to cells [95, 108, 117].

The permeation of the membranes by anthracyclines occurred in three steps: partition within the interfacial region of the bilayer, followed by diffusion through the hydrophobic core and lastly desorption from the interface on the opposite side. At physiological pH, these molecules could partition within the interfacial regions through electrostatic and hydrophobic interactions and then cross the hydrophobic core in their unprotonated form [97]. Studies performed at pH 5 showed that the protonated form was unable to cross membranes [108].

Fluorescence studies were used to compare the effect of doxorubicin, pirarubicin and daunorubicin on membranes of phosphatidylcholine (PC), phosphatidic acid (PA) and cholesterol at various molar ratios. It was shown that although all three penetrate into the membrane, the permeability is decreased as the amount of PA and/or cholesterol is elevated [95]. This is confirmed by other studies such as the one by Gallois and colleagues, which compared the effects of doxorubicin and daunorubicin with LUVs of similar constitutions and observed that at low molar ratios of drug/liposomes, both drugs interacted with the membrane as monomers. Doxorubicin displayed two types of interactions: electrostatic, in which the dihydroxyanthraquinone ring remained outside the bilayer, in the aqueous phase, and hydrophobic, in which the dihydroxyanthraquinone ring intercalated with the lipid acyl chains inside the bilayer. The proportions of these interactions depended on the composition of the membrane, which means that at low molar ratios between PA and doxorubicin, it binds to the membrane mainly through electrostatic interactions, remaining at the interface. When

this ratio increases, however, a hydrophobic interaction begins to prevail. Daunorubicin, being more lipophilic, displayed only hydrophobic interactions [95].

In general, the rate of uptake was the lowest for doxorubicin and the highest for pirarubicin, since it was the most hydrophobic and showed the highest pKa (highest neutral/protonated form ratio) [108]. The permeability coefficients were the highest for the lowest amounts of PA and/or cholesterol in the membrane [108], although cholesterol didn't seem to exert as much as an important effect in this case as it does when the more lipophilic drugs idarubicin and idarubicinol are studied [95].

It is interesting to notice that a very limited number of model membrane types is chosen for the displayed studies. These types of model membranes were described previously. The specific choice of these, however, resides in a set of properties they possess and/or share with cells and that can therefore give credibility to the results. Lipid monolayers are used not only for their simplicity and ease of production, but mostly for the possibility of controlling all of the conditions surrounding them. Monolayers might not produce results that can be directly linked to cell membranes, but monolayer techniques provide a wide basic knowledge on the behavior and interactions of a desired lipid or set of lipids with desired drugs [97]. Micelles achieve similar results, although they are perhaps a slightly more accurate model due to lipid curvature. Liposomes, however, seem to be the most used models. This may be because they combine two of the main characteristics they share with cell membranes: a bilayered structure of phospholipids and a curvature that allows it to become a closed vesicle. Being so, they are most likely the models that are closest to the cell structure, and can therefore provide more biologically accurate data. MLVs and LUVs are the most frequently used. MLVs are the easiest to obtain and are constituted of a number of membranes that can be analyzed. LUVs are of especial importance, though, since the degree of curvature of their lipid membranes is the most similar to that of actual cell membranes [97].

Chapter 2

Aim

The previous chapter described the state of the art in this field and as a result 3 main factors become evident: drug-membrane interaction studies are essential to the advance of pharmacology and medical science in general, but biophysical studies such as these are not as common as they should be; cells are complex, time-consuming and expensive models for this kind of study; membrane models such as liposomes can be a good alternative. As a result, there are two needs that arise - further investigation on drug-membrane interactions and the development of better models to perform them in.

In this context, this work was designed to tackle both of these needs. The objective was to develop an innovative set of liposome formulations that can mimic the membranes of normal and tumoral cells and be henceforth used in biophysical studies to determine the way the anticancer drugs interact with biomembranes.

For that purpose, two anticancer drugs were chosen for the study, daunorubicin and doxorubicin, since they are currently among the most used and the most effective and also due to the fact that they present similar structures except for one functional group, which leads to their use in different types of cancer. Four liposome models were designed, two to mimic the normal membranes (one with and one without cholesterol in its composition) and two to simulate a tumoral cell membrane (also one with and one without cholesterol).

The effect of the two drugs in size, zeta potential, partition coefficient, membrane location and membrane fluidity were assessed for the four formulations and for a tumoral cell line. These biophysical studies may help to get a higher knowledge about complementary mechanisms of action at the lipid membrane level of these two anticancer drugs using simple but reliable membrane models. It is important to stress that the simplification of the membranes and therefore a complete control of such complex structures is critical to understand the interactions at the molecular level. Nevertheless, some of the interaction studies performed in the model membranes were also performed in tumor cell lines (MDA-MB-231), to assess the degree of similarity regarding biophysical parameters and regardless the simplicity of the models. These studies in cells are a novelty and their development and standardization can be a big step ahead in membrane biophysics studies.

Chapter 3

Materials and Methods

The current chapter describes all the methodologies employed in this work for the study of anticancer drug-membrane interactions. The theoretical foundation behind each technique will be exploited as well as their practical application in the case of this study. The results obtained are shown and discussed in the next chapter.

3.1- Drug Choice

Daunorubicin and doxorubicin were chosen for the aforementioned studies. These are, as has been established in the introduction, two of the most frequently used chemotherapeutic drugs, being highly effective in a wide range of tumors [47]. It seems, therefore, like a good starting point to study drugs with a wide range of therapeutic and toxic effects as it can provide information that can be narrowed down to more specific inferences in future research. These two anthracyclines are very similar in structure except for one group, as is represented in figure 8.

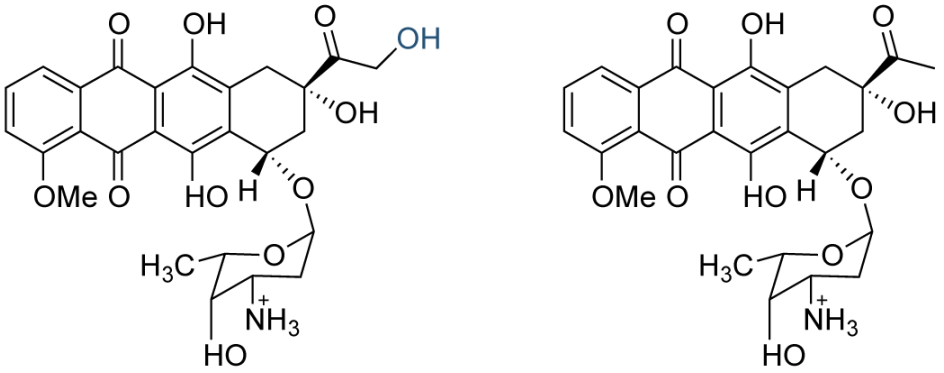

Figure 8 Chemical structures of doxorubicin, Dox (left) and daunorubicin, Dan (right). These two anthracyclines present almost identical structures except for an extra alcohol group in doxorubicin, in the figure represented in blue (Image from [118]).

It is evident that the structures of the two drugs vary only in a single functional alcohol group that is present in doxorubicin but not in daunorubicin. However, while daunorubicin is

almost only used to treat acute leukemia, doxorubicin has a very wide range of application, being used in the treatment of non-Hodgkin's and Hodgkin's lymphoma, multiple myelomas, as well as lung, ovarian, gastric, thyroid, breast and pediatric cancers [119]. Also, although both drugs cause the same kind of side-effects (see Table 2), being the most concerning by far cardiotoxicity, it appears that these side effects are usually more severe when doxorubicin is used, and as such this drug could be considered more aggressive [120]. In fact, several cases of cardiomyopathy have been correlated with cumulative exposure to doxorubicin [120, 121].

So, these two drugs, although sharing the same mechanism of action and side effects, peak in antitumoral activity efficacy in different types of tumors and cause side effects with different levels of severity. In this context, it was thought that studying these two drugs and their interaction with the membrane specifically could be a way to justify these differences.

3.2- Reagents

DMPC (1,2-dimyristoyl-sn-glycero-3-phosphocholine), DOPC (1,2-dioleoyl-sn-glycero-3-phosphocholine), DPPS (1,2-dipalmitoyl-sn-glycero-3-phospho-L-serine) and cholesterol were purchased from Avanti Polar Lipids Inc. (Alabaster, AL, USA), and daunorubicin and doxorubicin were obtained from Biovision Inc. (Milpitas, CA, USA) and used without further purification. DPH (l,6-diphenyl-l,3,5-hexatriene) and TMA-DPH (1-(4-trimethylammoniumphenyl)-6-phenyl-1,3,5-hexatriene p-toluenesulfonate) were obtained from Molecular Probes (Invitrogen Corporation, Carlsbad, CA, USA). Methanol, chloroform, DMSO (Dimethyl Sulfoxide), Hepes Hemisodium Salt, Trizma Maleate and NaCL (Sodium Chloride) were purchased from Sigma-Aldrich Chemical Co. (St. Louis, MO, USA). The cell medium RPMI 1640 with UltraGlutamine I and Hepes, trypsin-EDTA (ethylenediamine tetraacetic acid), PBS (phosphate-buffered saline), FBS (fetal bovine serum) and Trypan Blue were purchased from Gibco by Life Technologies (Invitrogen Corporation, Carlsbad, CA, USA).

Drug solutions were prepared either with Hepes buffer (10 mM, pH 7.4) or Tris buffer (0.1 M, pH 6.3). The ionic strength of Hepes buffer was adjusted to physiological conditions with NaCl (I = 0.1 M). The buffers were prepared using double-deionised water (conductivity inferior to 0.1 μScm^{-1}).

The medium used on the culture of MDA-MB-231 cells was RPMI 1640 with UltraGlutamine I and Hepes to which 5% of FBS was added.

3.3- Liposome Models and Preparation

3.3.1. Liposome Models

Since our aim was to study the effects of the two anticancer drugs on both normal and tumoral membranes, membrane models for both cases were designed. For each case, another model was designed without any cholesterol content in order to help determine the influence of this molecule on the membrane itself and on the interaction studies. The prepared models and respective properties are shown in Table 5.

The normal membrane models were mainly composed of DMPC since PC is the biggest constituent of membranes. The model containing cholesterol was prepared with 25% of this lipid. The tumoral formulations were prepared using a mixture of DMPC (as main constituent), DPPS, to represent the exposed PS on the outer leaflet of the membranes of tumoral cells, and DOPC, which is an unsaturated phospholipid that is included to mimic the increase in fluidity observed for tumoral membranes [57, 60]. The lipid stechiometry used is also represented in table 5 and was decided taking into account what is found in the literature regarding the differential lipid content of cell membranes [50, 52-60].

Table 5 Membrane mimetic models designed for the present study, along with their composition and pH conditions.

Model	Lipid Composition (Molar Proportions)	pH (Buffer)
Normal	DMPC	7.4 (Hepes)
Normal with Cholesterol	DMPC:Chol (3:1)	
Tumoral	DMPC:DOPC:DPPS (3:1:1)	6.3 (Tris)
Tumoral with cholesterol	DMPC:DOPC:DPPS:Chol (3:1:1:1)	

The formulations were designed to be made up of LUVs 100 nanometers in diameter since these mimic the natural cell membrane's curvature the best [75, 76].

3.3.2. Preparation

Multilamellar vesicles (MLVs) were prepared by the classical method of the lipid film hydration [122]. The lipid solution, prepared using chloroform/methanol (3:2) as solvent, was evaporated to dryness with a nitrogen stream at 60ºC in a rotative evaporator. For the DPH and TMA-DPH labelled liposomes used in the fluorescence measurements, probe stock solutions were prepared using the organic solvents used for the lipids [chloroform/methanol (3:2)]. A specific volume of this solution was then added to the lipid in chloroform/methanol (3:1) at a lipid:probe molar ratio of 300:1, which is the ideal ratio for good signal detection without altering the membranes' properties [100]. The mixture containing lipid and probe was then dried together. The resultant dried lipid film was dispersed with convenient buffer, either Hepes buffer or Tris buffer, and the mixture was vortexed to create MLVs. In order to obtain 100 nanometer unilamellar liposomes (LUVs), the mixture was extruded 10 times through polycarbonate filters with a pore diameter of 100 nm [123], at 60 °C (a temperature above the phase transition temperature of the lipids).

3.4- Cell Culture

3.4.1. Cell Type

The cells used for the membrane location studies were the MDA-MB-231 cell line. These are from mammary gland adenocarcinoma and were chosen because breast cancer is one of the most frequent types of cancer to arise specially in women above 45 years of age, and still

has a very high mortality rate [6]. As such, the decision was made to use this cell type as the first one tested to validate the tumoral liposome models described above.

3.4.2. Culturing Conditions

MDA-MB-231 cells were cultured in 75 cm^2 flasks at 37 ºC in an atmosphere with 5% CO^2 (Unitherm CO^2 Incubator 3503 Uniequip; Planegg, Germany) in RPMI 1640 U1 with Hepes medium supplemented with 5% of FBS. Every three days, when cells were at approximately 80% confluence, the old cell medium was removed, the cells were washed with PBS and detached from the surface using trypsin-EDTA, being the resulting cell suspension adequately dilluted onto a new flask with fresh medium.

For the location assays, cells at 80-90% confluence were detached in the same way, but after ressuspension with medium they were centrifuged at 1500 rpm for 5 minutes so as to precipitate the biomass only. The supernatant medium was then removed and the cells were ressuspended in 3 mL of the same buffer used for tumoral liposome models, Tris buffer (pH 6.3). Cells were labelled with DPH at a concentration of 1 mM or with TMA-DPH at 10.3 μM by incubation in the dark in ice for 1 hour. These concentrations of fluorophore were used since this protocol is still under optimization and these were the concentrations tested that allowed the acquisition of detectable signal.

3.4.3. Cell Counting and Viability Assessment

Cell counting was performed for each replica through the Trypan Blue Exclusion assay in order to make possible the determination of the volume of cell suspension to add to the samples so that their cell concentration was 1.6 x 10^5 cells/mL.

Figure 9 Picture and representation of a Neubauer chamber. The cells on the chamber quadrants represented with "C" are counted.

In order to count the cells, a mixture of cell suspension and 0.4% Trypan Blue solution in PBS at a 1:1 proportion would be prepared and loaded onto a hematocytometer (Neubauer chamber) represented in figure 9 [124].

The cells in the areas marked with a "C" in figure 9 are counted, and the cell concentration in the suspension is therefore calculated by the following equation:

$$[\text{Cells}] = \frac{n \times 10^4 \times F_d}{4} \qquad \textbf{Equation 1}$$

where n represents the number of cells counted in the four areas marked as "C", 10^4 is the volume of those areas and F_d is the dilution factor, which in this case is 2.

Cells were counted in the beginning of any methodology and after incubation with the fluorescent probes to ensure that the probes were not toxic to the cells and that the methodologies could proceed. Since the studied drugs are cytotoxic, cells were also counted

after the execution of the techniques for a number of samples to ensure that the techniques were executed with enough live cells to produce viable results.

3.5- Size and Zeta Potential Determination

Before starting an actual biophysical study of drug-membrane interaction, the characterization of the model membranes that were prepared for this study is important to ensure that the preparation methods described in topic 3.3.2 were able to generate liposomes with the intended characteristics and as such ready to be applied to the biophysical methods ahead [125, 126].

The size and membrane surface charge of liposomes, the latter analysed through the determination of the zeta potential, were assessed through Dynamic Light Scattering (DLS) and Electrophoretic light Scattering (ELS), respectively.

Light Scattering involves the incidence of a polarized laser beam on a sample and its scattering towards a detector placed at a 90º angle from the incident beam. Disperse particles suspended in a liquid medium undergo Brownian motions, which means that they are continuously moving, vibrating, translating and rotating. This causes the laser to be scattered at different intensities [125]. The scattered intensities fluctuate with time and provide information on the translational diffusion coefficient (D_t) of the particles. In a DLS apparatus, the signal obtained is processed by a correlator, and the fluctuations are interpreted by autocorrelation. It is through specific correlation of intensity fluctuations caused by the Brownian motions of the molecules in the sample along a period of time and with the aid of electrodynamics and theory of time dependent statistical mechanics that it is possible to obtain information regarding the structure and molecular dynamics of the particles in the medium [125, 126].

This method is one of the most used to determine the size of a particle in suspension as well as the range of particle sizes in said suspension. It is also useful for the determination of the surface charge via zeta potential, which is a measure of the electrical potential of the double layer at the interface between the dispersed medium and the stationary fluid adhered to the dispersed particle, and thus it gives us the information of the membrane surface behaviour in terms of charge [127, 128].

Ultimately, this technique was used to confirm if the prepared liposomes were approximately 100 nanometers in diameter, and if the surface charge was close to neutral in the normal models and negative in the tumoral models. For that purpose, samples for each model at a lipid concentration of 500 μM in the respective buffer were used. To determine if the chosen drugs had effect on liposome size and charge, samples with liposomes from each model at a lipid concentration of 500 μM were prepared with increasing concentrations of each drug, namely 5, 40 and 75 μM, and analysed through DLS (ZetaPALS BrookHaven Corporation Instruments; Software: PALS Zeta Potential Analyser v.5, Brookhaven Instruments; Holtsville, NY, USA). The assays were performed three times independently.

3.6- Biophysical modifications of the membrane

The membrane structure is very important not only because of membrane permeability and interaction with exogenous molecules but also due to the action of endogenous molecules attached to the membrane (proteins, receptors, channels) and the molecular mechanisms involved in pharmacological effects exhibited by a variety of drugs [92, 93, 156]. Experimental work on membrane mimetic systems has demonstrated that their structural properties are strongly affected by membrane associated molecules. Many drugs are able to directly or indirectly influence cell membrane properties. For instance, interactions between proteins and phospholipids or the formation of complexes between ligand molecules and phospholipids or sterols can lead to disruption of the membrane so that it becomes highly permeable [129]. Some compounds can actually affect the fluidity of membranes, and some examples can be found in Chapter 1, Table 4 [46, 78-82, 84, 88, 91, 93, 94]. Additionally, changes in membrane fluidity can affect receptor and enzyme activity and influence the ability of drugs to pass through the membrane, which in turn can affect their efficacy.

The importance of studying the action of anticancer drugs in the biophysical properties of the membrane is not limited to the understanding of their therapeutic effects but also to the elucidation of their side effects. A single biophysical method is not sufficient for a detailed analysis of the complexity of membrane dynamics and thermodynamics in the absence and presence of drug molecules.

In this context, the next topics present several techniques that when combined provide a detailed description of the membrane biophysical changes resultant from the actions of drugs.

3.6.1. Membrane partitioning

The first step for the study of the interaction of drugs with membrane models should be the determination of the partition coefficient, which characterizes the extent of the interaction of a drug with a micro-heterogeneous system in a quantitative manner. Every bioactive compound needs an adequate balance between liposolubility (solubility in membranes) and hydrosolubility (solubility in blood and cytosol) and this balance is often expressed by the partition coefficient. The partition coefficient is therefore a key aspect for understanding the pharmacokinetics and pharmacodynamics of drugs, since it is associated with their passive permeation into or across membranes to access their sites of action [130], which in turn has implications in their therapeutic effects [129]. Additionally, the partition coefficient can be useful to predict toxic effects that arise from the bioaccumulation of drugs in tissues [130].

The partition coefficient (*P*) is defined by the ratio at equilibrium of the drug concentration in the organic phase and the concentration of the same drug in the aqueous phase [129]:

$$P = \frac{[Drug]_{organic}}{[Drug]_{water}} \qquad \textbf{Equation 2}$$

The partition coefficient in the octanol/water system ($K_{O/w}$) is the most commonly used parameter for determining the lipophilicity of a compound [131-133]. This biphasic mixture is widely used as a standard system mainly because it was the first system to be developed for the determination of the partition coefficient. Despite its successful application in drug

design, the octanol/water system may be an oversimplification and has been often seen as inadequate since an isotropic medium bears little similarities to biomembranes [129, 133], especially if we take into account that the organic phase in this system, octanol, lacks the amphiphilic nature of phospholipids, which have hydrophilic head groups and hydrophobic acyl chains [131-134]. Consequently, the $K_{o/w}$ does not take into account the electrostatic interactions of compounds with the organic phase and provides information only on the hydrophobic interactions with the aqueous phase. The fact that more than 60% of the marketed drugs are ionisable (which includes the ones in this study, daunorubicin and doxorubicin [95]) makes the use of $K_{o/w}$ somewhat unreliable [135]. Finally, the relative toxic nature of octanol also dictates the need to use less pollutant alternative systems for partition coefficient determination [131].

Liposomes and micelles can advantageously replace octanol/water systems due to their anisotropic nature and their lipid ordered structure similar to that of natural membranes, and also by the possibility of studying the influence of electrostatic interactions in the partition phenomenon. Thus, the determination of the partition coefficient in liposomes or micelles/ water systems (K_p) gives more reliable data regarding the drug-membrane interactions, being these lipid model systems able to mimic the diverse membrane environments, from the polar surface to the lipophilic core.

Some K_p determination methods in membrane model/aqueous systems involve phase separation while others don't. Since phase separation is laborious and may cause equilibrium perturbation, the method selected to evaluate the lipophilicity of the anticancer drugs studied in the course of this work doesn't involve phase separation. The quantification analysis was performed by derivative spectroscopy that will be further described in the next subchapter.

i. Derivative spectroscopy

For most of the cases, the partition coefficient of a molecule between a lipid and an aqueous phase can be evaluated by UV-Vis spectrophotometry as long as there is a difference in an absorbance parameter of the partitioning molecule (e.g., molar absorptivity, ε, and/ or wavelength of maximum absorbance, λ_{max}) when in aqueous solution and after incorporation into the membrane [131-133, 136]. Therefore, it is possible to calculate K_p of a drug as long as its incorporation in the membrane leads to a change in the λ_{max} in the order of 5-10 nm, and/ or a change in the ε between the two solvents (≥ 10%). The difference in the wavelength of maximum absorption in the presence of liposomes in relation to absorption maximum in buffer solution can also provide information about the distribution of the drug between the aqueous and lipid phase. Indeed, batochromic deviations (λ_{max} deviations for higher wavelengths) are indicative of decrease of polarity in the drug's surroundings and indicates an incorporation of the investigated compounds into the hydrophobic part of the lipid bilayer [137]) whereas hypsochromic deviations (λ_{max} deviations for lower wavelengths) are indicative of the presence of the drug in a more polar microenvironment [137]). The use of UV-Vis spectrophotometry has plenty advantages, not only because most compounds have easily measurable spectroscopic properties, which depend on the chemical nature of the medium and are proportional to the concentration of compound at each stage, but also because the sensitivity of this technique allows the use of concentrations similar to those found in natural systems [138].

Given the definition of the partition coefficient and the conditions under which the law of Lambert-Beer is applied, the absorbance of a solution containing a certain concentration of drug (*Abs*), that is distributed between the lipid (*l*) and aqueous (*w*) phase, can be related with K_p according to Equation 3 [136, 139]:

$$Abs_T = Abs_w + \frac{(Abs_l - Abs_w)K_p[L]V_\varphi}{1+K_p[L]V_\varphi} \qquad \textbf{Equation 3}$$

where Abs_T, Abs_w and Abs_l correspond to the total, aqueous and lipid absorbance of the compound, respectively, K_p is the partition coefficient (dimensionless), [*L*] the lipid concentration ($molL^{-1}$) and V_φ the lipid molar volume ($Lmol^{-1}$).

Despite the apparent simplicity of Equation 3, its application is limited to systems with low scattering of light, such as micellar/aqueous systems. However, especially in cases where liposomes are used as membrane models, the presence of microstructures of heterogeneous sizes causes light scattering [132, 136, 140, 141], particularly at wavelengths below 300 nm, which results in a decrease of the light that reaches the detector. The spectroscopic interference of light scattering and the absorbance produced by the microstructures will turn the analysis of changes in the absorbance of the drug upon partition into a difficult task. To eliminate the background signal intensity caused by the vesicles, the absorption spectra of vesicle suspensions (references) with the same lipid concentration as the samples are measured and these spectra are subtracted to the correspondent sample spectra. However, even if the suspensions in the samples and references are prepared to contain the same amount of lipid vesicles, the counterbalance of the sample and reference beams is always incomplete being usually difficult to cancel completely the effects of the strong background signals, to obtain a flat and zero-level base line. The problem of the background interference of the medium due to light scattering of the vesicles is only eliminated by the use of derivative spectrophotometry (in order to wavelength, λ). In this context, the derivative spectrophotometry for the calculation of K_p is advantageous because it allows the elimination of interference caused by organized systems (difficult to cancel in zero-order spectrophotometry), without the need to employ techniques of phase separation. Furthermore, the derivative analysis of the spectra leads to a better resolution of overlapping bands [136, 140, 142].

The calculation of K_p by derivative spectrophotometry is based on an equation similar to Equation 3 [136, 143]:

$$D = D_w + \frac{(D_l - D_w)K_p[L]V_\varphi}{1+K_p[L]V_\varphi} \qquad \textbf{Equation 4}$$

where

$$D = \frac{\partial^n Abs}{\partial \lambda^n} \qquad \textbf{Equation 5}$$

The partition coefficients are then calculated by fitting Equation 4 to experimental derivative spectrophotometric data (*D* vs. [*L*]) through a nonlinear regression method where the adjustable parameters are D_l and K_p.

Even with the aforementioned advantages of derivative spectroscopy, the overall analysis of spectra required for K_p determination is a time consuming process that involves many steps. Therefore, a friendly-use application for *Microsoft Excel*® created by Doctor Cláudia

Nunes, the *K_p Calculator*, was used during the course of this study to completely overcome this drawback.

To assess the K_p values of all liposome models described, samples containing a fixed drug concentration of 40 μM and increasing concentrations of lipid (100, 200, 300, 400, 500, 600, 700, 800, 900 and 1000 μM) were prepared.

The therapeutic drug concentration of daunorubicin is 25.5 μM [144] and of doxorubicin about 29.4 μM [145]. In this study, most conditions were maintained as close as therapeutic conditions as possible. However, in the case of the drug concentrations used in research, concentrations often have to be adapted to the equipment's sensitivity, and the drug concentration was chosen to be 40 μM since it has been proven to be an ideal concentration that allows good detection in previous published [146, 147] and unpublished work [148] using other drugs, and also produced the same good results when different concentrations were tested using daunorubicin and doxorubicin by MSC Catarina Alves and the author of this work. Identical samples without any drug content were also prepared to serve as references and allow the removal of some of the noise caused by micro scattering associated with the liposomes. Samples containing only drug at 40 μM were also prepared. All of the samples were incubated for 30 minutes at 37ºC. After that time their absorption spectra were recorded at physiological temperature (37ºC) in 96-well plates in a UV-Vis spectrophotometer (BioTek Synergy HT, Software: Gen 5, BioTek Instruments, Inc., Winooski, VT, USA). After measurements, each reference spectrum (background) was subtracted from the correspondent sample spectrum to obtain corrected absorption spectra. Derivative spectra were calculated using the Savitzky–Golay method [149] in which a second-order polynomial convolution of 13 points was employed. This was performed according to the Nature protocol by Magalhães et al. [150]. Three independent assays were performed.

3.6.2. Membrane location

For compounds whose target sites are membranes or that interact at the membrane level, the orientation and location in the membrane are relevant parameters describing their effects. The study of membrane location thus allows a deeper understanding of the mode of action of drugs, contributing to the development of new types of drugs, more potent, more selective and with fewer side effects.

In the case of this study, indirect methods of determining the membrane location of a compound will be used. These require the presence of a foreign compound that is normally a fluorescent probe included in the membrane. This probe works as a reporter and if any changes are observed on the fluorescence of this probe, those changes can be then related to the location of the drug. For example, if the molecular location of a probe within membranes is known with certainty, the deactivation of the probe's fluorescence (also known as fluorescence quenching) induced by a drug can be used to reveal the location of the drug in the membrane [131, 143, 151, 152].

i. Steady-state fluorescence quenching

In this study, the membrane location of drugs was assessed by fluorescence quenching of membrane bound extrinsic fluorophores (fluorescent probes). These fluorophores, usually

amphiphilic molecules, whose membrane location is known and well characterized, emit constant fluorescence in situations where there is no interference with their environment. However, when a drug partitions into the membrane, it can have a location close to the fluorophore and induce a decrease in its emitted fluorescence.

Consequently, the decrease in the emitted fluorescence, also known as fluorescence quenching, of a membrane bound fluorophore provides a measure of its accessibility to the drug (quencher) and can be related with the concentration of the quencher [*Q*] by the Stern-Volmer equation (Equation 6) [100]:

$$\frac{I_0}{I} - 1 = K_{SV}[Q] \qquad \textbf{Equation 6}$$

where I_0 and I are, respectively, the corrected fluorescence intensity of fluorophores in the absence and presence of drug and K_{SV} is the Stern-Volmer constant.

Plotting the values of corrected fluorescence intensities (I_0/I-1) as a function of drug concentration ([*Q*]) a linear relationship is obtained, where the slope is the Stern-Volmer constant (K_{SV}).

The corrected fluorescence intensities used on Equation 6 were the result of a previous correction of the fluorescence values to eliminate the inner filter effect. The inner filter effect occurs when the drug absorbs at the wavelength of excitation of the fluorophore and decreases the effective intensity of the exciting light beam decreasing the measured fluorescence intensity. Since the absorption increases with the increase of the quencher concentration, this induces an apparent quenching and increases the values of the Stern-Volmer quenching constants obtained from steady-state experiments. Therefore, fluorescence intensities should be corrected to eliminate this apparent quenching by Equation 7 [153]:

$$I_{corr} = I \frac{A_Q}{A_F} \frac{1-10^{-A_F}}{1-10^{-A_Q}} \qquad \textbf{Equation 7}$$

where I_{corr} is the corrected fluorescence intensity, I the experimental fluorescence and A_Q and A_F are the absorbance of the sample in the absence and presence of the quencher, respectively.

ii. Fluorescence Quenching Mechanism

There are two kinds of mechanisms responsible for fluorescence quenching [100, 154]:

a) Static quenching: in static quenching a non-fluorescent complex is formed between the fluorophore and the quencher. When this complex absorbs light it immediately returns to the ground state without emission of any photon;

b) Dynamic or collisional quenching: in the case of collisional quenching, the quencher must diffuse to the fluorophore during the lifetime of the excited state. Upon contact, the fluorophore returns to the ground state, with emission of a photon. In general, quenching occurs without any permanent change in the molecules, that is, without chemical reaction.

Static and dynamic quenching can be distinguished by their differing dependence on temperature, viscosity and lifetime measurements [100]. The most effective way to distinguish the type of quenching is by lifetime measurements, and if the quenching process has a dynamic nature it will occur an equivalent decrease in fluorescence intensity and lifetime [100, 154]:

$$\frac{I_0}{I} = \frac{\tau_0}{\tau}$$ **Equation 8**

where I_0, τ_0 and I, τ are respectively, the corrected fluorescence intensity and lifetime of the fluorophore in the absence and presence of the quencher. The decrease in lifetime occurs because quenching is an additional rate process that depopulates the excited state. Thus, in cases of collisional quenching the graphical representation of the values of fluorescence intensity (I_0/I-1) or lifetime (τ_0/τ-1) as a function of the concentration of the drug ([Q]) originates a linear fit in which the slope corresponds to the Stern-Volmer constant (K_{SV}) that in this case is also called dynamic constant (K_D).

In the case of the static quenching, occurs the formation of a non-fluorescent complex between the fluorophore and the drug and thus the residual detectable fluorescence corresponds to the fraction of non complexed fluorophores. The fraction of fluorophore molecules that are not complexed by the drug remains undisturbed, and consequently the lifetime of the excited state remains also constant [100]:

$$\frac{\tau_0}{\tau} = 1$$ **Equation 9**

iii. Deviations from the linear Stern-Volmer plots

When the Stern-Volmer plot (I_0/I -1 as a function of [Q]) is linear this indicates that only one type of quenching occurs. However, deviations from the linearity may also occur [100, 154].

The negative deviations correspond to non-linear Stern-Volmer plots with a downward curvature towards the x-axis and may indicate the presence of fractions of fluorophore with different accessibility to the quencher, i.e., fractions that are not exposed together with fractions that are more accessible [100]. This negative deviation of Stern-Volmer plots is especially common in proteins. Indeed, proteins usually contain several tryptophan residues that work as fluorophores and are positioned in distinct environments. Each residue can be differently accessible to quencher. Hence one can expect complex Stern-Volmer plots, and even spectral shifts due to selective quenching of exposed versus buried tryptophan residues.

The positive deviations correspond to non-linear Stern-Volmer plots with an upward curvature and are frequently observed when the extent of quenching is large and can be attributed to problems of distribution of the quencher and/ or the fluorophore [100]. Two models can explain this deviation: combined static and dynamic quenching and the sphere of action model [100].

In the case of this particular study, combined static and dynamic quenching might be the most adequate explanation. In many instances the fluorophore can be quenched both by collisions and by complex formation with the same quencher, translated by the following equation [100]:

$$\frac{I_0}{I} - 1 = (K_D + K_S)[Q] + K_D K_S [Q]^2$$ **Equation 10**

where I_0 and I are, respectively, the corrected fluorescence intensity of fluorophores in the absence and presence of the quencher; [Q] is the concentration of the quencher and K_D and K_S are respectively the Stern-Volmer constants for dynamic and static quenching. For simplicity, Equation 10 can be re-written as follows:

$$\left[\frac{I_0}{I}-1\right]\frac{1}{[Q]}=(K_D+K_S)+K_DK_S[Q] \qquad \textbf{Equation 11}$$

A plot of $(I_0/I - 1)/ [Q]$ versus $[Q]$ yields a straight line with an intercept of $K_D + K_S$ and a slope of K_SK_D (Figure 10).

Moreover, the efficiency of the quenching or the accessibility of the fluorophores can also be assessed by the calculation of the bimolecular quenching rate constant [100]:

$$Kq=\frac{K_{SV}}{\tau} \qquad \text{Equation 12}$$

If the quenching is known to be dynamic, the Stern-Volmer constant will be represented by K_D, otherwise this constant will be described as K_{SV}. Diffusion-controlled quenching typically results in values of near 1 x 10^{10} $M^{-1}s^{-1}$. Values of Kq smaller than the diffusion-controlled value can result from steric shielding of the fluorophore or a low quenching efficiency. Apparent values of Kq larger than the diffusion-controlled limit usually indicate some type of binding interaction.

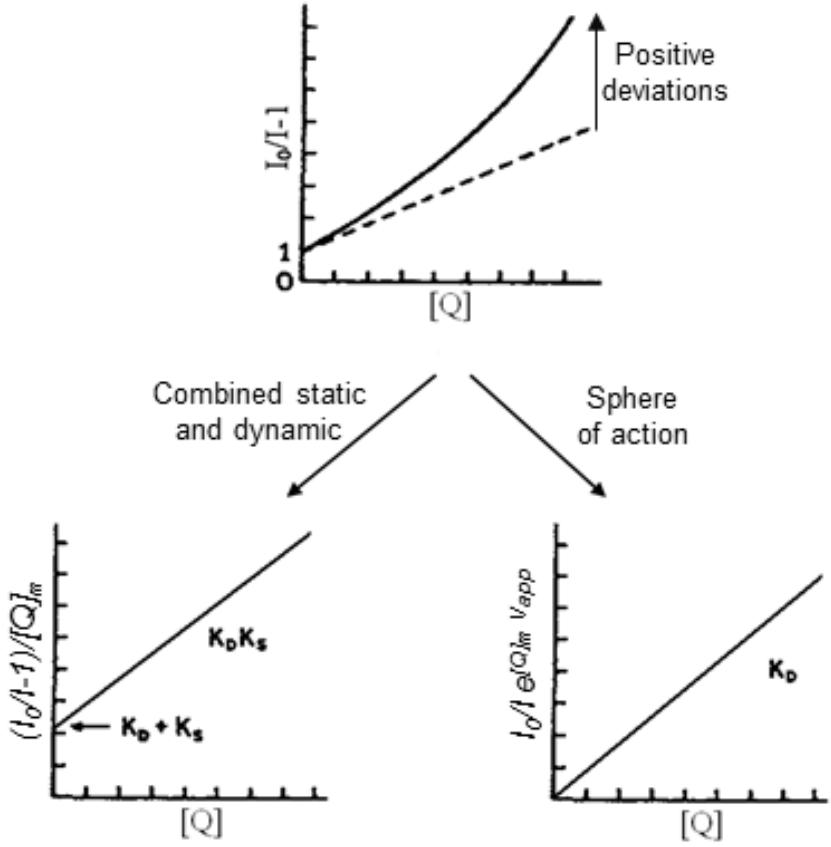

Figure 10 Positive deviations to the Stern-Volmer equation and alternative models of linearization. Adapted from [100].

iv. Fluorescence probes

Fluorescence probes contain fluorophores groups that allow obtaining a great variety of information through analysis of their excitation and emission spectra, their fluorescence quantum yield and the lifetime of the excited state and their polarization [129, 155]. The information reported by a probe inserted into a membrane (natural or model membrane) can

be used in the evaluation of membrane fluidity, the location of molecules in the membrane, intracellular ionic concentrations and membrane potential, among others [156].

Currently, there is a wide range of compounds used as fluorescence probes in several studies. In this work, the fluorophores chosen for assessing the membrane location of daunorubicin were DPH and TMA-DPH. TMA-DPH, contains a DPH phenyl ring located within the hydrophobic acyl chains of the membrane phospholipids and a cationic group, that anchors the probe to the polar headgroups of the phospholipids [157, 158]. Therefore, TMA-DPH reports to the interfacial region of lipid membranes, while DPH provides information regarding the hydrophobic area of the membrane [157-159].

v. Time-resolved fluorescence quenching

Time-resolved measurements are widely used in fluorescence spectroscopy, particularly for studies of biological macromolecules and increasingly for cellular imaging [100].

Time-resolved measurements provide more information than the available from the steady-state data. One of the examples of the necessary use of time-resolved measurements is to distinguish between static and dynamic quenching using lifetime measurements [100, 154]. Lifetime measurements are thus important, as they determine the time available for the fluorophore to interact with or diffuse in its environment, and hence the information available from its emission [100, 154].

There are essentially two types of methods for measuring fluorescence lifetimes that are in widespread use today: the time-domain and frequency-domain methods.

In time-domain or pulse fluorometry, the sample is excited with a pulse of light. The width of the pulse is made as short as possible, and is preferably much shorter than the decay time τ of the sample. The time dependent intensity is measured following the excitation pulse, and the decay time τ is calculated from the slope of a plot of $log\ I(t)$ versus t, or from the time at which the intensity decreases to $1/e$ of the intensity at $t = 0$ [100, 154].

The alternative method of measuring the fluorescence lifetime is the frequency-domain or phase-modulation method, which was the one used in this work. In this case, the sample is excited with intensity-modulated light, typically sine-wave modulation (Figure 21). The intensity of the incident light is varied at a range of frequencies, usually 10-250 MHz. Its reciprocal frequency is comparable to the reciprocal of decay time τ [100, 154]. When a fluorescent sample is excited in this manner the emission is forced to respond at the same modulation frequency. The lifetime of the fluorophore causes the emission to be delayed in time relative to the excitation, shown as the shift to the right in figure 11. This delay is measured as a phase shift (φ), which can be used to calculate the decay time. The phase shift and modulation of the emission depend on the relative values of the lifetime and the light modulation frequency. The emission occurs at the same frequency as the excitation. Because of the loss of electron energy (Stokes' shift) between excitation and emission, the emission waveform is demodulated and phase-shifted in comparison to the excitation. Thus the demodulation ratio (m_ω) and phase-angle shift (φ) constitute two separate observable parameters that are both directly related, via a Fourier transformation, to the initial fluorescence intensity and lifetime, τ, for a population of fluorophores [100, 154].

The shape of the frequency response is determined by the number of decay times displayed by the sample. If the decay is a single exponential, the frequency response is simple. One can use the phase angle or modulation at any frequency to calculate the

lifetime. For a single-exponential decay, the phase and modulation are related to the decay time (τ) by [100, 154]:

$$\tan\varphi_\omega = \omega t \qquad \textbf{Equation 13}$$

and

$$m_\omega = (1+\omega^2\tau^2)^{-1/2} \qquad \textbf{Equation 14}$$

where ω is the modulation frequency in radians/s and m_ω is the demodulation ratio of the emission. The origin of the phase shift and demodulation can be understood by considering the time-dependent excitation intensity and the time of intensity decay of the fluorophore.

Most samples of interest display more than one decay time. In this case the lifetimes calculated from the value of φ_ω or m_ω, measured at a particular frequency, are only apparent values and are the result of a complex weighting of various components in the emission. For such samples it is necessary to measure the phase and modulation values over the widest possible range of modulation frequencies.

When the fluorescence decay of a fluorophore is multi-exponential, the lifetime is defined by [154]:

$$<\tau>=\sum_{i=1}^{n} f_i\tau_i \qquad \textbf{Equation 15}$$

where f_i is the fractional contribution of component i to the total lifetime.

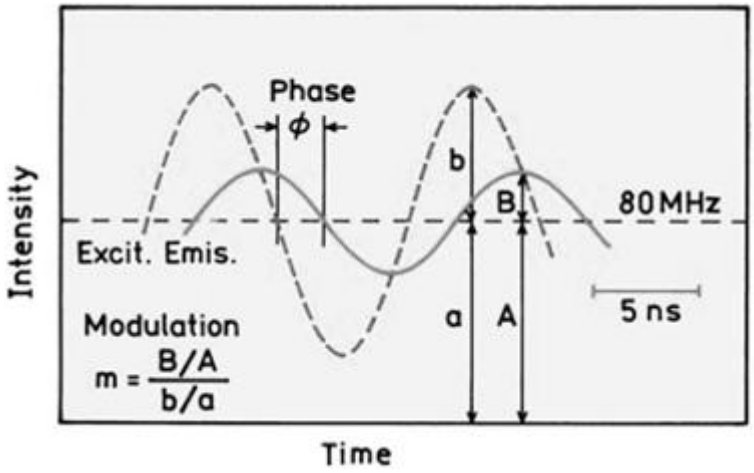

Figure 11 Frequency-domain lifetime measurements. The ratios B/A and b/a represent the modulation of the emission and excitation, respectively. In this example the assumed decay time is 5 ns and the light modulation frequency is 80 MHz. Adapted from [100].

In Figure 12, is shown an example of a frequency domain lifetime measurement, performed in a previous work by Doctor Cláudia Nunes, on a suspension of LUVs of DPPC, labelled with TMA-DPH, upon addition of a NSAID (Piroxicam). From the variation of phase angle and modulation as a function of frequency (Figure 12 A), is possible to obtain the lifetime values, considering the discrete components and their contribution to the fluorescence. Additionally, the residue of adjustment for the multi-exponential model can be seen (Figure 12 B), and a distribution around zero shows a good fit for the phase angle and modulation.

The curve fitting is performed, by the least-squares method, in the frequency domain, i.e. directly using the variations of the phase shift φ and the modulation ratio M as functions of the modulation frequency.

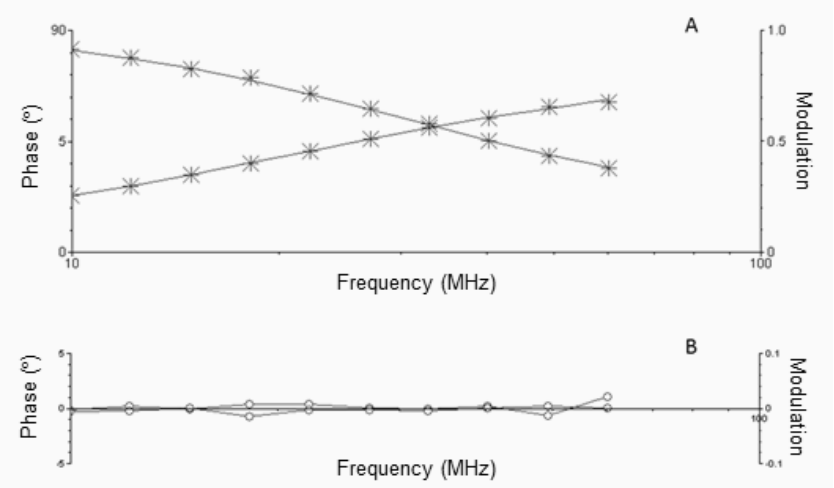

Figure 12 (A) Frequency-domain data for a double exponential decay obtained from LUVs of DPPC labelled with TMA-DPH after incubation with Piroxicam. The phase angle increases and the modulation decreases with increasing modulation frequency. (B) Residue model fit representing the small deviations between the theoretical multi-exponential fit and the experimental data.

Usually phase data and modulation are analysed simultaneously, being the reduced chi squared (x^2) given by [154]:

$$\chi^2 = \frac{1}{\upsilon}\left[\sum_{1=1}^{N}\frac{\left[\Phi(\omega_i)-\Phi_c(\omega_i)\right]^2}{\sigma_\Phi(\omega_i)}+\sum_{i=1}^{N}\frac{\left[M(\omega_i)-M_c(\omega_i)\right]^2}{\sigma_M(\omega_i)}\right] \qquad \textbf{Equation 16}$$

where N is the total number of frequencies. In this case, the number of data points is twice the number of frequencies, so that the number of degrees of freedom is $\upsilon = 2N - p$ (p = number of fitted parameters). The subscript c is used to indicate calculated values for assumed values of f_i and τ_i, and σ_ϕ and σ_M are the uncertainties in the phase and modulation values, respectively.

In order to assess the quality of the fit is essential to observe the x^2, whose value should be close to 1 for a good fit. Acceptable values are in the 0.8–1.2 range [100, 154]. Lower values indicate that the data set is too small for a meaningful fit and higher values are caused by a significant deviation from the theoretical model (e.g. insufficient number of exponential terms). Systematic errors (arising for instance from radiofrequencies interfering with the detection) can also explain higher values.

For these studies, DPH- and TMA-DPH-labelled liposomes were incubated with various concentrations of the drug daunorubicin. Samples contained a fixed concentration of lipid of 500 μM and increasing concentrations of daunorubicin (0, 5, 10, 15, 20, 25, 40 and 75 μM). Before fluorescence measurements, the resulting suspensions were incubated for 30 minutes at physiological temperature (37ºC) so that the drug could reach the partition equilibrium between the lipid membranes and the aqueous medium. Fluorescence measurements were carried out at a controlled temperature for each pH value of 37 °C, at excitation and emission wavelengths defined as 357 nm and 429 nm, for the DPH probe, and 359 nm and 429 nm, for TMA-DPH. Fluorescence steady-state measurements were performed in a spectrofluorimeter (Jasco FP 6500, Software Spectra Manager, Jasco Analytical Instrumments, Easton, MD, USA)) equipped with a constant temperature cell holder. All data were recorded in a 1 cm path length cuvette. For each measurement, fluorescence emission was

automatically acquired during 30 s. Fluorescence intensity values were corrected for inner filter effects at the excitation wavelength [153]. The same measurements were performed using the same samples in a plate-reading spectrofluorimeter (BioTek Cytation 3, Software Spectra Manager, BioTek Instruments, Inc., Winooski, VT, USA), in order to compare results and validate this method, since the plate reader is a much easier and faster method that could facilitate future studies. The same measurements were performed using cells by preparing samples at the same concentrations of daunorubicin with a steady concentration of cells of 1.6 x 10^5 cell/mL per sample.

Fluorescence time-resolved measurements were made with a Fluorolog Tau-3 Lifetime system. Modulation frequencies were acquired between 10 and 250 MHz. Integration time was 10 s. The fluorescence emission was detected with a 90° scattering geometry. All measurements were made using Ludox as a reference standard (τ= 0.00 ns). Two independent assays were performed for each case.

3.6.3. Steady-state anisotropy

The steady-state fluorescence anisotropy (r_{ss}) is based on determining the degree and extent of rotational diffusion of the fluorophore (probe) during the lifetime of the excited state. Small changes in the stiffness of the matrix surrounding the probe produce changes in the rotational movement of the probe and, as such, cause changes in the anisotropy [100].

To determine the steady-state anisotropy, the sample is excited with vertically polarized light and fluorescence intensities are measured with the emission polarizer oriented parallel ($I_{\parallel}$) and perpendicular ($I_{\perp}$) to the excitation polarizer [100].

The steady-state anisotropy (r_{ss}) is then defined by the following relationship between the relative intensities of fluorescence:

$$r_{ss} = \frac{I_{\parallel} - GI_{\perp}}{I_{\parallel} + 2GI_{\perp}} \qquad \textbf{Equation 17}$$

where G is an instrumental correction factor, given by the ratio of the sensitivities of the detection system for vertically and horizontally polarized light [100]:

$$G = \frac{I_{\perp}}{I_{\parallel}} \qquad \textbf{Equation 18}$$

The determination of steady-state anisotropy involves the use of probes (extrinsic fluorophore) inserted into the membrane, whose photoselective excitation is performed by polarizers. If the molecules of fluorophore are present in a highly ordered membrane, as seen in the gel or solid-crystalline state or in a viscous solvent, their movement is highly restricted and it is induced a parallel orientation of the fluorophore molecules to the vertical excitation polarizer. As a result, the molecules of fluorophore emit polarized light because they remain immobile during the lifetime of the excited state. However, if the environment surrounding the fluorophore is the fluid state, the notorious free rotation of the fluorophore molecules pushes a random fluorophore orientation, resulting in a decrease in the emission of polarized light. The explanation for this decrease is based on the lack of alignment with the vertical excitation polarizer (Figure 13) [100].

The application of studies of steady-state anisotropy to membrane models allows the determination of the main phase transition temperature of the lipid. The essence of this

technique consists on monitoring the anisotropy in a range of temperatures, of a labelled suspension of liposomes.

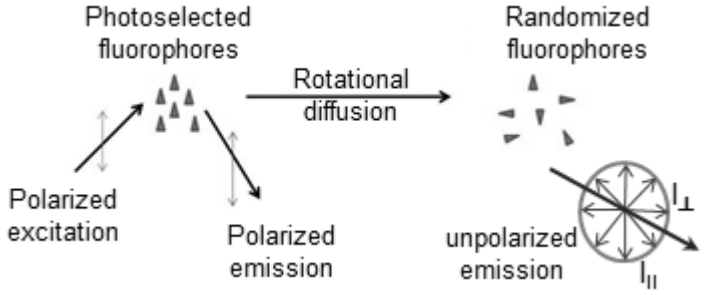

Figure 13 Effects of polarized excitation and rotational diffusion on the anisotropy of the emission. Adapted from [100].

Typically, sigmoid curves are obtained which show the variation of the anisotropy of fluorophores in liposomes with the temperature, allowing analysing: the influence of the drug on the phase transition temperature (T_m) and influence on the anisotropy before and after the transition and the transition profile. The parameters of cooperativity (B) and T_m, are calculated from the slope and the inflection point of the data fitted to sigmoid curves, respectively, using the following Equation 19 [160]:

$$r_{ss} = r_{s1} + p_1 T + \frac{r_{s2} - r_{s1} + p_2 T - p_1 T}{1 + 10^{B(1/T - 1/T_m)}} \qquad \textbf{Equation 19}$$

where T is the absolute temperature, T_m is the midpoint of the phase transition, B is a measure of the cooperativity of the transition, p_1 and p_2 correspond to the slopes of the straight lines at the beginning and at the end of the plot, and r_1 and r_2 are the anisotropy intercepting values at the y axis. Cooperativity is a concept associated with the transfer of energy that is occurring between the molecules at the measured conditions – the higher the cooperativity, the more synergistic the energy transfer in the model studied [161].

Due to strong packing, the lipid molecules are unable to disorder gradually, and thus, when the phase transition occurs, there is a sudden increase in the movements of phospholipids. Therefore, the phase transition is a cooperative process where all the lipid molecules are involved. The presence of a foreign molecule in the acyl chain region of the membrane decreases cooperativity, turning the lipid melting into a more gradual, smooth and therefore less cooperative process [162]. It is more frequent that the drugs decrease the cooperativity of a process. However, some drugs also increase the cooperativity of the transition, from which can be inferred that the drugs are located within the lipid bilayer but closer to the polar zone, so its presence does not cause any delay on the lipid melting process [163].

The measurement of fluorescence anisotropy is therefore very useful in evaluating the fluidity of the membrane, by providing information about the microviscosity of the lipid environment where the probe is inserted and has even applied to assess pathologies and the therapeutic action of drugs. For example, fluorescence anisotropy studies have shown that patients with active rheumatoid arthritis (pain) have an increased stiffness of the membranes of lymphocytes [164]. In turn, using the same technique, it was found that the drugs used for the treatment of this disease induce the increase of membrane fluidity of lymphocytes, suggesting that the study of changes in membrane fluidity, by means of steady-state

anisotropy measurements, can be used to monitor the effectiveness of the treatment of drugs [165].

In this work, LUVs at a concentration of 500 μM per sample of the defined models labelled with either DPH or TMA-DPH were used. The liposome suspensions were incubated without drug and with either daunorubicin or doxorubicin at increasing concentrations – 5, 10, 15, 20, 25, 40 and 75 μM for 30 minutes at 37 ºC and steady-state anisotropy and temperature-resolved anisotropy was measured for these concentrations. The monitoring of the anisotropy was also done for a range of temperatures from 10 to 60ºC for samples with no drug and drug at the concentrations of 40 and 75 μM – temperature-resolved anisotropy. The same was performed using cell suspensions labelled with the referred probes also at drug concentrations of 0, 40 and 75 μM, but the temperature range was 10-50ºC. The cells were used at a concentration of 1.6 x 10^5 cells/mL per sample. Two independent assays were performed for each case.

3.7- Statistical Analysis

Statistical analysis was performed using IBM® SPSS® Statistics software (v.20.0.0.0; IBM, Armonk, NY, USA). The measurements were repeated at least twice and data was expressed as mean ± standard deviation (SD). Data was statistically analysed through the one-way analysis of variance (ANOVA) method and differences between groups were compared by Bonferroni and Tukey post-hoc tests in which a p value lower than 0.05 ($p<0.05$) was considered statistically significant.

Chapter 4

Results and Discussion

4.1- Liposome Characterization

The formulations designed were characterized as explained above, to guarantee they possessed the characteristics of interest for the following studies. Particle size was measured through DLS and is presented in figure 14.

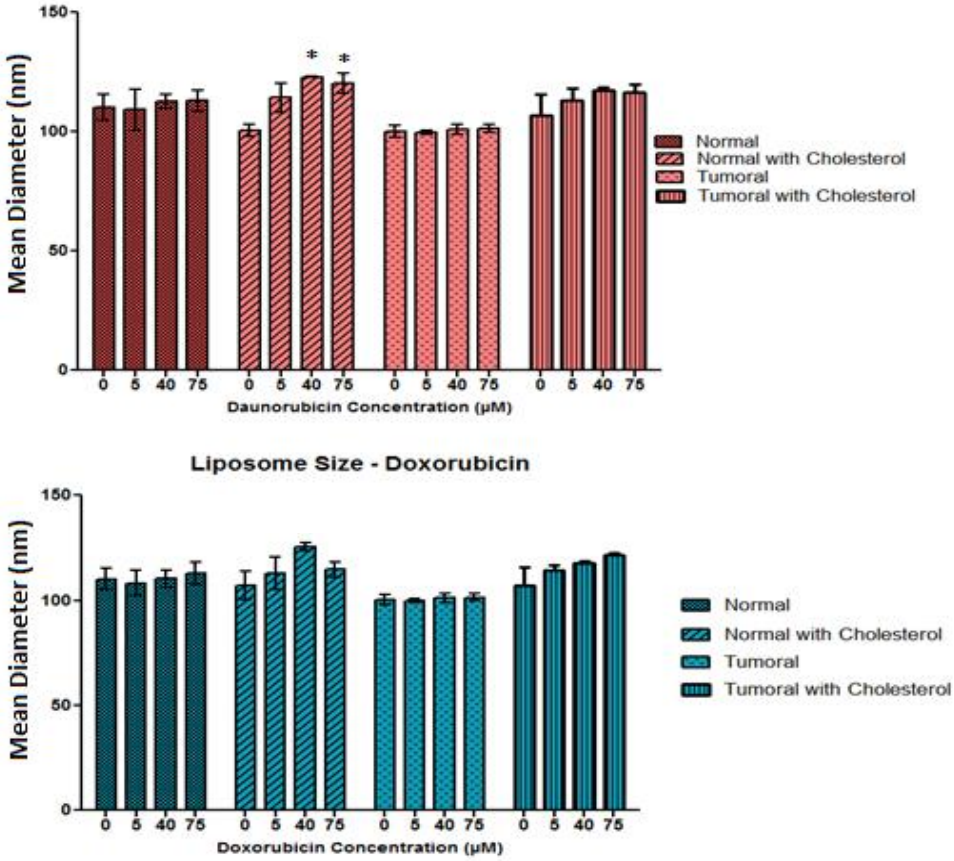

Figure 14 Size distribution of liposomes in the four fourmulations designed (normal, normal with cholesterol, tumoral, and tumoral with cholesterol) with increasing concentrations of daunorubicin and doxorubicin ranging from 0 to 75 μM. * represents that means are significantly different ($p<0.05$) relatively to the suspensions without drug (0 μM) of the same model.

From figure 14 it is possible to verify that the liposomes produced were in fact 100 nm in diameter as desired. Even though some statistically significant differences can be seen for the normal with cholesterol model, overall the addition of the drugs does not appear to produce substantial effects in the size of the liposome formulations studied.

As described previously in this document, normal cell membranes are composed of a number of molecules charged differently, but these are present at certain equilibrium so that the surface charge is close to 0 as described in the literature [54, 56]. Contrarily, tumor cell membranes expose to the outer leaflet of the membrane anionic lipids such as PS, having therefore a negative surface charge [54, 56]. The determination of the zeta potential of the designed mimetic membrane models helps comprehend if these changes can also be mimicked.

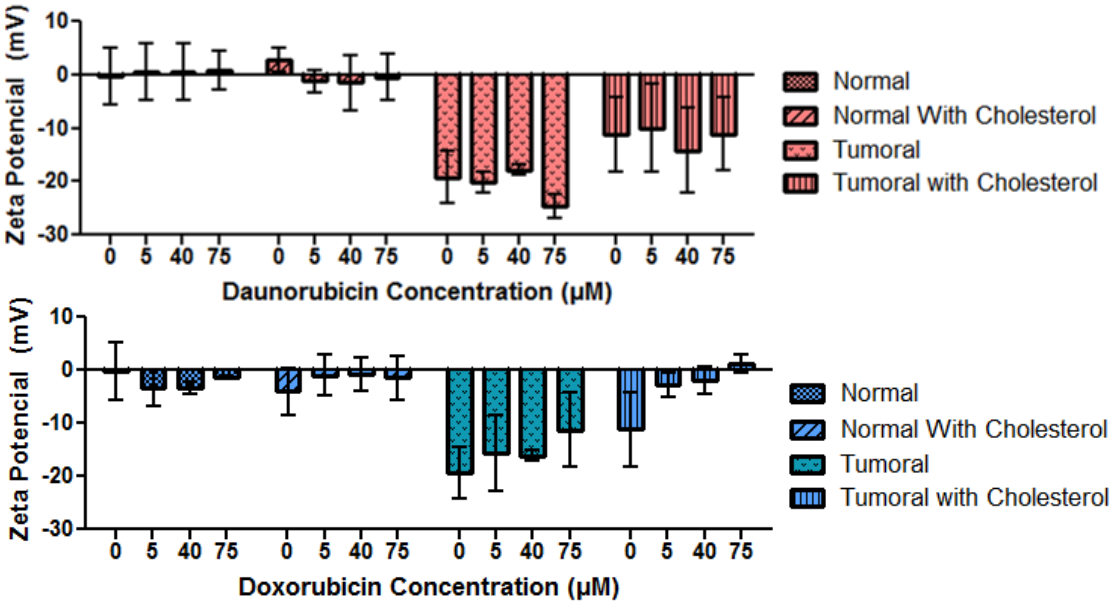

Figure 15 Zeta potential of liposomes in the four formulations designed (normal, normal with cholesterol, tumoral, and tumoral with cholesterol) in increasing concentrations of daunorubicin and doxorubicin ranging from 0 to 75 µM. * represents that means are significantly different ($p<0.05$) relatively to the suspensions without drug (0 µM) of the same model.

Figure 15 represents the zeta potential for the four models prepared without any drug and with 3 concentrations of either daunorubicin or doxorubicin – 5, 40 and 75 µM. First, these values will be used to assess the similarities of the models to actual cell membranes. Secondly, the effect of each drug and the referent concentrations on the surface charge of the models will be explored, and finally, an overall review of the meaning of the zeta potential values obtained will be done.

It can be observed that for the normal formulations with or without cholesterol, the zeta potential values are around 0, which indicates neutral surface charge, while for the tumoral formulations negative values of zeta potential were obtained. This is consistent with what is found in actual cell membranes (normal and tumoral, respectively), and as such we can conclude that the proposed formulations successfully mimic the surface charge of the cell membranes they're intended to be models for.

A tendency can be observed for the tumoral models as it appears that the zeta potential becomes less negative and tends towards neutrality as the drug concentration is increased. That is likely to happen because both drugs (pKa=8.4)[95] are positively charged at the pH values used during the assays due to their amine group (see figure 8). This might mean that

the positively charged amine group is able to interact with the negatively charged phosphate groups at the polar heads of the anionic phospholipids (especially due to the increase in the amount of PS on the outer leaflet of the membrane), neutralizing those charges via these interactions.

In general, liposome formulation characterization allowed to confirm that the membrane models were prepared as intended, with surface charge that is similar to that of normal and tumoral cells and a diameter that creates a membrane curvature similar to that of actual cells.

Although it can't be said without doubt that interactions between the two drugs and the four models are occurring, the results give some indications that that might be happening. To confirm and help understand these interactions, further studies were performed.

4.2- Membrane Partition Studies

The membrane partition, analysed by the measure of the partition coefficient (K_p), was performed through derivative spectrophotometry. As explained in the chapter 3, lipid suspensions were prepared at a range of lipid concentrations from 100 to 1000 μM – these were the reference samples. Similar ones were prepared with drug at a fixed concentration of 40 μM. 40 μM solutions of only drug in buffer were also prepared. All of these were placed in 96-well plates and the absorbance spectra were measured. Studies were performed 3 times independently. Once confirmed that the values of all three replicas were coincident, the mean values of the samples, references and drug spectra were introduced in a *Microsoft Excel*® application created by Doctor Cláudia Nunes – *Kp Calculator* [150]. The mentioned absorbance spectra obtained are represented as an example in figure 16.

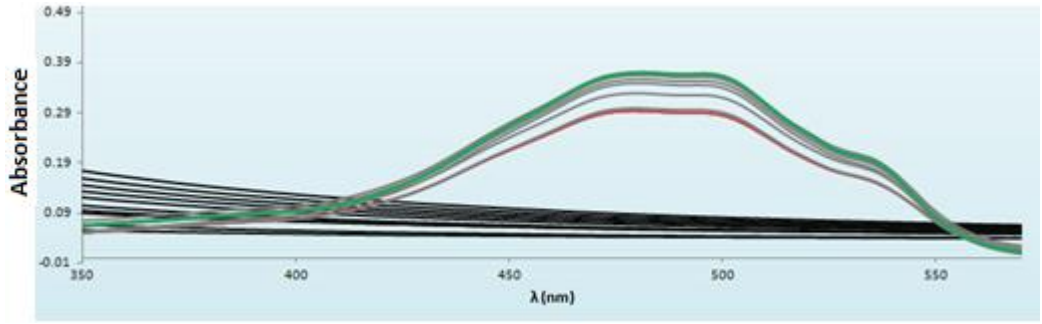

Figure 16 Absorbance spectra plotted from the experimental data. In this case it is shown the data plotted from the normal model for the drug daunorubicin.

The absorbance spectra values from the reference samples were subtracted to the values referent to the samples containing drug. From this data, and to decrease the noise associated with the microscattering as previously explained, the first, second and third derivative were calculated, being an example of the third derivative represented in figure 17. The third derivative is usually chosen for the following steps since it allows for a better reduction of the noise caused by the microscattering associated with the liposomes. From the spectrum of the third derivative, four peaks are chosen and the values for each drug concentration at the four wavelengths chosen are collected, as is represented for one wavelength in figure 17. These values were then inserted into the Origin Pro 8.5.1 software, plotted and a non-linear curve fitting was calculated using Equation 4, described in Chapter 3 of this document. The

resulting plot of the derivative data and the fitting associated are also represented in figure 17.

From this fitting it is possible to obtain the K_p value for each wavelength tested, being the final K_p the average of these values for that drug using that mimetic model. To obtain adimensional K_p values and remove the influence of the different microenvironments of the different models, the values obtained before are divided by the specific molar volume of the lipids used in that specific mimetic model.

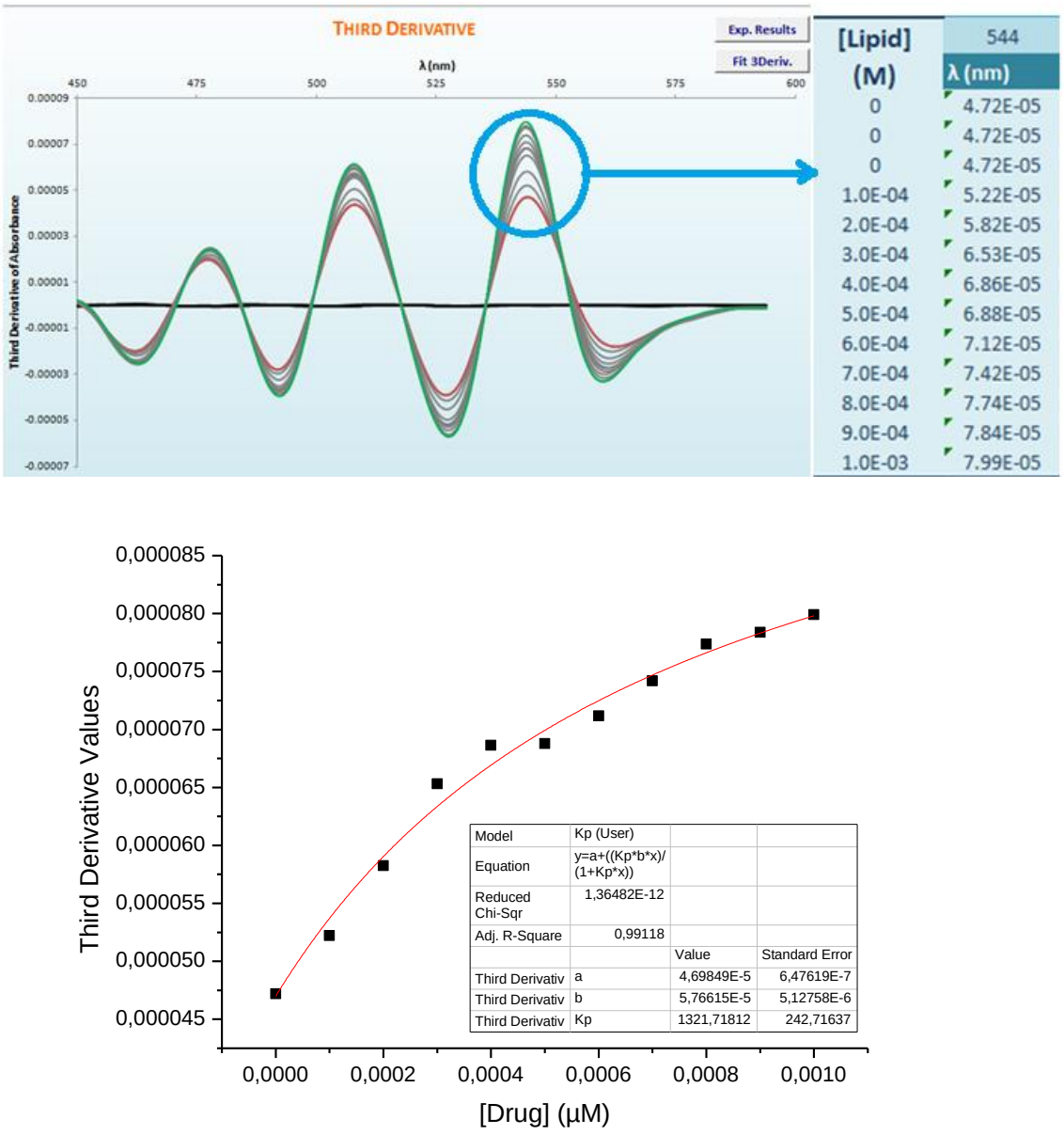

Figure 17 Third derivative spectrum of the data from figure 16 and the respective actual data for a particular wavelength (above). Below is the fitting performed using the Origin Pro software.

The adimensional K_p values found for both daunorubicin and doxorubicin using the four mimetic models are represented in figure 18. These allow the analysis of 3 main factors. First the two drugs will be compared; then, the effect of cholesterol in the membrane models will be evaluated; finally, a comparison of normal vs. tumoral models can be made.

Regarding the two compounds tested, it is very clear that they partition very differently into the different membrane models. In the normal model, the drug doxorubicin partitions into the membrane approximately 12 times more than daunorubicin does. In the case of the normal model containing cholesterol, the same tendency applies, with doxorubicin partitioning 38 times more than daunorubicin. Since the only difference between the two drugs is that doxorubicin has an alcohol group, the results indicate that this alcohol group is likely to be involved in the higher partition of the drug into the normal membrane models. A hypothesis that can be formulated is that, besides the interaction of the drugs' amine group with the membrane, this OH group might be establishing hydrogen bonds with the ester groups of the phospholipids. In the case of the normal model with cholesterol, this partition decreases, once the model becomes more rigid it does not have as many ester groups available do establish the hydrogen bonds. This is not observed for the tumoral models. Both drugs partition similarly into the membranes of the tumoral model. However, for the tumoral model with cholesterol, doxorubicin partitions slightly less into the membrane than daunorubicin.

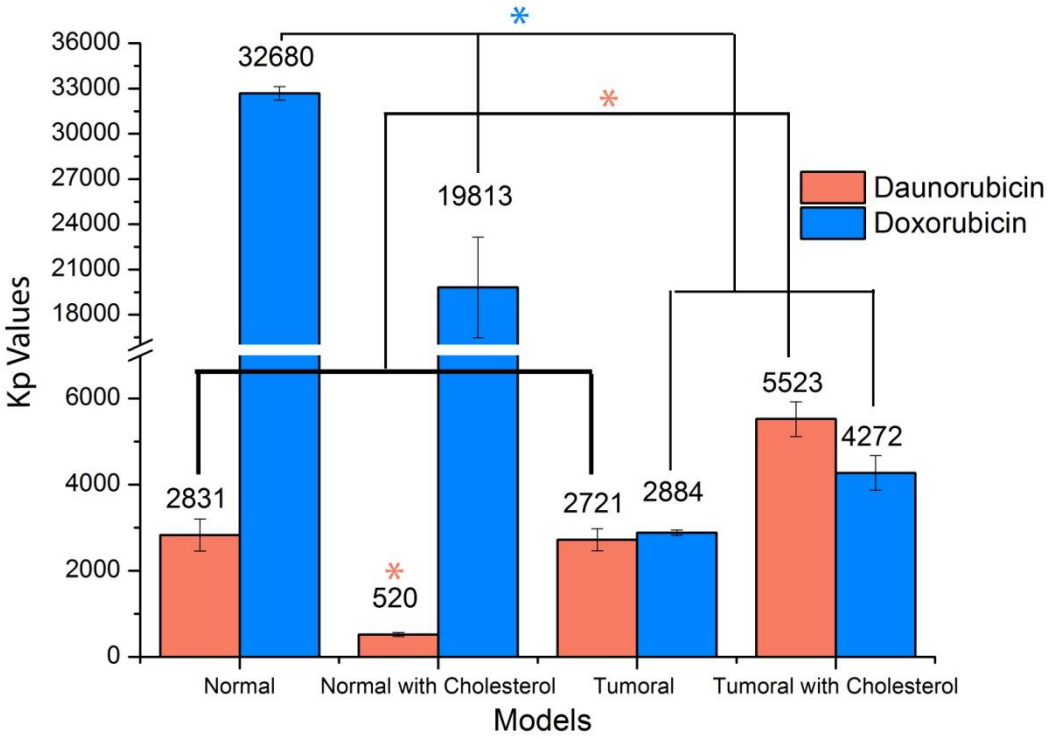

Figure 18 Partition Coefficient (K_p) values for both drugs used in the sudy, daunorubicin and doxorubicin, determined though derivative spectrophotometry using four different lipidic mimetic models of the membrane – normal, normal with cholesterol, tumoral and tumoral with cholesterol.* represents significant difference ($p<0.05$), comparing the models for the same drug.

From the results obtained it appears that the presence of cholesterol has a particular effect in the different model membranes. In the normal models, drug partition is lower when cholesterol is present in the membrane, which was to be expected since it is known that in nature cholesterol generally makes the membrane more rigid and more compact. In the case of daunorubicin, there is very little partition into the normal with cholesterol membrane, being this value by far significantly the lowest of all. However, in the tumoral models, the drugs partition more when cholesterol is present. A possible explanation for this resides in the fact that cholesterol creates microdomains such as lipid rafts by associating with other components of the membrane such as the PS. These are localised structures that are rigid and

overall tend to decrease the fluidity of the membrane. It might be the case that cholesterol is forming these microdomains in the tumoral mimetic model that contains cholesterol, and that the remaining lipids of the membrane outside of these microdomains are becoming more permeable due to the absence of cholesterol there to compact, and as a result the cholesterol is improving drug partition in the case of the tumoral membrane models. It is also interesting to notice that in the literature, lower amounts of anionic phospholipids in the membrane were seen to cause an increase in their permeability for both anthracyclines [95, 108]. Therefore it may be fair to conclude that the decreased proportion of PS, an anionic lipid, in the membrane of the tumoral with cholesterol is favorable for the uptake of both drugs, which might be related to the possibility that PS is one of the main lipids to form complexes or domains with cholesterol.

Finally, comparing the models taking into account the type of tissue they try to mimic, it's clear that daunorubicin partitions much better into the tumoral model containing cholesterol, which is a factor of much value to its therapeutic effect especially since it seems that the drug has higher affinity towards tumoral models. Doxorubicin, while partitioning less into the tumoral membranes than into the normal ones, still has very high partition coefficients in the case of the tumoral models, which also plays in favor of its effectiveness in treatment. These findings are in accordance to the literature, which suggests that membrane models of higher heterogeneity (mixtures of lipids) usually promote the interaction, partition or even penetration of drugs such as doxorubicin into the the membranes [87-89].

Overall, it can be concluded that, with the exception of daunorubicin in the normal with cholesterol model, the drugs partition very well into all the membranes of the tested models, which could explain why they are to this day some of the most used for chemotherapy but also why they have such severe side effects - since the high partition is also verified for the normal cell-mimicking models, there is high cytotoxicity not only for the tumoral cells, but also to the normal ones.

Table 6 Logarithmic values of the partition Coefficient (Kp) values for both drugs used in the sudy, daunorubicin and doxorubicin, determined though derivative spectrophotometry using four different lipidic mimetic models of the membrane – normal, normal with cholesterol, tumoral and tumoral with cholesterol, as well as the partition coefficient for each drug found via the octanol/water method.

	Octanol/Water Method	**Derivative Spectrophotometry [log(Kp)]**			
	Log(P) [166]	Normal	Normal with Cholesterol	Tumoral	Tumoral with Cholesterol
Daunorubicin	1.83	3.27 ± 0.05	2.49 ± 0.04	3.28 ± 0.04	3.55 ± 0.03
Doxorubicin	1.27	4.34 ± 0.01	4.07 ± 0.07	3.30 ± 0.01	3.44 ± 0.04

In fact, while doxorubicin causes the same kind of side effects as daunorubicin, the effects associated with the first are much more severe, being doxorubicin considered a more aggressive drug [119-121]. The findings described are consistent with that, showing a partition of doxorubicin into normal membranes that is several times higher than that of daunorubicin and than that of doxorubicin in tumoral models.

The results obtained using the method of derivative spectrophotometry were then compared to the values of partition for both drugs described in the literature determined

through the octanol/water partition method. Since these values are usually presented, from a pharmaceutical point of view, in the logarithmic form, table 6 presents the partition coefficient of both drugs in logarithmic form using both methods.

As mentioned before, octanol, the organic phase of the octanol/water method, lacks the amphiphilic nature that is so characteristic of phospholipids and essential for the cell membranes' structure [131-134]. As such, this method bears very little resemblance to the actual biomembranes found in nature. On the other hand, using liposomes as model membranes solves this problem as these are very similar to biomembranes. In table 6 it is shown that the partition coefficient values found in this study using derivative spectrophotometry are very different from those found using the octanol/water method. The K_p values found in this study are actually much higher than those of the octanol/water method. This proves that the interactions between the two drugs and the membranes involve not only hydrophobic but also electrostatic and Van der Waals interactions as well as hydrogen bonds, which are facts supported by previous research [95, 108]. Thus, the liposomes/water system appears to be a much more effective, complete and accurate way of determining the partition coefficient and therefore obtaining information regarding the way the drugs partition into the biomembranes. The transition in industry and research of the use of the octanol/water method to the use of model membranes to determine partition coefficient could in the future prove to be a great improvement in both fields.

4.3- Membrane Location of Daunorubicin

Membrane location assays were performed for the drug daunorubicin using the four models designed for this study. The same assays were performed for a line of tumoral cells, the line MDA-MB-231 that can be seen in figure 19, in order to produce results that could be comparable to those of the models. The assays were performed using liposomes and cells labeled with either DPH or TMA-DPH. These are two fluorescent probes that have a known and described location in the membrane. Since their location in the membrane is known, the proximity of the drug to these probes can give information on their own location in the membrane. That is because the probes' fluorescence is deactivated by the proximity of the drug, a phenomenon called quenching.

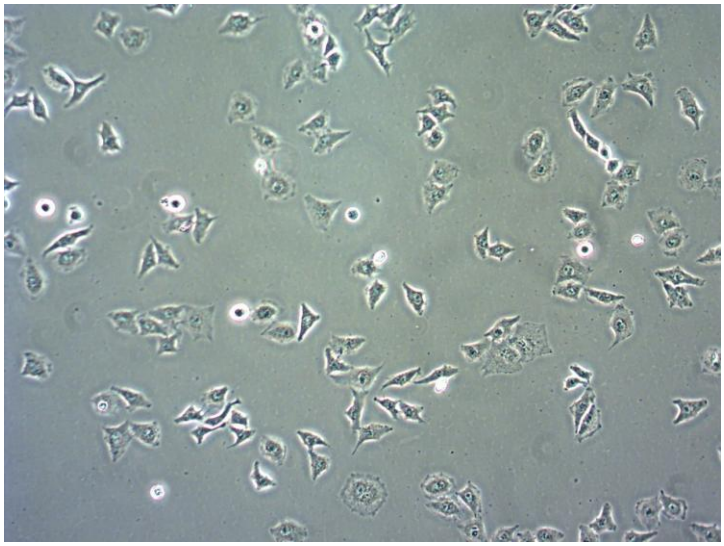

Figure 19 MDA-MB-231 cells cultured with RPMI U1 25mM Hepes and 5% FBS observed after 2 days of growth under an inverse microscope at a magnification of 1000x.

As explained in Chapter 3, there are two types of mechanisms for fluorescence quenching: static and dynamic or collisional quenching. When quenching is static, a permanent complex is formed between the fluorophore and the quencher and the lifetime measurements remain constant for each sample, which would mean that the K_D would equal zero. The dynamic or collisional mechanism involves the interaction of the quencher with the fluorophore in the excited state, but this is temporary since the fluorophore then returns to ground state. If this is the mechanism, the I0/I values would form a linear plot, that should be superimposable with $\tau 0/\tau$, meaning that K_{SV} is equal to K_D. Since neither case is observed, it is fair to infer that the mechanism of quenching involves combined static and dynamic quenching.

The chosen fluorescent probes to be used in this study were DPH and TMA-DPH. These are interesting because they insert into the lipid bilayer, possessing however an important distinction. The DPH probe possesses a structure that is hydrophobic (represented in figure 20) and as such inserts into the acyl chain region of the phospholipidic membranes, being therefore more internally located. The TMA-DPH (figure 20) is very similar to DPH, however it contains an amine group which is polar and therefore able to interact with the polar heads of the phospholipids. DPH will tend to be nearest to the center of the bilayer due to its affinity to the fatty acid tails of the phospholipids. TMA-DPH, although being partially inserted between the acyl chains, also interacts with the polar regions, therefore locating at a sort of transition region between the polar and apolar zones of the phospholipids, allowing the acquisition of information at a more superficial level.

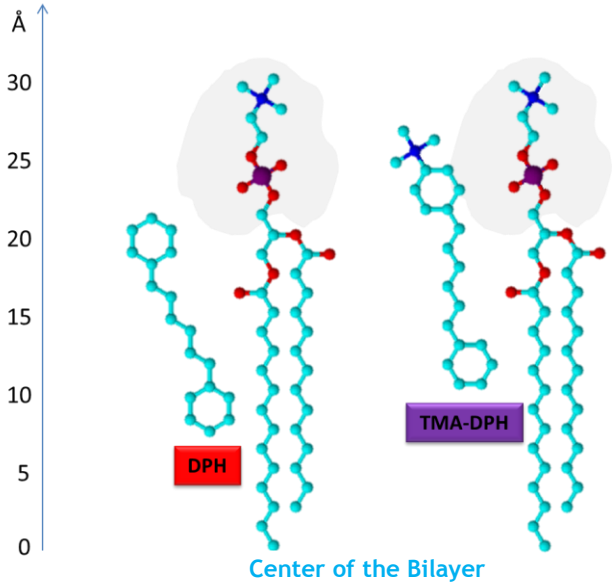

Figure 20 Schematic representation of the structure of the fluorescent probes DPH and TMA-DPH and their average location next to an example of phospholipid (to the right of each probe), which is the constituent of a lipid bilayer. This image was kindly provided by MSc Ana Catarina Alves.

The closest the drug's proximity, the more the deactivation of the probe's natural fluorescence. With that information, correlations can be made using an array of samples of increasing drug concentrations to in turn determine biophysical parameters that can help shine light on the drug location. The determination of the drug-induced quenching involves the measurement of the fluorescence emission spectra of samples at a lipid concentration of 500 μM and drug concentrations from 0 to 75 μM. These spectra can be obtained through a regular spectrofluorimeter, in which each sample has to be changed manually, or by a plate

reading spectrofluorimeter, in which all samples are introduced in a 96-well plate and all the samples are inside the equipment throughout the whole reading process. Now, a regular spectrofluorimeter has the advantage of a higher sensitivity. However, since it can only hold one sample at a time and these have to be manually changed, it is a much more morose and time-consuming process to use this device. Also, in cases such as this when it is very important to keep the samples in the dark to avoid fluorescence bleaching and always at 37ºC to ensure the measurements are done at that specific temperature, this method involves some sample disturbance by having to transport them at room temperature from the incubator to the device and having to open the sample holder sometimes to measure the temperature, which might impair both needs. On the other hand there is the plate reader, which is a slightly less sensitive equipment. However, it has the advantage of allowing the introduction of all the samples at the same time, which reduces light and room temperature exposure. Also, it can be programmed to incubate the samples at the desired temperature for a certain time, ensuring that the spectra readings are done at that temperature. In this case, the plates were incubated for 10 minutes at 37ºC prior to reading. The measurements are also programmed once the plate is inserted, which makes the process much more expeditious since the operator does not need to be present during the measurements.

The plate reading spectrofluorimeter seems to be a more practical and advantageous alternative, but its use needed to be validated to ensure that this methodology works in this apparatus once there is no described protocol. For that purpose, the fluorescence spectra (emission and excitation) measurements were performed in both devices. The results for both equipments can be seen in Annex I.

The dynamic constant (K_D) remains the same since the measurements for its determination were performed in a different fluorimeter (one able to perform lifetime measurements). The comparison must therefore be done between mainly the static constants represented (K_S), which were obtained directly from the slopes of fitting curves obtained using equation 11 on the emission spectra maximum values. Since K_D values are the same and the Stern-Volmer constant, K_{SV}, is a calculated as K_S+K_D, this constant can also be used to compare the two devices used.

Overall, it can be observed that the values of K_D and K_{SV} obtained using the two devices were quite similar, and, as such, the use of the plate reader on its own is a valid choice. Small differences in the values between devices are easily explained by the vast array of disturbing conditions the samples suffer in the regular spectrofluorimeter measurements, such as more light incidence and temperature variations, even with the utmost care from the operator. The results for the regular spectrofluorimeter present very small values of standard deviation, while in general the results obtained with the plate reader have wider standard deviation values, which is according to the fact that the latter has a lower detection limit, allowing for less precise measurements. In the end, we conclude that although the regular fluorimeter is more precise, both of the devices are very accurate and can be used for these procedures.

To make easier the visualization and understanding of the results, only the results obtained using the plate reading spectrofluorimeter will be shown in figure 21.

The Stern-Volmer quenching constant (K_{SV}) indicates the sensitivity of the fluorophore to a quencher. Higher values of the Stern-Volmer constant mean higher deactivation (quenching) of the fluorophore. The bimolecular quenching constant, or Kq, represented in figure 22, is often used to reflect the efficiency of quenching or the accessibility of the fluophores to the

quencher. Kq eliminates the contribution of the intrinsic lifetime of the probe and therefore, when comparing different probes with different lifetimes, Kq represents a much more accurate parameter. In this sense, all the comparisons beneath will take that constant into account.

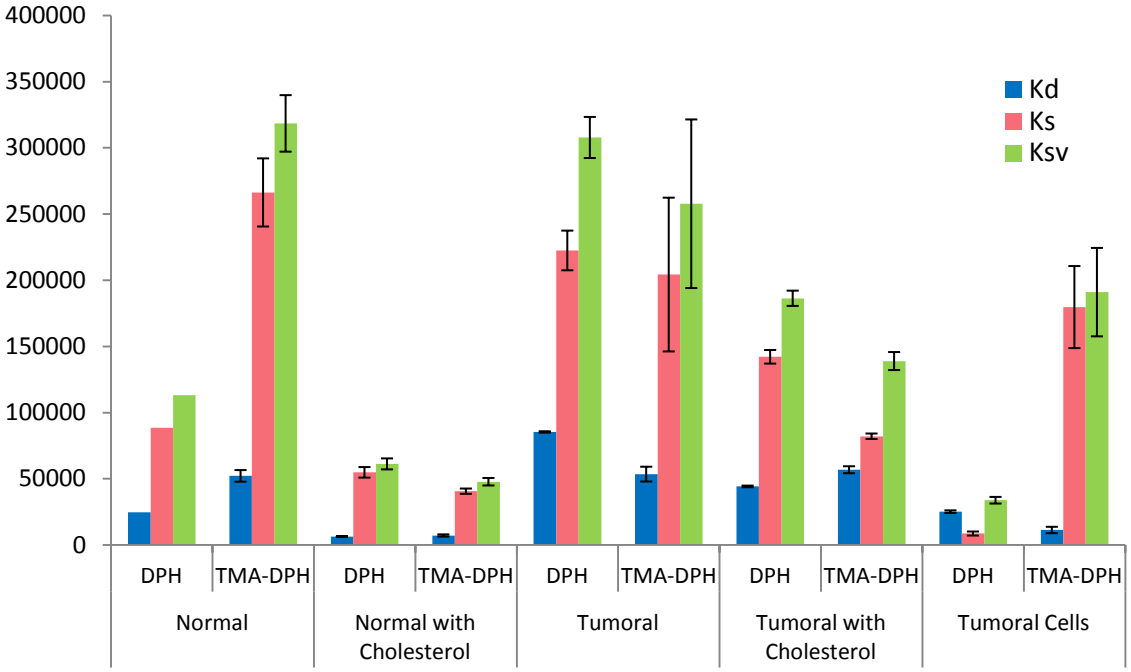

Figure 21 Plotted results of the static, dynamic and Stern-Volmer constants determined using a a plate reading spectrofluorimeter. These constants were determined for all four models plus the tumoral cells MDA-MB-231, under the effect of daunorubicin, for the two probes, DPH and TMA-DPH.

In figure 22 it is evident that for the normal and tumoral model without cholesterol drug locates closer to the location site of TMA-DPH, while for both models with cholesterol the Kq value is close between the two probes.

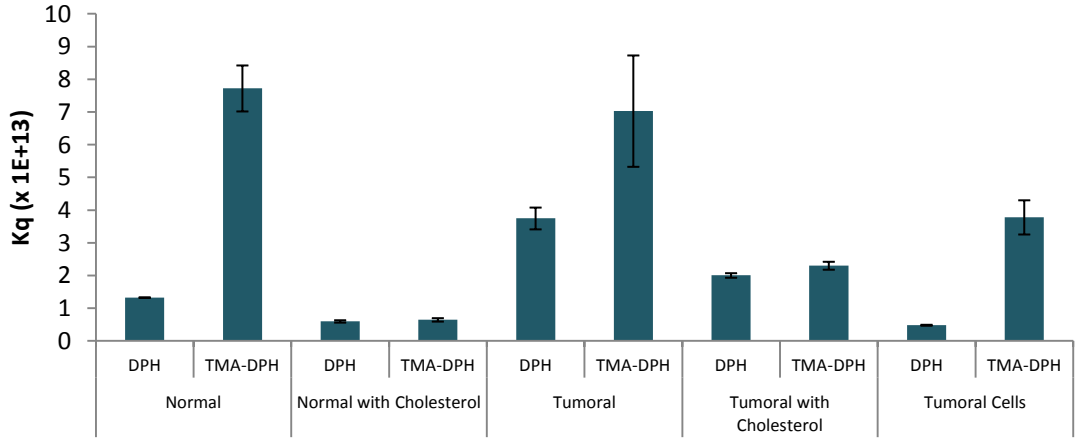

Figure 22 Bimolecular quenching constant (Kq) determined using a a plate reading spectrofluorimeter. These constants were determined for all four models plus the tumoral cells MDA-MB-231, under the effect of daunorubicin, for the two probes, DPH and TMA-DPH.

This leads to conclude that, for the models without cholesterol, daunorubicin is located at a more superficial zone, having its amine group interacting with the phosphate groups of

the polar heads of the phospholipids while the rest of the drug molecule inserts in between the acyl chains of the lipids.

In the case of the models with cholesterol, it is possible that cholesterol, having a small headgroup with affinity to choline, may prevent the interaction of the amino group of daunorubicin with the phosphate group due to steric hindrance. Therefore the quenching effect is less noticeable at the TMA-DPH region when comparing with the model without cholesterol. Nevertheless and comparing with all the other lipid models, the normal model containing cholesterol resulted in very low values for all the constants. This means that very little drug could be found nearing either location of the probes. This is consistent with the very low partition coefficient obtained for daunorubicin – if the drug isn't able to partition into the membrane or partitions very little, then there's very little drug to interact with the fluorophores and the resulting constant values are very low.

For the tumoral cells, the obtained Kq values also point to a drug location closer to TMA-DPH. However, the constant values found for DPH using the tumoral cells were much lower than those of the tumoral model, which makes sense considering the much higher complexity of a biomembrane, containing a wide variety of different domains and molecules in large quantities that might prevent the drug from penetrating it with ease.

4.4- Membrane Fluidity

4.4.1.Temperature-Resolved Anisotropy

When measuring anisotropy along a range of temperatures, an anisotropy profile is obtained such as is shown in figure 23 as an example.

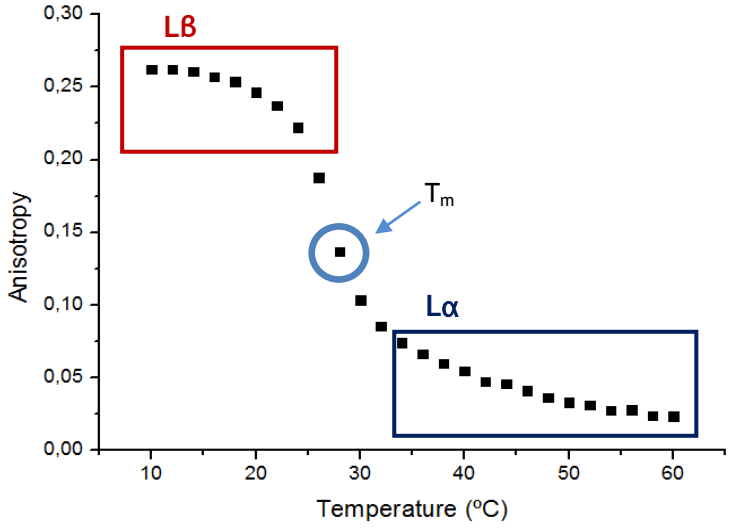

Figure 23 Anisotropy profile from 10 to 60ºC to the normal model with no drug for the probe DPH. The gel phase and liquid-crystalline phases are represented as Lβ and Lα, respectively. The phase transition temperature or Tm is the inflexion point of the plot.

At lower temperatures, a plateau of high anisotropic values exists, which represents the solid-crystalline or gel phase of the lipids (L_β). The temperature at which the arrangement of the lipids shifts to form a fluid or liquid-cristaline phase (L_α) is known as the phase transition temperature or T_m.

Revealing information can be gathered from both observing the obtained anisotropy profiles for each sample and calculating the phase transition temperature. Since we

performed the phase transition temperature measurements for liposome suspensions without drug and with two concentrations of drug (daunorubicin and doxorubicin) for the two fluorescent probes, it is possible to determine if the drugs are causing higher fluidity of the membranes, the phase they are causing differences on and the membrane location where those changes are happening as well.

However, it is also interesting to know the differences in fluidity for the different models without the involvement of the drugs, mainly because it can allow a comparison with the fluidity of biomembranes in nature. Figure 24 represents the profiles for the liposome suspensions of each model for both probes.

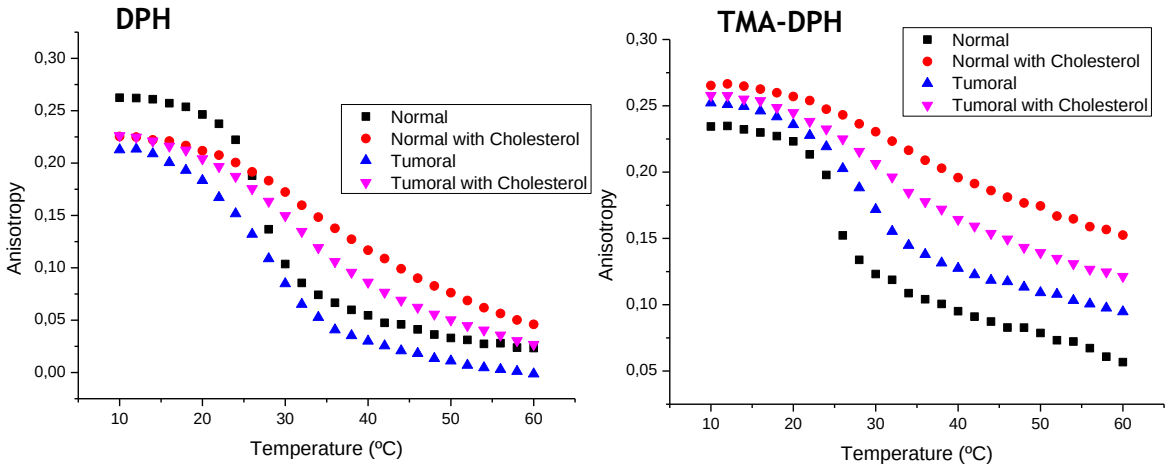

Figure 24 Anisotropy profiles for the four different liposome models membranes labelled with both of the fluorescent probes used (DPH and TMA-DPH).

From figure 24 it is clear that the models have very different behaviors in terms of fluidity in the range of temperature used. Moreover, different profiles depending on the used probe are obtained. As the TMA-DPH reports to a zone closer to the polar head groups it represents higher anisotropy values when compared with the profile obtained for DPH.

For DPH, the normal model shows the highest rigidity in the gel phase but one of the lowest in the fluid phase, which means that in the gel phase the normal model is the most rigid but that does not happen after the phase transition. It is also possible to see, in the acyl chains region, a stabilizing effect of cholesterol, for both models with cholesterol, fluidizing the gel phase and stiffening the fluid phase. In what concerns the head group region, cholesterol has a stiffening effect due to its electrostatic interaction with the choline group. Moreover, and due to the increment of serine in the tumoral model, which has a bulky head group, the tumoral mimetic model is more rigid in this region contrarily to the very simple normal model.

It is also worth pointing out that in both regions the probes report to, the tumoral models tend to be more fluid overall and particularly near the 37ºC temperature than the normal with cholesterol model, which in reality is the one with physiological interest since normal biomembranes are never made of only one lipid (like is the case of the normal model). This is in accordance with what was intended, and as such it is proof that these models were indeed able to mimic the higher fluidity of tumoral cell membranes.

Figure 25 gathers the anisotropy profiles of the four models labeled with two probes without drug and for two drug concentrations (40 and 75 μM).

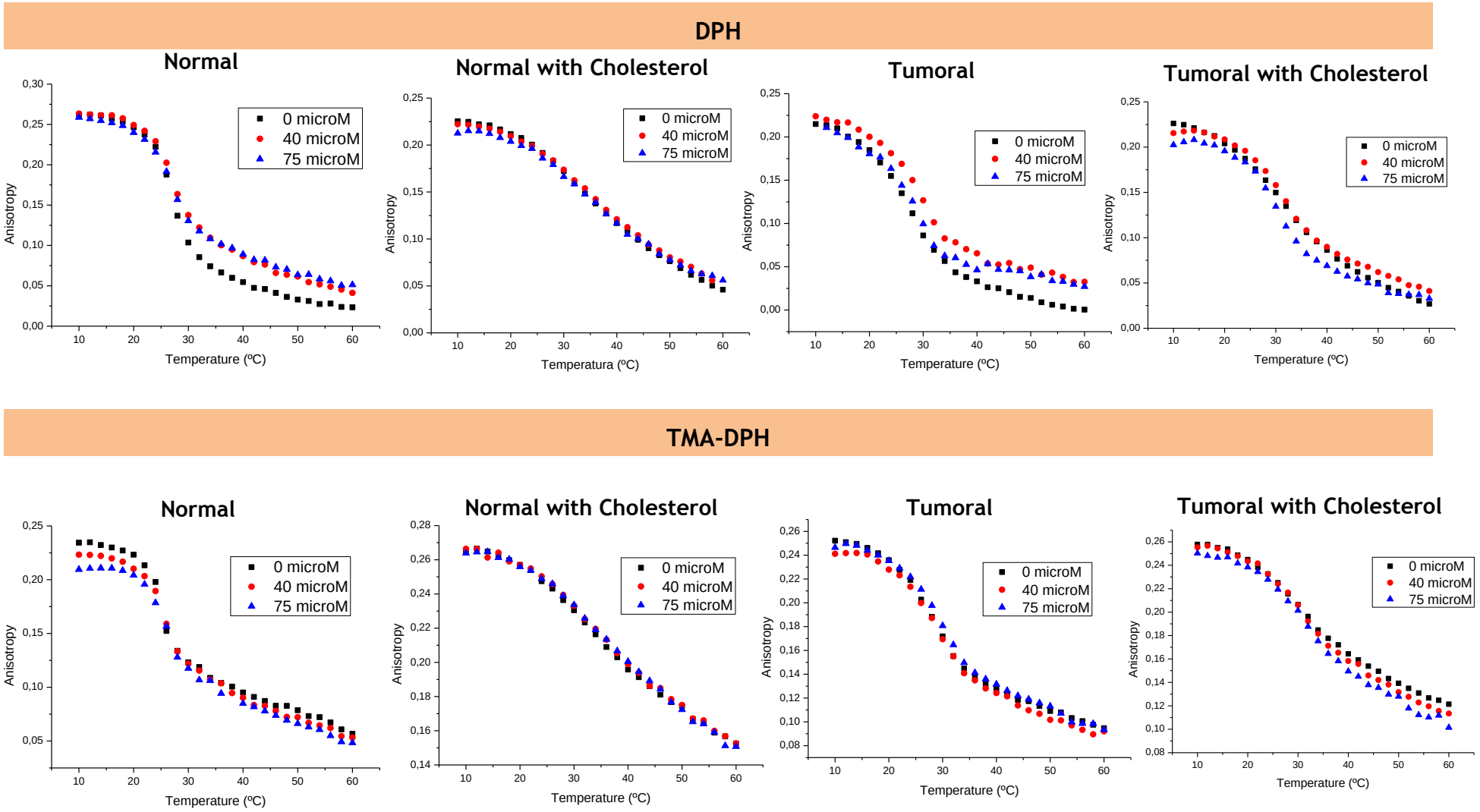

Figure 25 Anisotropy profiles for the four different liposome models designed labelled with both of the fluorescent probes used (DPH and TMA-DPH). For each model and each probe a sample with no drug and two other at drug concentrations of 40 and 75 μM were prepared and the profiles obtained are shown in this figure. This figure shows profiles where the drug used was daunorubicin.

In general, the normal model with cholesterol appears to be unchanged with the addition of drug for both probes. If we look back to the partition coefficients obtained for the model normal with cholesterol, these were very small for daunorubicin, which is consistent with the lack of alteration in fluidity.

For the tumoral models, at physiological temperature, the presence of daunorubicin seems to result in an increase in membrane rigidity at least at a more internal level of the bilayer, as seen in the profile obtained using DPH. The more interfacial or superficial zone of the membrane (given by TMA-DPH) seems to suffer no alterations. However, the tumoral model containing cholesterol appears to become more fluid in the same conditions in both regions, which is consistent with the fact that both drugs partition more into this model than the one without cholesterol. This observation supports the hypothesis that cholesterol, by bonding with the polar heads of certain lipids, creates microdomains that are rigid, but might be localized and leave the rest of the surface area more fluid. This is consistent with the values of K_p, which are higher for both drugs for the tumoral model that contains cholesterol.

Table 7 Phase transition temperatures (Tm) and Cooperativity values for the four models and the two probes (DPH and TMA-DPH) without daunorubicin and at daunorubicin concentrations of 40 and 75 μM.

		Tm (ºC)			Cooperativity		
		Drug Concentration			Drug Concentration		
Model	**Probe**	**0 μM**	**40 μM**	**75 μM**	**0 μM**	**40 μM**	**75 μM**
Normal	**DPH**	27.3 ± 0.7	27 ± 1	27.1 ± 0.8	166 ± 12	148 ± 12	150 ± 24
	TMA-DPH	25.14 ± 0.09	25.7 ± 0.1	25.6 ± 0.7	213 ± 11	168 ± 37	145.2 ± 0.6
Normal with Cholesterol	**DPH**	40 ± 3	39.6 ± 0.6	40 ± 0	62.2 ± 0.1	71 ± 8	69.52 ± 0.01
	TMA-DPH	38 ± 3	36 ± 2	40 ± 0	57 ± 5	70 ± 5	55 ± 5
Tumoral	**DPH**	29.00 ± 0.02	29 ± 1	29.2 ± 0.4	95 ± 10	168 ± 34	209 ± 10
	TMA-DPH	28.8 ± 0.9	29.1 ± 0.5	30 ± 1	111.5 ± 0.4	97 ± 36	156 ± 15
Tumoral with Cholesterol	**DPH**	35.0 ± 0.5	32 ± 1	30.88 ± 0.08	76 ± 8	122 ± 32	137 ± 12
	TMA-DPH	33.36 ± 0.06	31.44 ± 0.02	32 ± 1	70 ± 6	93 ± 12	97 ± 13

More information can be gathered from observing the phase transition temperature (T_m) and cooperativity values of the membrane models labeled with the two probes at these three concentrations of daunorubicin. This information can be seen in table 7.

The only clear tendency regarding the T_m is that it decreases for the tumoral with cholesterol model with the DPH probe, which means that the membrane becomes more fluid. The same appears to happen with the probe TMA-DPH. For the remaining models no tendency can be observed. That might be better explained by associating again with the results obtained for the membrane partition. Daunorubicin partitions the most into the membrane of the tumoral with cholesterol model, and that would make it so that this drug is more able to interact with the fluorescent probes in this model than in the other ones, justifying the aforementioned findings.

Regarding cooperativity, the cooperative zone is usually associated with the first segment of the acyl chains bound to the polar head of a phospholipid, commonly the C1-C8 region [110]. In this sense, daunorubicin appears to be located the interfacial region,since the cooperativity in this model increases with the increase in concentration of drug, and the

increase in cooperativity values is associated with an interaction with the polar heads [167]. Since the drug has a positively charged amine group at the pH values used in the study, these interactions with the polar heads are most likely between this amine group and the negatively charged phosphate groups of phospholipids.

The normal with cholesterol model is the one with which daunorubicin partitions the least, which is consistent with the lack of alteration in Tm and the very low values of cooperativity.

In the case of the models without cholesterol, it is shown that, although they partition similarly, the cooperativity values decrease in the case of the normal model but increase in the tumoral model. That might occur because the tumoral model is much more heterogeneous, and, since the drug is a small molecule, it can function the way that cholesterol does for the models containing cholesterol and organize the membrane lipids. In fact, phosphatidylserine, one of the lipids in the tumoral model membrane, possesses a very large polar head, that can favour the packing of a smaller molecule like daunorubicin. In a membrane as heterogeneous as the one from the tumoral model, the energy transmission is very heterogeneous as well. However, if the packing increases in the membrane as an effect of daunorubicin as theorized above, the energy transfer can become more homogeneous, which could explain the increase of cooperativity. The normal model is already very homogeneous since it is composed of only one lipid type. As such, any interference, like the inclusion of daunorubicin into the membrane, hinders the energy transfer, hence leading to the decrease in cooperativity.

The tumoral model becomes more rigid, which can be observed by the anisotropy profile for this model with DPH as well as by the increase in cooperativity. This doesn't seem to happen in the tumoral with cholesterol model. This could be explained by the possibility that daunorubicin, as explained above, may be associating with other constituents of the tumoral model membrane that make the membrane more rigid, while it can be making the tumoral with cholesterol membrane more fluid by disorganizing the membrane structure in this model, leading to the decrease in Tm.

The temperature-resolved anisotropy was also measured with the tumoral cells to assess the effect of daunorubicin, but the results produced did not make possible the acquisition of phase transition temperatures or cooperativity values. However, from the anisotropy profiles, depicted in figure 26, some inferences can be made. For example, it is noticeable that in the absence of drug, the polar region of the cell membrane bilayer is more rigid than the hydrophobic center. Curiously, the addition of daunorubicin seems to cause the polar regions of the membrane to become more fluid, while the hydrophobic chains become slightly more rigid. The biggest alterations in profile are found for the probe TMA-DPH, which indicates that also in the cell membrane of tumor cells the drug appears to locate in the cooperative zone, inserting in the acyl chains but also interacting with the polar heads. The observations for the tumoral cell anisotropy profiles are in fact similar to those made for the liposome tumoral with cholesterol model. This is more evidence that the models designed are in fact in the right path towards the validation of models for biophysical membrane studies.

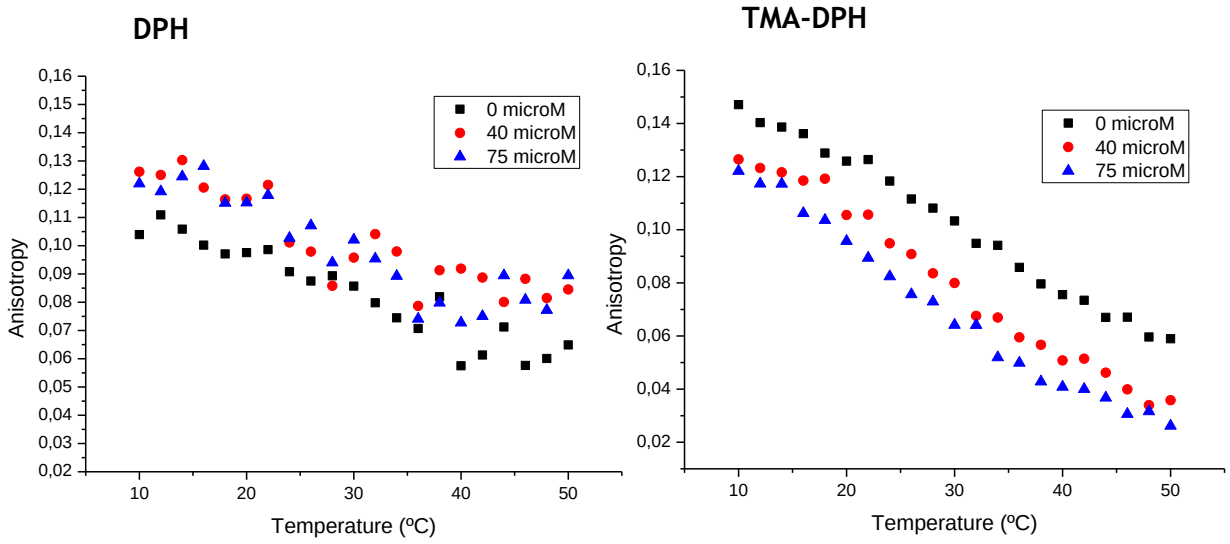

Figure 26 Anisotropy profiles for the tumoral cell line MDA-MB-231 labelled with both of the fluorescent probes used (DPH and TMA-DPH). Anisotropy was measured for samples with no drug, and at two concentrations of drug, 40 and 75 μM.

Temperature-resolved anisotropy measurements were also performed for a range of temperatures from 10 to 60ºC using the same models and probes but testing the drug doxorubicin. The anisotropy profiles of the four models labeled with two probes without drug and for two drug concentrations (40 and 75 μM) of doxorubicin are shown in figure 27.

Overall, the profiles found for doxorubicin are very similar to those found using the other drug tested, daunorubicin. As such, the same observations made for daunorubicin regarding fluidity by analysis of the anisotropy profile can be applied to the case of doxorubicin.

The phase transition temperature, Tm, and cooperativity were also determined for doxorubicin and are established in table 8.

Table 8 Phase transition temperatures (Tm) and Cooperativity values for the four models and the two probes (DPH and TMA-DPH) without doxorubicin and at doxorubicin concentrations of 40 and 75 μM.

		Tm (°C)			Cooperativity		
		Drug Concentration			Drug Concentration		
Model	**Probe**	**0 μM**	**40 μM**	**75 μM**	**0 μM**	**40 μM**	**75 μM**
Normal	**DPH**	26.83 ± 0.09	27.6 ± 0.1	27.80 ± 0.02	115 ± 2	127 ± 2	121 ± 12
	TMA-DPH	25.21 ± 0.01	25.7 ± 0.2	25.7 ± 0.9	198 ± 33	167 ± 40	139 ± 21
Normal with Cholesterol	**DPH**	39 ± 1	40.5 ± 0.6	38 ± 3	66 ± 10	62 ± 3	70 ± 12
	TMA-DPH	40.001 ± 0.002	40.000 ± 0.003	40.007 ± 0.008	67 ± 4	53 ± 5	71 ± 21
Tumoral	**DPH**	29 ± 0.8	30 ± 1	30.5 ± 0.8	89 ± 15	110 ± 20	118 ± 28
	TMA-DPH	29.1 ± 0.4	29.3 ± 0.8	31.2 ± 0.4	118 ± 5	111 ± 16	168 ± 31
Tumoral with Cholesterol	**DPH**	33 ± 0	31 ± 2	31 ± 1	87 ± 0	83 ± 25	94 ± 12
	TMA-DPH	33.34 ± 0.05	31.39 ± 0.08	32 ± 1	70 ± 6	91 ± 14	85 ± 3

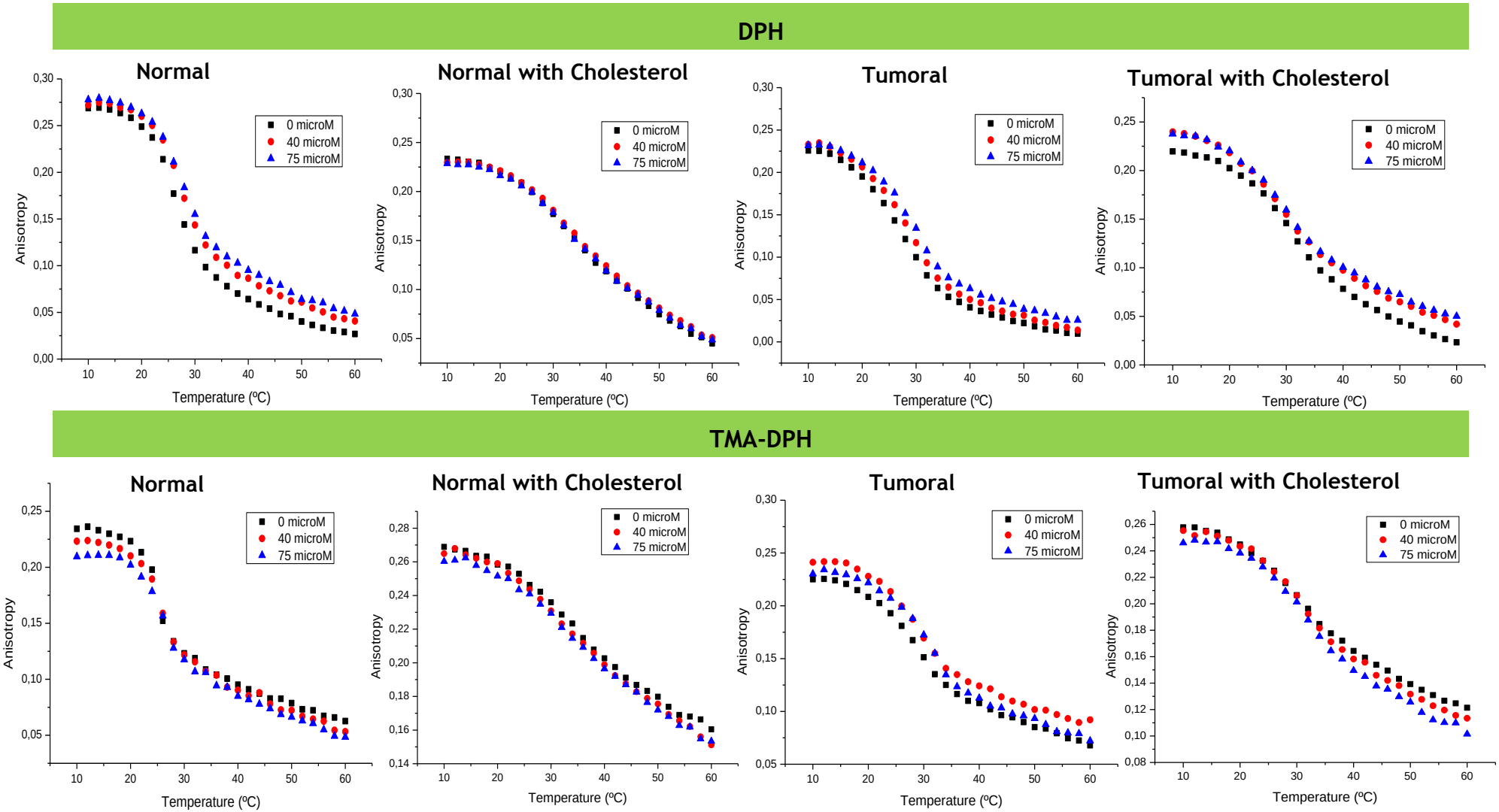

Figure 27 Anisotropy profiles for the four different liposome models designed labelled with both of the fluorescent probes used (DPH and TMA-DPH). For each model and each probe a sample with no drug and two other at drug concentrations of 40 and 75 μM were prepared and the profiles obtained are shown in this figure. This figure shows profiles where the drug used was doxorubicin.

However, as opposed to what occurs in relation to daunorubicin, doxorubicin does not seem to produce any tendency towards Tm alteration in any of the membrane models, but some similarities in the tendencies of the cooperativity values can be seen. A tendency towards a decrease in cooperativity can be observed using the probe TMA-DPH for the normal model, which means that the energy transfer at the polar head region of the bilayer in being impaired with the addition of doxorubicin. As such, an explanation might be that the normal bilayer, made up of only one type of lipid, is very homogeneous, and therefore in normal conditions, energy transfer happens smoothly and homogeneously. When an exogenous factor is introduced, in this case, the doxorubicin drug molecule, the homogeneity is impaired, and the energy transfer as a result is as well, resulting in a decrease in cooperativity. This means that the molecules can be located near the phospholipid headgroup, then moving away. In the case of the tumoral model, the opposed tendency happens, so the cooperativity increases. This might be again because the tumoral model membrane is already heterogeneous, and in such a case, the doxorubicin molecule might actually come to have a stabilizing effect, with its amine group interacting with the phosphate groups from the polar heads of the phospholipids and the remaining of the molecule interacting via hydrogen bonds or Van der Waals forces with the cooperative zone. A more stable structure facilitates the passage of energy, which explains the increase in cooperativity for this model with the increase in doxorubicin concentration.

4.4.2. Steady-State Anisotropy

Steady-state anisotropy was also measured using liposomes of the four models labeled with either DPH or TMA-DPH to assess the effect of increasing concentration of daunorubicin at 37ºC. The results of such measurements are represented in figure 28.

Using the probe DPH, it can be seen that the normal with cholesterol membrane model suffers no alterations in fluidity at the physiological temperature, which is consistent with all the previous data. The normal and tumoral models seem to become slightly more rigid at the hydrophobic area at concentrations of drug up to 20 μM. This is in agreement with the findings through temperature-resolved anisotropy. Interestingly, above that concentration of drug, this effect stagnates, which seems to suggest that a saturation level is achieved, and that these models can only incorporate the drug up to a certain concentration, which would be, as mentioned, approximately 20 μM. It could perhaps be useful to try to perform temperature-resolved anisotropy measurements for these (or all) models again but using drug concentrations below 20 μM. In that situation, the measurements would be performed in conditions where the drug was still being incorporated and not after the membrane was saturated, which could allow the determination of more distinct profiles with more accurate phase transition temperatures and cooperativity values.

As for the tumoral with cholesterol model, it does not suffer alterations until higher concentrations of drug are achieved (40 and 75 μM), at which point the membrane becomes more fluid. The same seems to happen to tumoral cells, which presents another biophysical similarity between the models designed and the cells they were designed after.

When focusing on the more superficial area of the bilayer by attending to the anisotropy at 37ºC obtained for TMA-DPH-labeled cells, one can once again verify no changes in fluidity associated with the normal with cholesterol model. Unexpected, however, could be the fact

that no changes can be seen for the tumoral with cholesterol model either, which is very different than what is found for tumoral cells, whose membrane appears to become more fluid also at the polar regions. However, one must keep in mind that these are still very simple models compared to cells, which usually possess a variety of proteins, ions and molecules anchored to its surface, something that was not mimicked in this study. As for the normal and tumoral models, no alterations can be seen unless at higher concentrations of drug (40 and 75μM), at which the membrane becomes slightly more fluid.

As such, it can be concluded that the drug daunorubicin appears to have a packing effect on the hydrophobic region of the phospholipids, probably at the cooperative zone, for the models without cholesterol, while making the membrane of the tumoral with cholesterol model more fluid at that region, being consistent with the findings for tumoral cells.

Summarily, this is in accord with the idea that the drug probably is located in the cooperative zone while also interacting with the polar heads of phospholipids. Furthermore, it confirms some more similarities between the models of this study and the membranes of tumoral cells, which proves this study to be a great and crucial step towards the validation and standardized use of liposomes as model membranes in biophysical studies.

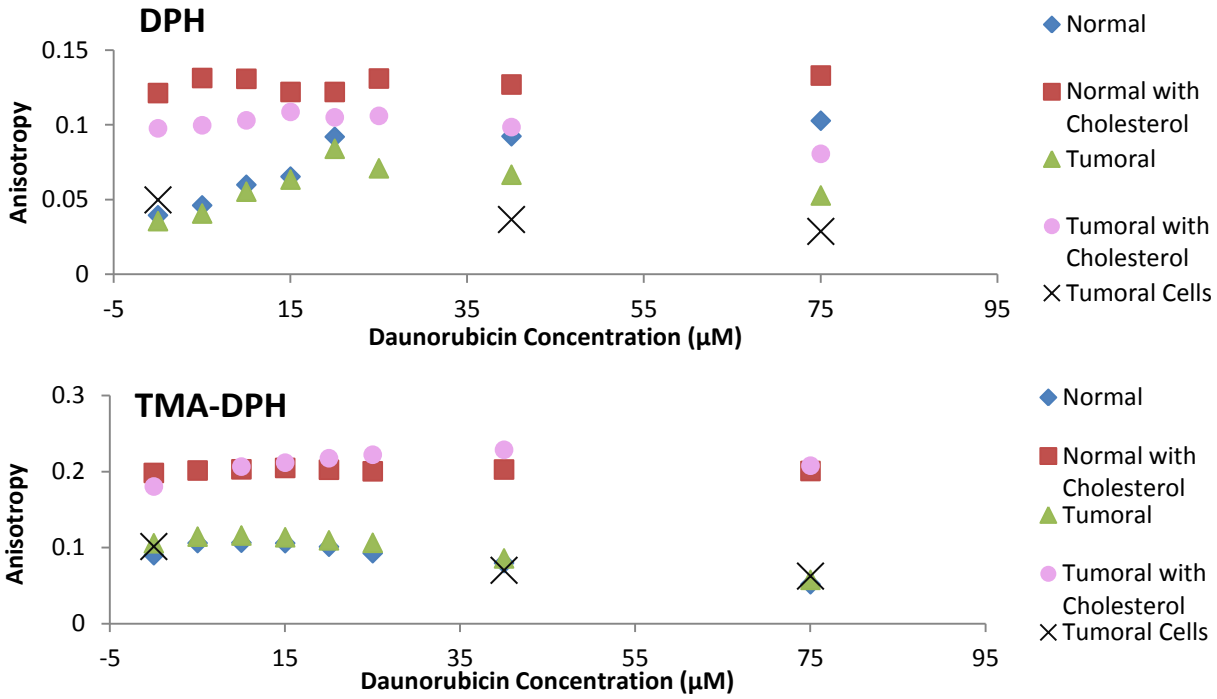

Figure 28 Steady-state anisotropy values found using DPH and TMA-DPH fluorescent probes on for the four membrane models and the tumoral cells MDA-MB-231 with no drug or under the effect of daunorubicin.

4.5- Cell Viability

To ensure that the probes and drug used did not induce a level of cytotoxicity that could jeopardize the results, cell viability was confirmed by counting the live cells via the Trypan Blue Exclusion method before and after incubation with the compounds. Although this assay is not a valid choice when viability is in fact the key parameter in study, since the intention was only to confirm that there was a high percentage of live cells even after the assays were finished, a simple counting method such as this was employed.

Figure 29 shows the percentage of cells before and after the addition and incubation for 1 hour with the used probes.

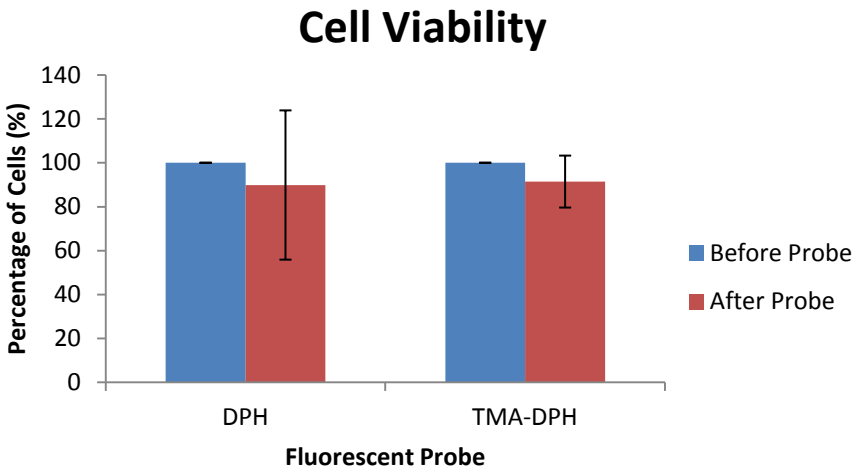

Figure 29 Percentage of cells counted before and after the incubation of the cells for 1 hour with the probes.

The number of cells counted before the addition of any probe was normalized to correspond to 100%. The results show that the both of the probes appear to be innocuous, since the percentage of cells after incubations remains approximately the same. As such, the methodologies could proceed.

Since the drugs used are cytotoxic, the assays were performed by keeping the time of contact between the cells and the drugs to a minimum. To ensure that the measurements were correctly performed, cells were counted once again after the different methods were employed and the results are presented in figure 30.

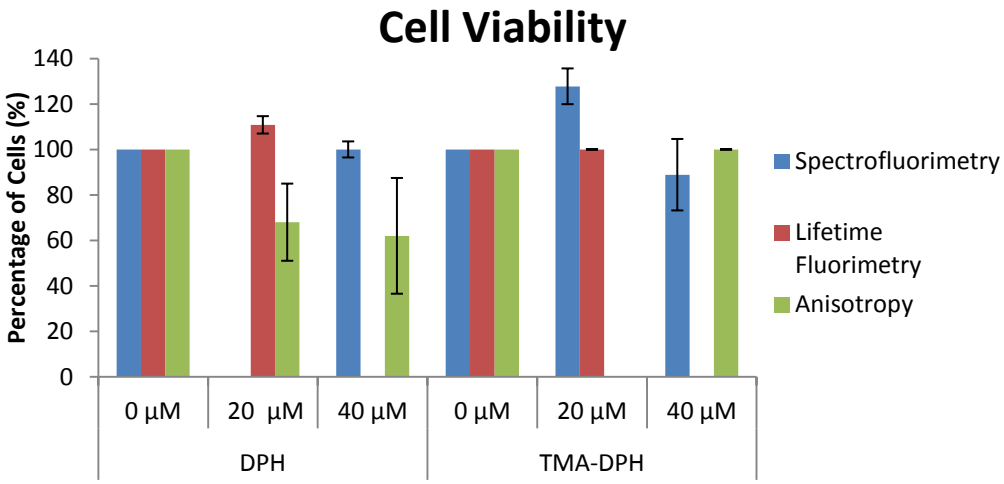

Figure 30 Percentage of cells counted after the employed methodologies. The number of cells counted for the suspension without drug (0 µM) was normalized to represent 100%. The samples containing 20 µM and 40 µM of daunorubicin (for both probes) were chosen and the cells in them counted to ensure viability after the assays.

As can be seen, the percentage of cells counted after the execution of the assays was never below 60%, and as such it can be considered that the techniques were performed correctly and the measurements obtained corresponded in fact to the labeled cells.

In both figures though, the standard deviation values can be quite high. However, one have to keep in mind that the counting method is very subjective, highly depending on the operator, the equipment used, and a number of other variables impossible to control, which makes this a not very precise assay. Nonetheless, it is reliable enough to guarantee that the techniques were correctly performed.

Chapter 5

Conclusions

Size measurements confirmed that the models were prepared as intended, with liposome diameters being close to 100 nm. Neither drug seemed to affect liposome size. Zeta potential confirmed that normal model membranes had a surface charge close to neutral and tumoral model membranes were slightly negatively charged, which is consistent with what happens naturally. Increase in drug concentration made the potential less negative, meaning that the drug, positively charged at the pH used, was most likely interacting with the membrane. This is consistent with what is found in literature since the mechanism of action of both drugs involves intercalating the DNA molecule, and to access the DNA the drug has to have the ability to cross the membrane, so a drug-membrane interaction needs to occur [7].

K_p determination showed that the two drugs, although very similar in structure, partition very differently into the different mimetic systems. The highest Kp is found for the normal model, since this is the simplest and therefore most homogeneous one, composed of only one fluid lipid that creates a quite porous membrane, which is confirmed by the fact that the normal model presents the lowest phase transition temperatures of all models studied. Partition for the two drugs decreases with the presence of cholesterol in the membrane for normal models, but the opposite occurs for the tumoral models. Doxorubicin partitions more than daunorubicin for all models except tumoral with cholesterol.

In both models without cholesterol, daunorubicin appears to localize between the acyl chains of phospholipids in the membrane while still interacting through electrostatic interactions with the polar heads, so it appears to locate at an intermediate region. A previous study showed that doxorubicin's location in DPPC models was between the acyl chains of the phospholipids [88]. This is an interesting finding – since doxorubicin is more hydrophobic, it locates in hydrophobic regions of the bilayer, while in our study we have found that daunorubicin, which is less hydrophobic, is able to locate between the acyl chains and also interact with the polar headgroup of phospholipids, which makes sense.

Using the tumoral cells results were obtained that indicate that the drug located at a more superficial level, and the impairment in the entrance into the membrane might be related to the high complexity and variety of its components. As such, some of similarities could be drawn between the tumoral models and the tumoral cells, which leads to believe that the formulations designed in this study did a quite good job at mimicking the cell

membranes they intended to mimic, which is very good considering this is a first step toward that objective. Also very interesting is to keep in mind that we were able to prove or confirm that membrane location can be assessed for cells through the same techniques employed for liposomes and that enlightening results can be obtained.

In terms of fluidity, the normal model with cholesterol appears to be the most rigid of all and remains unchanged by the drugs, while the normal model is highly fluid. Contrarily to what was expected, the tumoral model with cholesterol becomes more fluid at the interfacial or more superficial region (TMA-DPH region) with the addition of either drug fluid with the presence of drug, which does not happen in the tumoral model without cholesterol. The same is curiously found for the profiles obtained using the cells under the effect of daunorubicin, which further supports that the models were very good cell membrane simulators. Also, it is very important that profiles of anisotropy along a range of temperatures were obtaines for cells, which had not been described before either, and would be thought to be impossible due to the cells complexity.

It is also important to note that, looking at the viability results, the techniques could be performed while maintained a high rate of live cells in the sample (always above 60%), which proves that these methodologies can continue to be employed in this sense.

To justify the obtained results, the cholesterol might be forming microdomains with some of the lipids of the tumoral model, increasing the rigidity of the membrane in the areas those domains begin to exist, but making the remaining portion of the membrane more permeable. This hypothesis makes sense considering the higher partition into the tumoral with cholesterol model which is the most interesting one at a physiological level since it was designed to mimic the tumoral cell membrane. A high partition of both drugs into the membrane as well as the increase in membrane fluidity for this model is according to the fact that they are some of the most effective drugs in the treatment of cancer since a high partition indicates high interaction with the membrane and probably higher ability to cross the membrane. The fact that doxorubicin has higher partition coefficient for all the mimetic systems except the tumoral with cholesterol one can justify the higher severity of its side effects in comparison to daunorubicin [119-121].

Overall it appears that the models projected were a good example to study the interactions between these two drugs and the membrane, providing some enticing and clarifying information. The membrane location and fluidity studies using cells are a complete novelty in this field that produced interesting results, that to a certain degree allow validating the tumoral models in this study and can help in the future to develop even more accurate models that can be revolutionary to the world of membrane biophysics as we know it now.

This study and follow-up work can be a big step towards the validation of liposomes as models for cell membranes, and in the future allow the facilitation of drug-interaction studies. Possible future applications would involve not only the use in research but the introduction of the models at an industrial level for an easier, less expensive and quicker development of new drugs or delivery systems for the treatment of several diseases that are more efficient and with fewer side effects.

Chapter 6

Future Work

In the future, membrane location studies should also be performed using the four liposome models and the tumoral cells for the drug doxorubicin.

The same studies (membrane location and anisotropy) should also be performed on MCF 10A cells, which are cells from normal breast gland tissue and, as such, the normal counterpart of the tumoral cells used. These studies would not only allow a comparison with the results obtained for the normal models with intent to improve them but also allow a comparison of the behaviour of the drugs in normal and tumoral biomembranes.

It would also be interesting to determine the partition coefficient using both lines of cells (MDA-MB-231, tumoral, and MCF 10A, normal), which would be useful to compare with the findings from the other techniques. For that purpose, a protocol should be designed, since at the moment there is no protocol that confirms the possibility of use of the derivative spectrophotometry to determine the Kp using cells.

Further ahead, it would be important to perform all of these studies in other tumoral and normal cell lines, since the effect of drugs varies from cell type to cell type, not only due to their cell membrane but also due to internal molecular processes that differ depending on the tissue.

After the execution of these studies, we would be equipped to draw conclusions that would allow the alteration of the models in this study to further resemble the actual biomembranes. Eventually, with the knowledge acquired, validation of the models could be performed and there would henceforth be a model membrane for breast adenocarcinoma. With further research there could be in the future the development of models for several cancer types or even several diseases other than cancer. This could then allow the study of not only drug-membrane interactions, but also of the effect of proteins that exist inserted or anchored to the biomembranes using the models created, which is another very enticing and essential line of work.

Chapter 7

References

1. Singh, S., *Pharmacology for Dentistry* 1st ed. Apr, 2007: New age International.
2. Brown, A., J. Chen, and Y. Hitchcock, *The risk of second primary malignancies up to three decades after the treatment of differentiated thyroid cancer.* The Journal of Clinical Endocrinology & Metabolism, 2008. **93 (2)**: p. 504-515.
3. Rang, H.P., et al. 2007: Elsevier Science Health Science div. 829.
4. Doll, R., C.S. Muir, and J. Waterhouse, *Cancer incidence in five continents, Volume II*, 1970, International Unit Against Cancer: Geneva.
5. Brunton, L., et al., *Goodman and Gilman's Manual of Pharmacology and Therapeutics*. 2007: McGraw Hill Professional. 642.
6. Doyle, P. and B. Levin, *World Cancer Report 2008*, 2008, World Health Organization - International Agency for Research on Cancer: Lyon, France.
7. Katzung, B.G., S.B. Masters, and A.J. Trevor, *Basic and Clinical Pharmacology*. 11th edition ed. 2009: McGraw -Hill Medical.
8. Hanahan, D. and R.A. Weinberg, *Hallmarks of cancer: the next generation.* Cell, 2011. **144**(5): p. 646-74.
9. ACS. *American Cancer Society - Information and Resources for Cancer: Breast, Colon, Lung, Prostate, Skin*. 2014 [cited 2014; Available from: http://www.cancer.org.
10. Weinshilboum, R., *Inheritance and Drug Response.* New England Journal of Medicine, 2003. **348**(6): p. 529-537.
11. Bateman, D.N. and M. Eddleston, *Clinical pharmacology: the basics.* Medicine, 2008. **36**(7): p. 339-343.
12. Hacker, M.P., W.S. Messer, and K.A. Bachmann, *Pharmacology: Principles and Practice*. 2009: Academic Press.
13. Golan, D.E., et al., *Principles of Pharmacology - The Pathophysiologic Basis of Drug Therapy*. 2nd ed, ed. L.W. Wilkins. 2011.
14. Kalow W, Tang BK, and E. I., *Hypothesis: comparisons of inter- and intra-individual variations can substitute for twin studies in drug research.* Pharmacogenetics, 1998. **8**: p. 283-9.
15. Eichelbaum, M., *Pharmacogenomics and individualized drug therapy.* Annual Review of Medicine, 2006. **57**: p. 119.
16. Achour, O., et al., *Cathepsin D activity and selectivity in the acidic conditions of a tumor microenvironment: Utilization in the development of a novel Cathepsin D substrate for simultaneous cancer diagnosis and therapy.* Biochimie, 2013. **95**(11): p. 2010-2017.
17. Fessler, E., et al., *Cancer stem cell dynamics in tumor progression and metastasis: Is the microenvironment to blame?* Cancer Letters, 2013. **341**(1): p. 97-104.
18. Cohen, A., et al., *A mass spectrometry-based plasma protein panel targeting the tumor microenvironment in patients with breast cancer.* Journal of Proteomics, 2013. **81**(0): p. 135-147.
19. Castaño, Z., et al., *The bed and the bugs: Interactions between the tumor microenvironment and cancer stem cells.* Seminars in Cancer Biology, 2012. **22**(5–6): p. 462-470.
20. Hu, M. and K. Polyak, *Molecular characterisation of the tumour microenvironment in breast cancer.* European Journal of Cancer, 2008. **44**(18): p. 2760-2765.
21. Filip, A.A., et al., *Circulating microenvironment of CLL: Are nurse-like cells related to tumor-associated macrophages?* Blood Cells, Molecules, and Diseases, 2013. **50**(4): p. 263-270.

22. Pal, S., B.S. Shankar, and K.B. Sainis, *Cytokines from the tumor microenvironment modulate sirtinol cytotoxicity in A549 lung carcinoma cells*. Cytokine, 2013. **64**(1): p. 196-207.
23. Liu, Y., et al., *The microenvironment in classical Hodgkin lymphoma: An actively shaped and essential tumor component*. Seminars in Cancer Biology, 2014. **24**(0): p. 15-22.
24. Turner, K.E., et al., *Proteomic Analysis of Neuroblastoma Microenvironment: Effect of the Host-Tumor Interaction on Disease Progression*. Journal of Surgical Research, 2009. **156**(1): p. 116-122.
25. McLeod, H.L. and W.E. Evans, *Pharmacogenomics: Unlocking the human genome for better drug therapy*. Annual Review of Pharmacology and Toxicology, 2001. **41**: p. 101-121.
26. Barrett, J.C. and R.W. Wiseman, *Cellular and molecular mechanisms of multistep carcinogenesis: relevance to carcinogen risk assessment*. Environ Health Perspect, 1987. **76**: p. 65-70.
27. Evans, W.E. and H.L. McLeod, *Pharmacogenomics — Drug Disposition, Drug Targets, and Side Effects*. New England Journal of Medicine, 2003. **348**(6): p. 538-549.
28. Zhang, X., et al., *Involvement of the Immune System in Idiosyncratic Drug Reactions*. Drug Metabolism and Pharmacokinetics, 2011. **26**(1): p. 47-59.
29. Pitot, H.C., T. Goldsworthy, and S. Moran, *The natural history of carcinogenesis: Implications of experimental carcinogenesis in the genesis of human cancer*. Journal of Supramolecular Structure and Cellular Biochemistry, 1981. **17**(2): p. 133-146.
30. Ingelman-Sundberg, M. and A. Gomez, *The past, present and future of pharmacoepigenomics*. Pharmacogenomics, 2010. **11**(5): p. 625-7.
31. Tesfa, D., M. Keisu, and J. Palmblad, *Idiosyncratic drug-induced agranulocytosis: Possible mechanisms and management*. American Journal of Hematology, 2009. **84**(7): p. 428-434.
32. Rang, H.P., et al., *Rang and Dale's Pharmacology*. 7th ed. 2012: Elsevier Inc. 792.
33. Evans, W.E. and M.V. Relling, *Moving towards individualized medicine with pharmacogenomics*. Nature, 2004. **429**(6990): p. 464-468.
34. Boon, W. and E. Moors, *Exploring emerging technologies using metaphors – A study of orphan drugs and pharmacogenomics*. Social Science & Medicine, 2008. **66**(9): p. 1915-1927.
35. Ferrara, N., *Vascular Endothelial Growth Factor*. Arteriosclerosis, Thrombosis, and Vascular Biology, 2009. **29**(6): p. 789-791.
36. Nebert, D.W. and E.S. Vesell, *Advances in pharmacogenomics and individualized drug therapy: exciting challenges that lie ahead*. European Journal of Pharmacology, 2004. **500**(1–3): p. 267-280.
37. Almarsdóttir, A.B., I. Björnsdóttir, and J.M. Traulsen, *A lay prescription for tailor-made drugs—focus group reflections on pharmacogenomics*. Health Policy, 2005. **71**(2): p. 233-241.
38. Issa, A.M., *Ethical considerations in clinical pharmacogenomics research*. Trends in Pharmacological Sciences, 2000. **21**(7): p. 247-249.
39. Mordini, E., *Ethical considerations on pharmacogenomics*. Pharmacol Res, 2004. **49**(4): p. 375-9.
40. Gosselin-Acomb, T., *Principles of Radiation Therapy*, in *Cancer Nursing Principles and Practice*, C. Henke Yarbro, M. Hansen Frogge, and M. Goodman, Editors. 2005, Jones and Bartlett Publishers, Inc.: Boston. p. 229-249.
41. Silberman, H. and A.W. Silberman, *Principles and Practice of Surgical Oncology: Multidisciplinary Approach to Difficult Problems*. 2009: Wolters Kluwer Health/Lippincott Williams & Wilkins.
42. Golan, D.E., et al., *Principles of Pharmacology - The Pathophysiologic Basis of Drug Therapy*. 3rd edition ed, ed. D.E. Golan. 2011: Lippincott Williams & Wilkins. 976 pages.
43. Cheng, N., et al., *Transforming Growth Factor-β Signaling-Deficient Fibroblasts Enhance Hepatocyte Growth Factor Signaling in Mammary Carcinoma Cells to*

Promote Scattering and Invasion. Molecular Cancer Research, 2008. **6**(10): p. 1521-1533.
44. Busto, J.V., et al., *Surface-active properties of the antitumour ether lipid 1-O-octadecyl-2-O-methyl-rac-glycero-3-phosphocholine (edelfosine)*. Biochimica et Biophysica Acta (BBA) - Biomembranes, 2007. **1768**(7): p. 1855-1860.
45. Hąc-Wydro, K., et al., *Edelfosine disturbs the sphingomyelin-cholesterol model membrane system in a cholesterol-dependent way – The Langmuir monolayer study*. Colloids and Surfaces B: Biointerfaces, 2011. **88**(2): p. 635-640.
46. Saint-Laurent, A., et al., *Membrane interactions of a new class of anticancer agents derived from arylchloroethylurea: a FTIR spectroscopic study*. Chemistry and Physics of Lipids, 2001. **111**(2): p. 163-175.
47. Corrie, P.G., *Cytotoxic chemotherapy: clinical aspects*. Medicine, 2011. **39**(12): p. 717-722.
48. Gabhann, F.M. and A.S. Popel, *Systems Biology of Vascular Endothelial Growth Factors*. Microcirculation, 2008. **15**(8): p. 715-738.
49. *Targeted Cancer Therapies Fact Sheet - National Cancer Institute*. 2014 [cited 2015; Available from: http://www.cancer.gov/about-cancer/treatment/types/targeted-therapies/targeted-therapies-fact-sheet.
50. Peetla, C., A. Stine, and V. Labhasetwar, *Biophysical interactions with model lipid membranes: applications in drug discovery and drug delivery*. Mol Pharm, 2009. **6**(5): p. 1264-76.
51. Dimanche-Boitrel, M.-T., et al., *Role of early plasma membrane events in chemotherapy-induced cell death*. Drug Resistance Updates, 2005. **8**(1–2): p. 5-14.
52. Lodish, H., et al., *Membrane Proteins*, in *Molecular Cell Biology*2000, W. H. Freeman: New York.
53. Szachowicz-Petelska, B., et al., *Characterization of the cell membrane during cancer transformation*. Journal of Environmental Biology, 2010. **31**(5): p. 845-850.
54. Yamaji-Hasegawa, A. and M. Tsujimoto, *Asymmetric distribution of phospholipids in biomembranes*. Biol Pharm Bull, 2006. **29**(8): p. 1547-53.
55. Ran, S., A. Downes, and P.E. Thorpe, *Increased exposure of anionic phospholipids on the surface of tumor blood vessels*. Cancer Res, 2002. **62**(21): p. 6132-40.
56. Zwaal, R.F., P. Comfurius, and E.M. Bevers, *Surface exposure of phosphatidylserine in pathological cells*. Cell Mol Life Sci, 2005. **62**(9): p. 971-88.
57. Selkirk, J.K., J.C. Elwood, and H.P. Morris, *Study on the Proposed Role of Phospholipid in Tumor Cell Membrane*. Cancer Research, 1971. **31**(1): p. 27-31.
58. Baro, L., et al., *Abnormalities in plasma and red blood cell fatty acid profiles of patients with colorectal cancer*. Br J Cancer, 1998. **77**(11): p. 1978-83.
59. Hildebrand, J., D. Marique, and J. Vanhouche, *Lipid composition of plasma membranes from human leukemic lymphocytes*. J Lipid Res, 1975. **16**(3): p. 195-9.
60. Liebes, L.F., et al., *Comparison of lipid composition and 1,6-diphenyl-1,3,5-hexatriene fluorescence polarization measurements of hairy cells with monocytes and lymphocytes from normal subjects and patients with chronic lymphocytic leukemia*. Cancer Res, 1981. **41**(10): p. 4050-6.
61. Alberts, B., A. Johnson, and J. Lewis, *The Lipid Bilayer*, in *Molecular Biology of the Cell*, G. Science, Editor 2002, Garland Science: New York.
62. Luostarinen, R., M. Boberg, and T. Saldeen, *Fatty acid composition in total phospholipids of human coronary arteries in sudden cardiac death*. Atherosclerosis, 1993. **99**(2): p. 187-193.
63. Mason, R.P. and R.F. Jacob, *Membrane Microdomains and Vascular Biology: Emerging Role in Atherogenesis*. Circulation, 2003. **107**(17): p. 2270-2273.
64. Perona, J.S. and V. Ruiz-Gutierrez, *Triacylglycerol molecular species are depleted to different extents in the myocardium of spontaneously hypertensive rats fed two oleic acid-rich oils**. American Journal of Hypertension, 2005. **18**(1): p. 72-80.
65. Diehn, M., R.W. Cho, and M.F. Clarke, *Therapeutic Implications of the Cancer Stem Cell Hypothesis*. Seminars in radiation oncology, 2009. **19**(2): p. 78-86.

66. Lladó, V., et al., *Regulation of the cancer cell membrane lipid composition by NaCHOleate: Effects on cell signaling and therapeutical relevance in glioma.* Biochimica et Biophysica Acta (BBA) - Biomembranes, 2014. **1838**(6): p. 1619-1627.
67. Li, Y., et al., *Implications of cancer stem cell theory for cancer chemoprevention by natural dietary compounds.* The Journal of Nutritional Biochemistry, 2011. **22**(9): p. 799-806.
68. Crea, F., et al., *Pharmacogenomics and cancer stem cells: a changing landscape?* Trends in Pharmacological Sciences, 2011. **32**(8): p. 487-494.
69. Pignatello, R., et al., *Biomembrane models and drug-biomembrane interaction studies: Involvement in drug design and development.* J Pharm Bioallied Sci, 2011. **3**(1): p. 4-14.
70. Gillies, R.J., et al., *A unifying theory of carcinogenesis, and why targeted therapy doesn't work.* European journal of radiology, 2012. **81**: p. S48-S50.
71. Dean, M., T. Fojo, and S. Bates, *Tumour stem cells and drug resistance.* Nat Rev Cancer, 2005. **5**(4): p. 275-284.
72. Wu, C. and B.A. Alman, *Side population cells in human cancers.* Cancer letters, 2008. **268**(1): p. 1-9.
73. van Thuijl, H.F., et al., *Genetics and pharmacogenomics of diffuse gliomas.* Pharmacology & Therapeutics, (0).
74. Berns, A., *Stem Cells for Lung Cancer?* Cell, 2005. **121**(6): p. 811-813.
75. Seddon, A.M., et al., *Drug interactions with lipid membranes.* Chem Soc Rev, 2009. **38**(9): p. 2509-19.
76. Pereira-Leite, C., C. Nunes, and S. Reis, *Interaction of nonsteroidal anti-inflammatory drugs with membranes: in vitro assessment and relevance for their biological actions.* Prog Lipid Res, 2013. **52**(4): p. 571-84.
77. Bildstein, L., et al., *Interaction of an amphiphilic squalenoyl prodrug of gemcitabine with cellular membranes.* European Journal of Pharmaceutics and Biopharmaceutics, 2011. **79**(3): p. 612-620.
78. Bilge, D., et al., *Interactions of tamoxifen with distearoyl phosphatidylcholine multilamellar vesicles: FTIR and DSC studies.* Spectrochimica Acta Part A: Molecular and Biomolecular Spectroscopy, 2014. **130**(0): p. 250-256.
79. Bilge, D., N. Kazanci, and F. Severcan, *Acyl chain length and charge effect on Tamoxifen-lipid model membrane interactions.* Journal of Molecular Structure, 2013. **1040**(0): p. 75-82.
80. Zhao, L., et al., *DSC and EPR investigations on effects of cholesterol component on molecular interactions between paclitaxel and phospholipid within lipid bilayer membrane.* International Journal of Pharmaceutics, 2007. **338**(1–2): p. 258-266.
81. Speelmans, G., et al., *The interaction of the anti-cancer drug cisplatin with phospholipids is specific for negatively charged phospholipids and takes place at low chloride ion concentration.* Biochimica et Biophysica Acta (BBA) - Biomembranes, 1996. **1283**(1): p. 60-66.
82. Pignatello, R., et al., *Lipophilic conjugates of methotrexate with glucosyl-lipoamino acids: calorimetric study of the interaction with a biomembrane model.* Thermochimica Acta, 2005. **426**(1–2): p. 163-171.
83. Pentak, D., *Physicochemical properties of liposomes as potential anticancer drugs carriers. Interaction of etoposide and cytarabine with the membrane: spectroscopic studies.* Spectrochim Acta A Mol Biomol Spectrosc, 2014. **122**: p. 451-60.
84. Pili, B., et al., *Interaction of a new anticancer prodrug, gemcitabine-squalene, with a model membrane: Coupled DSC and XRD study.* Biochimica et Biophysica Acta (BBA) - Biomembranes, 2010. **1798**(8): p. 1522-1532.
85. Li, X., et al., *Doxorubicin physical state in solution and inside liposomes loaded via a pH gradient.* Biochimica et Biophysica Acta (BBA) - Biomembranes, 1998. **1415**(1): p. 23-40.
86. Więcek, A., et al., *Interactions between an anticancer drug – edelfosine – and DPPC in Langmuir monolayers.* Colloids and Surfaces A: Physicochemical and Engineering Aspects, 2008. **321**(1–3): p. 201-205.

87. de Wolf, F.A., et al., *Characterization of the interaction of doxorubicin with (poly)phosphoinositides in model systems Evidence for specific interaction with phosphatidylinositol-monophosphate and -diphosphate*. FEBS Letters, 1991. **288**(1–2): p. 237-240.
88. Gaber, M.H., et al., *Interaction of Doxorubicin with phospholipid monolayer and liposomes*. Biophysical Chemistry, 1998. **70**(3): p. 223-229.
89. Nieciecka, D., et al., *Partitioning of doxorubicin into Langmuir and Langmuir-Blodgett biomimetic mixed monolayers: Electrochemical and spectroscopic studies*. Journal of Electroanalytical Chemistry, 2013. **710**(0): p. 59-69.
90. Preetha, A., N. Huilgol, and R. Banerjee, *Comparison of paclitaxel penetration in normal and cancerous cervical model monolayer membranes*. Colloids and Surfaces B: Biointerfaces, 2006. **53**(2): p. 179-186.
91. Labbé, J.-F., et al., *Spectroscopic characterization of DMPC/DOTAP cationic liposomes and their interactions with DNA and drugs*. Chemistry and Physics of Lipids, 2009. **158**(2): p. 91-101.
92. Gomide, A.B., et al., *Disrupting membrane raft domains by alkylphospholipids*. Biochimica et Biophysica Acta (BBA) - Biomembranes, 2013. **1828**(5): p. 1384-1389.
93. Jensen, M. and W. Nerdal, *Anticancer cisplatin interactions with bilayers of total lipid extract from pig brain: A 13C, 31P and 15N solid-state NMR study*. European Journal of Pharmaceutical Sciences, 2008. **34**(2–3): p. 140-148.
94. Jensen, M., et al., *Cisplatin interaction with phosphatidylserine bilayer studied by solid-state NMR spectroscopy*. J Biol Inorg Chem, 2010. **15**(2): p. 213-23.
95. Gallois, L., M. Fiallo, and A. Garnier-Suillerot, *Comparison of the interaction of doxorubicin, daunorubicin, idarubicin and idarubicinol with large unilamellar vesicles: Circular dichroism study*. Biochimica et Biophysica Acta (BBA) - Biomembranes, 1998. **1370**(1): p. 31-40.
96. Burger, K.N.J., R.W.H.M. Staffhorst, and B. De Kruijff, *Interaction of the anti-cancer drug cisplatin with phosphatidylserine in intact and semi-intact cells*. Biochimica et Biophysica Acta (BBA) - Biomembranes, 1999. **1419**(1): p. 43-54.
97. Bourgaux, C. and P. Couvreur, *Interactions of anticancer drugs with biomembranes: What can we learn from model membranes?* Journal of Controlled Release, 2014(0).
98. Seydel, J.K. and M. Wiese, *Drug-Membrane Interactions: Analysis, Drug Distribution, Modeling*, in *Methods and Principles in Medicinal Chemistry*, R. Mannhold, H. Kubinyi, and G. Folkers, Editors. 2002, Wiley-VCH Verlag GmbH: Weinheim, Germany.
99. Pallicer, J.M. and S.D. Krämer, *Evaluation of fluorescence anisotropy to assess drug-lipid membrane partitioning*. Journal of Pharmaceutical and Biomedical Analysis, 2012. **71**(0): p. 219-227.
100. Lakowicz, J.R., *Principles of Fluorescence Spectroscopy*. 3rd ed. ed. 2006, New York: Springer.
101. Martin, M.L., et al., *The role of membrane fatty acid remodeling in the antitumor mechanism of action of 2-hydroxyoleic acid*. Biochimica et Biophysica Acta (BBA) - Biomembranes, 2013. **1828**(5): p. 1405-1413.
102. Hunter, R.J., *Potential in Colloidal Science, Principles and Applications*. 3rd ed. ed. 1988, London: Academic Press Limited,.
103. Hąc-Wydro, K. and P. Dynarowicz-Łątka, *Biomedical applications of the Langmuir monolayer technique*. Ann UMCS Chem, 2008(63): p. 47–60.
104. Weiner, B.B., W.W. Tscharnuter, and D. Fairhurst *Zeta Potential: A New Approach*. 1993.
105. Park, J.-H., et al., *Interconnected hyaluronic acid derivative-based nanoparticles for anticancer drug delivery*. Colloids and Surfaces B: Biointerfaces, 2014. **121**(0): p. 380-387.
106. Pujol, M., et al., *Influence of alkyl length in the miscibility of several types of lecithins. Interaction of doxorubicin with these membrane models*. Thin Solid Films, 1996. **284–285**(0): p. 723-726.
107. Boyar, H. and F. Severcan, *Tamoxifen-model membrane interactions: an FT-IR study*. Journal of Molecular Structure, 1997. **408–409**(0): p. 265-268.

108. Frézard, F. and A. Garnier-Suillerot, *Permeability of lipid bilayer to anthracycline derivatives. Role of the bilayer composition and of the temperature*. Biochimica et Biophysica Acta (BBA) - Lipids and Lipid Metabolism, 1998. **1389**(1): p. 13-22.
109. Ambike, A., et al., *Interaction of self-assembled squalenoyl gemcitabine nanoparticles with phospholipid-cholesterol monolayers mimicking a biomembrane*. Langmuir, 2011. **27**(8): p. 4891-9.
110. Zhao, L. and S.-S. Feng, *Effects of lipid chain unsaturation and headgroup type on molecular interactions between paclitaxel and phospholipid within model biomembrane*. Journal of Colloid and Interface Science, 2005. **285**(1): p. 326-335.
111. Zhao, L. and S.-S. Feng, *Effects of lipid chain length on molecular interactions between paclitaxel and phospholipid within model biomembranes*. Journal of Colloid and Interface Science, 2004. **274**(1): p. 55-68.
112. Zhao, L., S.-S. Feng, and M.L. Go, *Investigation of molecular interactions between paclitaxel and DPPC by langmuir film balance and differential scanning calorimetry*. Journal of Pharmaceutical Sciences, 2004. **93**(1): p. 86-98.
113. Couvreur, P., et al., *Squalenoyl nanomedicines as potential therapeutics*. Nano Lett, 2006. **6**(11): p. 2544-8.
114. Preetha, A., N. Huilgol, and R. Banerjee, *Comparison of paclitaxel penetration in normal and cancerous cervical model monolayer membranes*. Colloids Surf B Biointerfaces, 2006. **53**(2): p. 179-86.
115. Zhao, L. and S.S. Feng, *Effects of cholesterol component on molecular interactions between paclitaxel and phospholipid within the lipid monolayer at the air-water interface*. J Colloid Interface Sci, 2006. **300**(1): p. 314-26.
116. Preetha, A., N. Huilgol, and R. Banerjee, *Interfacial properties as biophysical markers of cervical cancer*. Biomed Pharmacother, 2005. **59**(9): p. 491-7.
117. Speelmans, G., et al., *Transport Studies of Doxorubicin in Model Membranes Indicate a Difference in Passive Diffusion across and Binding at the Outer and Inner Leaflet of the Plasma Membrane*. Biochemistry, 1994. **33**(46): p. 13761-13768.
118. Brown, T. and T.B. Jr., *Nucleic Acid-Drug Interactions*, in *Nucleic Acids Book*. 2005, ATDBio Ltd.: Southampton, United Kingdom.
119. Cortes-Funes, H. and C. Coronado, *Role of anthracyclines in the era of targeted therapy*. Cardiovasc Toxicol, 2007. **7**(2): p. 56-60.
120. Minotti, G., et al., *Anthracyclines: molecular advances and pharmacologic developments in antitumor activity and cardiotoxicity*. Pharmacol Rev, 2004. **56**(2): p. 185-229.
121. Arcamone, F., *Properties of Antitumor Anthracyclines and New Developments in Their Application: Cain Memorial Award Lecture*. Cancer Research, 1985. **45**(12 Part 1): p. 5995-5999.
122. Lasic, D.D. and D. Needham, *The "stealth" liposome: a prototypical biomaterial*. Chemical reviews, 1995. **95**: p. 2601-2628.
123. Hope, M.J., et al., *Production of large unilamellar vesicles by a rapid extrusion procedure. Characterization of size distribution, trapped volume and ability to mantain a membrane potential*. Biochimica et Biophysica Acta, 1985. **812**: p. 55-65.
124. LifeTechnologies. *Trypan Blue Exclusion - Protocol*. 2015 [cited 2015; Available from: http://www.lifetechnologies.com/pt/en/home/references/gibco-cell-culture-basics/cell-culture-protocols/trypan-blue-exclusion.html.
125. Berne, B.J. and R. Pecor, *Dynamic Light Scattering: With Applications to Chemistry, Biology, and Physics*. Dover Books on Physics Series. 2000: Dover Publications Inc.
126. Wilczura-Wachnik, H., *Dynamic Light Scattering application in size detection of molecules and molecular aggregates* Journal of Modern Optics, 1991(38).
127. HORIBA. *Zeta Potential Analysis using Eletrophoretic Light Scattering*. 2014 [cited 2014 10.06]; Available from: http://www.horiba.com/scientific/products/particle-characterization/technology/zeta-potential/.
128. IUPAC, *Compendium of Chemical Terminology*. 2nd edition ed, ed. A.D.M.a.A. Wilkinson. 1997, Oxford: Blackwell Scientific Publications.

129. Seydel, J.K. and M. Wiese, *Drug-Membrane Interactions: Analysis, Drug Distribution, Modeling*. Methods and Principles in Medicinal Chemistry, ed. R. Mannhold, H. Kubinyi, and G. Folkers. 2002: Wiley-VCH.
130. Martinez, M.N. and G.L. Amidon, *A mechanistic approach to understanding the factors affecting drug absorption: A review of fundamentals*. Journal of Clinical Pharmacology, 2002. **42**(6): p. 620-643.
131. Ferreira, H., et al., *Utilização de modelos membranares na avaliação da actividade de fármacos*. QUÍMICA, 2005. **99**: p. 39-51.
132. Castro, B., et al., *A fast and reliable spectroscopic method for the determination of membrane-water partition coefficients of organic compounds*. Lipids, 2001. **36**: p. 89-96.
133. Santos, N.C., M. Prieto, and M.A.R.B. Castanho, *Quantifying molecular partition into model systems of biomembranes: an emphasis on optical spectroscopic methods*. Biochimica et Biophysica Acta, 2003. **1612**: p. 123-135.
134. Herbette, L.G., et al., *The molecular basis for Lacidipine's unique pharmacokinetics: optimal hydrophobicity results in membrane interactions that may facilitate the treatment of atherosclerosis*. Journal of Cardiovascular Pharmacology, 1994. **23**(5): p. S16-S25.
135. Kerns, E.H. and L. Di, *Drug-like properties: concepts, structure design and methods: from ADME to toxicity optimization*. 2008: Elsevier.
136. Kitamura, K., et al., *Second Derivative Spectrophotometric Determination of Partition Coefficients of Chlorpromazine and Promazine Between Lecithin Bilayer Vesicles and Water*. Analytica Chimica Acta, 1995. **304**: p. 101-106.
137. Lelkes, P.I. and I.R. Miller, *Perturbations of Membrane-Structure by Optical Probes .1. Location and Structural Sensitivity of Merocyanine-540 Bound to Phospholipid-Membranes*. Journal of Membrane Biology, 1980. **52**(1): p. 1-15.
138. Higson, S., *An introduction to the use of visible and ultraviolet light for analytical measurements*, in *Analytical Chemistry* 2003, Oxford University Press.
139. Kitamura, K. and N. Imayoshi, *Second-Derivative Spectrophotometric Determination of the Binding Constant Between Chlorpromazine and -Cyclodextrin in Aqueous Solutions*. Analytical Sciences, 1992. **8**: p. 497-501.
140. Omran, A.A., et al., *Determination of partition coefficients of diazepam and flurazepam between phosphatidylcholine bilayer vesicles and water by second derivative spectrophotometric method*. Journal of Pharmaceutical and Biomedical Analysis, 2001. **25**(2): p. 319-324.
141. Rodrigues, C., et al., *Interaction of rifampicin and isoniazid with large unilamellar liposomes: spectroscopic location studies*. Biochimica Et Biophysica Acta-General Subjects, 2003. **1620**(1-3): p. 151-159.
142. Ojeda, C.B. and F.S. Rojas, *Recent developments in derivative ultraviolet/visible absorption spectrophotometry (review)*. Analytica Chimica Acta, 2004. **518** p. 1-24.
143. Ferreira, H., et al., *Partition and location of nimesulide in EPC liposomes: a spectrophotometric and fluorescence study*
Analytica and Bioanalytical Chemistry, 2003. **377**: p. 293-298.
144. Chiodini, B., R. Bassan, and T. Barbui, *Cellular uptake and antiproliferative effects of therapeutic concentrations of idarubicin or daunorubicin and their alcohol metabolites, with or without cyclosporin A, in MDR1+ human leukemic cells*. Leuk Lymphoma, 1999. **33**(5-6): p. 485-97.
145. Drugs.com. *Doxorubicin Dosage*. 2015; Available from: http://www.drugs.com/dosage/doxorubicin.html.
146. Lúcio, M., et al., *Effect of anti-inflammatory drugs in phosphatidylcholine membranes: A fluorescence and calorimetric study*. Chemical Physics Letters, 2009. **471**(4-6): p. 300-309.
147. Nunes, C., et al., *Lipid-drug interaction: biophysical effects of tolmetin on membrane mimetic systems of different dimensionality*. J Phys Chem B, 2011. **115**(43): p. 12615-23.

148. Nunes, C., et al., *A biophysical investigation of the interaction of non-steroidal anti-inflammatory drugs with large unilamellar DPPC liposomes* REQUIMTE, Departamento de Química, Faculdade de Farmácia, Universidade do Porto.
149. Savitzky, A. and M.J.E. Golay, *Smoothing and differentiation of data.* Analytical chemistry, 1964. **36**: p. 1627-1639.
150. Magalhaes, L.M., et al., *High-throughput microplate assay for the determination of drug partition coefficients.* Nat. Protocols, 2010. **5**(11): p. 1823-1830.
151. Ferreira, H., et al., *Effect of anti-inflammatory drugs on splenocyte membrane fluidity.* Analytical Biochemistry, 2005. **339**(1): p. 144-149.
152. Mansilha, C.I.G.R., *Estudos de partição e localização de fármacos em lipossomas por técnicas espectroscópicas*, in *Departamento de Química da Faculdade de Ciências*2002, Universidade do Porto: Porto.
153. Coutinho, A. and M. Prieto, *Ribonuclease T1 and alcohol dehydrogenase fluorescence quenching by acrylamide.* Journal of Chemical Education, 1993. **70**: p. 425.
154. Valeur, B., *Molecular Fluorescence Principles and Applications*. 2002: Wiley-VHC.
155. Loura, L.M.S., et al., *Interaction of peptides with binary phospholipid membranes: application of fluorescence methodologies.* Chemistry and Physics of Lipids, 2003. **122**(1-2): p. 77-96.
156. Slavic, J., *Fluorescent probes in cellular and molecular biology*. 1994, Michigan CRC Press: Ann Arbor.
157. Repáková, J., et al., *Distribution, Orientation, and Dynamics of DPH Probes in DPPC Bilayer.* Journal of Physical Chemistry B, 2004. **108**: p. 13438-13448.
158. Kaiser, R.D. and E. London, *Location of diphenylhexatriene (DPH) and its derivatives within membranes: comparison of different fluorescence quenching analysis of membrane depth.* Biochemistry, 1998. **37**: p. 8180-8190.
159. Neves, P., et al., *Characterization of membrane protein reconstitution in LUVs of different lipid composition by fluorescence anisotropy.* Journal of Pharmaceutical and Biomedical Analysis, 2009. **49**(2): p. 276-281.
160. Grancelli, A., et al., *Interaction of 6-fluoroquinolones with dipalmitoylphosphatidylcholine monolayers and liposomes.* Langmuir, 2002. **18**(24): p. 9177-9182.
161. Ghosh, S.K. and P.K. Chattaraj, *Concepts and Methods in Modern Theoretical Chemistry: Electronic Structure and Reactivity*. 2013: CRC Press.
162. Engelke, M., et al., *Tamoxifen perturbs lipid bilayer order and permeability: comparison of DSC, fluorescence anisotropy, Laurdan generalized polarization and carboxyfluorescein leakage studies.* Biophysical Chemistry, 2001. **90**(2): p. 157-173.
163. Merino, S., et al., *Fluoroquinolone - Biomembrane interaction at the DPPC/PG lipid - Bilayer interface.* Langmuir, 2002. **18**(8): p. 3288-3292.
164. Beccerica, E., et al., *Diacetylrhein and Rhein - Invivo and Invitro Effect on Lymphocyte Membrane Fluidity.* Pharmacological Research, 1990. **22**(3): p. 277-285.
165. Beccerica, E., et al., *Effect of antirheumatic drugs on lymphocyte membrane fluidity in rheumatoid arthritis: a fluorescence polarization study.* Pharmacology, 1989. **38**: p. 16-22.
166. Sangster, J., *Octanol-Water Partition Coefficients of Simple Organic Compounds.* Journal of Physical and Chemical Reference Data, 1989. **18**(3): p. 1111-1229.
167. Jain, M. and N. Wu, *Effect of small molecules on the dipalmitoyl lecithin liposomal bilayer: III. Phase transition in lipid bilayer.* The Journal of Membrane Biology, 1977. **34**(1): p. 157-201.

Chapter 8

Annexes

Annex I Plotted results of the static, dynamic and Stern-Volmer constants determined using a regular spectrofluorimeter (left) and a plate-reading spectrofluorimeter (right. These constants were determined for all four models plus the tumoral cells MDA-MB-231 under the effect of daunorubicin for the two probes, DPH and TMA-DPH.

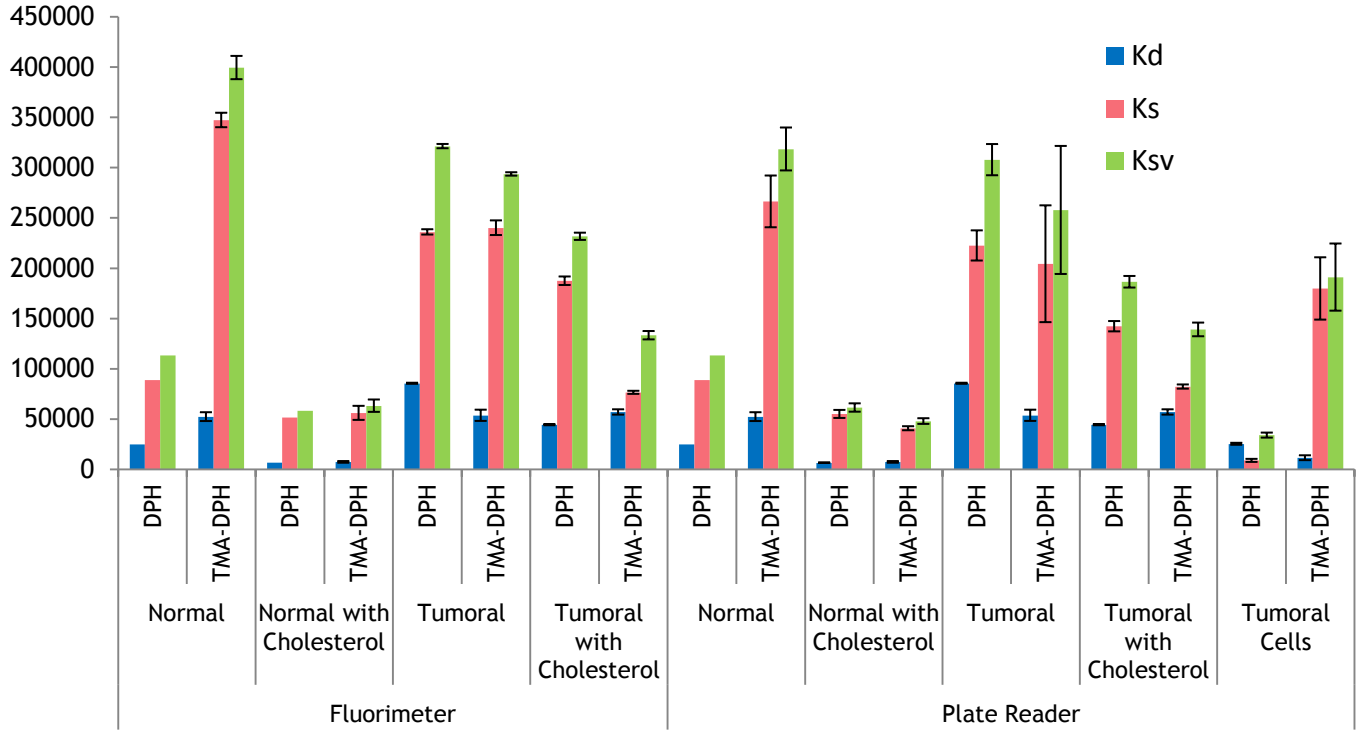

Annex II Static, dynamic and Stern-Volmer constants (K_s, K_D, K_{SV} respectively) obtained for the four models designed for this study plus the tumoral cells MDA-MD-231, for the two probes, DPH and TMA-DPH.

		Probes	K_D	K_S	K_{SV}
Fluorimeter	Normal	DPH	24660	88583	113243
		TMA-DPH	52170 ± 4385	347275 ± 7187	399445 ± 11572
	Normal with Cholesterol	DPH	6502	51592	58094
		TMA-DPH	7137 ± 842	55916 ± 6996	63053 ± 6154
	Tumoral	DPH	85352 ± 530	235949 ± 2649	321301 ± 2120
		TMA-DPH	53499 ± 5592	240108 ± 7276	293607 ± 1684
	Tumoral with Cholesterol	DPH	44208 ± 629	187358 ± 4229	231567 ± 3600
		TMA-DPH	56812 ± 2631	76351 ± 1528	133164 ± 4159
Plate Reader	Normal	DPH	24 660	88583	113243
		TMA-DPH	52170 ± 4385	266284 ± 25731	318454 ± 21346
	Normal with Cholesterol	DPH	6389 ± 161	54851 ± 3990	61240 ± 4151
		TMA-DPH	7137 ± 842	40624 ± 1995	47762 ± 2837
	Tumoral	DPH	85352 ± 530	222465 ± 14996	307817 ± 15526
		TMA-DPH	53499 ± 5592	204264 ± 58087	257763 ± 63679
	Tumoral with Cholesterol	DPH	44208 ± 629	142125 ± 5135	186333 ± 5764
		TMA-DPH	56812 ± 2631	82106 ± 2084	138918 ± 6798

Annex III Bimolecular constant (Kq) obtained for the four models designed for this study plus the tumoral cells MDA-MD-231, for the two probes, DPH and TMA-DPH. plus the tumoral cells MDA-MD-231, for the two probes, DPH and TMA-DPH.

Method	Model	Probe	Kq (x 1E+13)
Fluorimeter	Normal	DPH	1.4 ± 0.6
		TMA-DPH	9.68 ± 0.05
	Normal with Cholesterol	DPH	0.6
		TMA-DPH	0.85 ± 0.07
	Tumoral	DPH	3.9 ± 0.1
		TMA-DPH	8.01 ± 0.09
	Tumoral with Cholesterol	DPH	2.49 ± 0.03
		TMA-DPH	2.21 ± 0.08
Plate Reader	Normal	DPH	1.3
		TMA-DPH	7.7 ± 0.7
	Normal with Cholesterol	DPH	0.60 ± 0.04
		TMA-DPH	0.65 ± 0.05
	Tumoral	DPH	3.7 ± 0.3
		TMA-DPH	7 ± 2
	Tumoral with Cholesterol	DPH	2.01 ± 0.07
		TMA-DPH	2.3 ± 0.1
	Tumoral Cells	DPH	0.48 ± 0.01
		TMA-DPH	3.8 ± 0.5